ДОКЛАДЫ
АКАДЕМИИ НАУК СССР

SOVIET PHYSICS

"Doklady"

VOLUME 1 NUMBER 5

A Translation
of the
"Physics Section"
of the

Proceedings of the Academy of Sciences of the USSR

(RUSSIAN ORIGINAL VOL. 110, NOS. 1-6)

Published by the
AMERICAN INSTITUTE OF PHYSICS
INCORPORATED

SOVIET PHYSICS

"Doklady"

A translation of the "Physics Section" of the Proceedings of the Academy of Sciences of the USSR.

A publication of the

AMERICAN INSTITUTE OF PHYSICS

Governing Board

Allen V. Astin
Robert F. Bacher
W. S. Baird
H. A. Bethe
R. T. Birge
Frank D. Dexter
I. C. Gardner
S. A. Goudsmit
Charles Kittel
Hugh S. Knowles
R. B. Lindsay
William F. Meggers
Harry F. Olson
R. R. Palmer
R. F. Paton
Eric Rodgers
Ralph A. Sawyer
Frederick Seitz
H. D. Smyth
Mark W. Zemansky

Officers and Staff

Frederick Seitz
Chairman, Governing Board
Henry A. Barton
Director
Wallace Waterfall
Executive Secretary
Mark W. Zemansky
Treasurer
Theodore Vorburger
Advertising Manager
Ruth F. Bryans
Publication Manager
Kathryn Setze
Assistant Treasurer
Alice Mastropietro
Circulation Manager
Eugene H. Kone
Director of Public Relations

American Institute of Physics Advisory Board on Russian Translations

Elmer Hutchisson, *Chairman*
Dwight Gray, Morton Hamermesh, Vladimir Rojansky, Victor Weisskopf

SOVIET PHYSICS—"Doklady" is a bi-monthly journal published by the American Institute of Physics for the purpose of making available in English reports of current Soviet research in physics as contained in the "Physics Section" of the Proceedings of the Academy of Sciences of the USSR. The Proceedings appears thirty-six times per year and the "Physics Sections" are accumulated and English translations of them are published in six issues per year.

Transliteration of the names of Russian authors follows the system employed by the Library of Congress.

This translating and publishing project was undertaken by the Institute in the conviction that dissemination of the results of research everywhere in the world is invaluable to the advancement of science. The National Science Foundation of the United States encouraged the project initially and is supporting it in large part by a grant. Translation and printing are being handled by Consultants Bureau, Inc.

The American Institute of Physics and its translators propose to translate faithfully all of the scientific material in the "Physics Section" of the Proceedings of the Academy of Sciences of the USSR appearing after January 1, 1956. The views expressed in the translated material, therefore, are intended to be those expressed by the original authors, and not those of the translators nor of the American Institute of Physics.

One volume is published annually. Volume 1 will consist of six issues and will contain all scientific material published in the "Physics Section" of the original Russian journal during the 1956 calendar year.

Subscription Prices:

Per year (6 issues)	
United States and Canada	$25.00
Elsewhere	27.50
Back Numbers	
Single copies	$ 6.00

Subscriptions should be addressed to the American Institute of Physics, 57 East 55th Street, New York 22, N. Y.

Copyright by American Institute of Physics 1957

SOVIET PHYSICS

"Doklady"

A translation of the "Physics Section" of the Proceedings of the Academy of Sciences of the USSR.

VOLUME 1, NUMBER 5 SEPTEMBER-OCTOBER, 1956

ENERGY DISTRIBUTION OF INCOHERENT RADIATION FROM SYNCHROTRON ELECTRONS

Iu. M. Ado and P. A. Cherenkov

(Presented by Academician D. V. Skobeltsyn March 21, 1956)

According to classical theory when electrons move in a magnetic field they emit electromagnetic radiation with frequencies which are multiples of the orbital angular frequency of the electrons in their circular trajectory [1-3].

The intensity I_n of the nth harmonic is given by

$$I_n = \frac{2\omega_0 e^2 n^{1/3}}{R\sqrt{\pi}}\left[-\Phi'(y) - \frac{y}{2}\int_y^\infty \Phi(y)\,dy\right], \tag{1}$$

where e, E_0, E and ω_0 are the charge, rest energy, total energy and circular frequency, respectively, of an electron moving in a trajectory or radius R; $\Phi(y)$ is an Airey function;* $\Phi'(y)$ is its derivative; $y = n^{2/3}(E_0/E)^2$.

The radiation is strongly oriented and practically confined inside a cone whose axis coincides with the direction of instantaneous velocity of the electron and whose vertex angle α is given by

$$\alpha = \frac{2}{n^{1/3}}. \tag{2}$$

The maximum radiation belongs to the harmonic $n_{\max}$ which satisfies the relation

$$n_{\max} = \frac{2}{3}\left(\frac{E}{E_0}\right)^3, \tag{3}$$

and for electron accelerators whose orbital radius is of the order of 100 cm; this lies in the visible portion of the spectrum for electron energies $E \simeq 100$ Mev. With increasing energy the maximum, as follows from (3) is shifted towards shorter wave lengths.

Radiation from electrons moving in a magnetic field has been studied experimentally in several articles [4-6]. But the optical characteristics of this radiation have been measured for the total emission during the entire cycle of acceleration.

In the present work we have measured the relative energy distribution in the radiation from monoenergetic electrons at 150, 225, 250 Mev in the spectral region from 400 to 6100 A.**

The electrons were accelerated in the synchrotron of the P. N. Lebedev Physics Institute of the Academy of Sciences USSR to a maximum energy of 250 Mev. The experimental arrangement is shown in Fig. 1. The

---

* The Airey functions have been tabulated [7].

** Similar experiments have been performed for the ultraviolet region using a different method [4, 5].

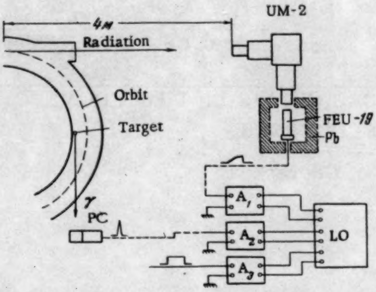

Fig. 1. Arrangement of apparatus. PC) Pulse ionization chamber; A_1) amplifier of light signal channel; A_2) amplifier of ionization chamber pulse; A_3) amplifier of envelope of accelerating voltage pulse; LO) loop oscillograph.

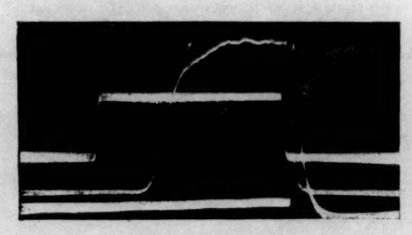

Fig. 2. Pulse oscillograms: 1) light pulse; 2) ionization chamber pulse; 3) pulse of envelope of high frequency accelerating potential.

radiation from the electrons left the synchrotron chamber through a tube with a plexiglas window which was placed along a tangent to the orbit.

Spectral analysis of the radiation was performed by a UM-2 prism monochromator whose entrance slit was perpendicular to the plane of the orbit, which passed through its middle. In front of the exit slit of the monochromator a FEU-19 photomultiplier was placed, screened by 12 cm lead blocks from the gamma-ray background.

The signal from the photomultiplier output was fed to a dc amplifier with negative feedback (A_1) in which voltage pulses were transformed into current pulses. The signal then passed to a loop oscillograph (LO) where it was recorded on film by a vibrator of 5000 cycle natural frequency. Simultaneously with the light pulse the loop oscillograph recorded signals from the pulse ionization chamber PC which were proportional to the intensity of bremsstrahlung and thus proportional to the number of accelerated electrons in each cycle. The data from these records enabled us to normalize the oscillograms to the same number of electrons.

Pulses of the envelope of the high-frequency accelerating potential were also recorded. The recording of the signals took place at the rate of 0.5 m/sec. One of the oscillograms is reproduced in Fig. 2.

For each wave length selected 8 to 10 cycles were recorded. The monochromator prism was rotated by a special remote control transmitting mechanism which enabled us to obtain spectra in 5 to 6 minutes.

The monochromator-photomultiplier system was calibrated by a standard temperature-limited tube with a brightness temperature of 2198°. The spectral sensitivity of the apparatus enabled us to take spectra from 4000 to 6100 A.

The light pulses on the oscillogram photographs were measured at the instant when the accelerating potential was cut off and reduced to a single intensity. The energy acquired by the electron up to this time was determined by supplementary magnetic measurements.

In Fig. 3 the solid curves represent the energy distribution in the emission spectrum in relative units for electrons at 150, 225 and 250 Mev, as calculated from (1) and converted to intensity per A. The experimental values are given by dots with indications of the errors, which included both errors in reading the oscillograms and errors in determining the spectral sensitivity of the apparatus.

In using the experimental data it was necessary to take into consideration the change of angle α with change of n, as follows from Eq. (2). However it can be shown that during observation of emission from electrons in a synchrotron the apex angle of the cone (which is a little larger because of betatron oscillations) in which the radiation is concentrated, will change by only 2% in the transition from $\lambda_1 = 4000$ A to $\lambda_2 = 6100$ A;

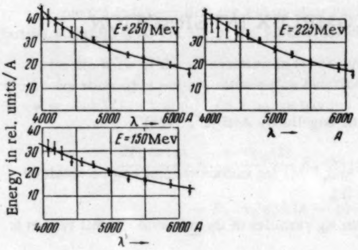

Fig. 3. Energy distribution of emission spectrum: dots are experimental values; the solid curve is theoretical.

this error is unimportant.

As can be seen from Fig. 3, the experimental intensity distributions in the emission spectra of electrons with fixed energy confirm the theory within the limits of experimental error. The observed systematic deviation of the experimental points for short wave lengths (which does not exceed the limit of experimental error, however) can evidently be attributed to lower accuracy in calibrating the spectral sensitivity of the apparatus in this region.

LITERATURE CITED

[1] D. Ivanenko and A. Sokolov, Doklady Akad. Nauk SSSR 59, 1551 (1948).

[2] L. A. Artsimovich and I. Ia. Pomeranchuk, J. Exptl.-Theoret. Phys. (U.S.S.R.) 16, 379 (1946).

[3] J. Schwinger, Phys. Rev. 75, 1912 (1949).

[4] P. L. Hartman and D. H. Tomboulian, Phys. Rev. 91, 1577 (1953).

[5] P. L. Hartman and D. H. Tomboulian, Phys. Rev. 87, 233 (1952).

[6] F. R. Elder, et al., Phys. Rev. 74, 52 (1948).

[7] V. A. Fok, Tables of Airey Functions (1946).

Received March 16, 1956

P. N. Lebedev Physics Institute,
Academy of Sciences USSR

EQUATIONS WITH VARIATIONAL DERIVATIVES AND DISTRIBUTION FUNCTIONS FOR SYSTEMS WITH COMPLEX INTERACTION

I. P. Bazarov

(Presented by Academician N. N. Bogoliubov April 17, 1956)

Equilibrium distribution functions $F_s(x_1, x_2 \ldots, x_s)$ $(s = 1, 2, \ldots)$ for various systems can be obtained much more easily when a certain generating functional is used [1].

Let us take a system consisting of M kinds of particles with N_a particles of the ath kind. If this system is in an external field $\varphi(\vec{r})$ the Gibbs distribution will be

$$D = \frac{1}{Q} \exp\left\{ -\frac{1}{\theta}\left(U + \sum_{\substack{1<a<M \\ 1<i<N_a}} \varphi_a(\mathbf{r}_i) \right)\right\}, \tag{1}$$

where $U = \Sigma \Phi_{ab}(|\mathbf{r}_{a,i} - \mathbf{r}_{b,j}|)$ is the potential energy of the interaction between particles; $\vec{r}_{a,i}$ determines the position of the ith molecule of the ath class; the summation is performed over all pairs of molecules; Q is a configuration integral; the mutual potentials Φ_{ab} are assumed to be symmetrical functions with respect to a and b.

The free energy of this system:

$$F = -\theta \ln Q = -\theta \ln \exp \int \left\{ -\frac{1}{\theta}\left(U + \sum_{a,i} \varphi_a(\mathbf{r}_i) \right)\right\} d\tau \tag{2}$$

is a functional of the external field $\varphi(\vec{r})$.

The distribution functions of groups of particles $F_{a_1, \ldots a_s}(\vec{r}_1, \ldots, \vec{r}_s)$ which are normalized in such a way that $\frac{1}{V^s} F_{a_1, \ldots, a_s}(\vec{r}_1, \ldots, \vec{r}_s)\, d\vec{r}_1, \ldots, d\vec{r}_s$ defines the probability that s definite molecules of classes $a_1, \ldots, a_s$ have the indicated coordinates in volume V, can be expressed in terms of the variational derivatives of the Functional (2):

$$F_a(x|\varphi) = \frac{V}{N_a} \frac{\delta F}{\delta \varphi_a(x)}, \tag{3}$$

$$F_{ab}(x, y|\varphi) = \frac{N_b}{N_b - \delta_{ab}} F_a(x|\varphi) F_b(y|\varphi) -$$

$$- \frac{V}{N_b - \delta_{ab}} F_a(x|\varphi) \delta(x - y) - \frac{\theta V}{N_b - \delta_{ab}} \frac{\delta F_a(x|\varphi)}{\delta \varphi_b(y)},$$

$$\ldots\ldots\ldots\ldots\ldots\ldots\ldots\ldots\ldots\ldots \tag{4}$$

where $\delta_{ab} = 1$ for $a = b$; $\delta_{ab} = 0$ for $a \neq b$ and $\vec{r}_i$ is denoted by x, y,. . . . Assuming in (3) and (4) that $\varphi = 0$ we obtain the distribution functions in the absence of the field.

From (4) it is seen that the binary distribution function is completely expressed in terms of unitary distribution functions with the aid of the variational derivative.

On the basis of the distribution in (1) and the definition of the distribution functions it is easy to obtain a closed equation for a unitary distribution function with a variational derivative; thus in the limiting case $N \to \infty$, $V \to \infty$, but $V/N = v$ and $N_a/N = n_a$ we have:

$$\frac{\partial F_a(x\,|\,\varphi)}{\partial x^\alpha} + \frac{1}{\theta}\frac{\partial \varphi_a(x)}{\partial x^\alpha} F_a(x)\,|\,\varphi) + \frac{1}{\theta}\sum_{1<b<M}\int \frac{\partial \Phi_{ab}(|x-y|)}{\partial x^\alpha}\left\{\frac{n_b}{v} F_a(x\,|\,\varphi) F_b(y|\varphi) - \right. \\ \left. - F_a(x\,|\,\varphi)\,\delta(x-y) - \theta\frac{\delta F_a(x\,|\,\varphi)}{\delta\varphi_b(y)}\right\} dy = 0 \quad (\alpha = 1, 2, 3) \tag{5}$$

or in variational derivatives of the Functional $F(\varphi)$:

$$\frac{\partial}{\partial x^\alpha}\frac{\delta F}{\delta\varphi_a(x)} + \frac{1}{\theta}\frac{\partial\varphi_a(x)}{\partial x^\alpha}\frac{\delta F}{\delta\varphi_a(x)} + \frac{1}{\theta}\sum_{1<b<M}\int\frac{\partial\Phi_{ab}(|x-y|)}{\partial x^\alpha}\left\{\frac{\delta F}{\delta\varphi_a(x)}\frac{\delta F}{\delta\varphi_b(y)} - \right. \\ \left. - \frac{\partial F}{\delta\varphi_a(x)}\delta(x-y) - \theta\frac{\delta^2 F}{\delta\varphi_a(x)\,\delta\varphi_b(y)}\right\} dy = 0. \tag{6}$$

Eq. (5) can be represented in the form

$$\frac{\partial F_a(x\,|\,\varphi)}{\partial x^\alpha} + \frac{1}{\theta}\frac{\partial\psi_a(x)}{\partial x^\alpha} F_a(x\,|\,\varphi) = 0, \tag{7}$$

where

$$\psi_a(x) = \varphi_a(x) + \sum_{1<b<M}\int \Phi_{ab}(|x-y|)\left\{\frac{n_b}{v}F_b(y\,|\,\varphi) - \delta(x-y) - \theta\frac{\delta}{\delta\varphi_b(y)}\right\} dy.$$

Eq. (7) for $F_a(x\,|\varphi)$ is formally the same type of equation as in the case of motion of particles of an ideal gas in a given external field $\psi_a(x)$. The actual interaction between the particles is expressed by the fact that $\psi_a(x)$ is not an ordinary but an operator field.

When in Eq. (7) we neglect the operator character of the external field we obtain an equation which defines the distribution function $F_a(x\,|\varphi)$ for a system with Coulomb interaction. When $F_a(x\,|\varphi)$ is expanded in powers of $\underline{v}$ we obtain for the binary Function (4) a value which agrees with Debye's results [2].

When in (6) we replace the functional argument $\varphi(x)$ by $u(x)$ through the formula

$$\varphi(x) = -\theta\ln[1 + vu(x)],$$

then (for M = 1) it will become

$$-\frac{\partial}{\partial x^\alpha}\frac{\delta F}{\delta u_x} + \frac{1}{\theta^2}\int\frac{\partial\Phi(|x-y|)}{\partial x^\alpha}(n + u_y)\left(\frac{\delta F}{\delta u_x}\frac{\delta F}{\delta u_y} - \theta\frac{\delta^2 F}{\delta u_x\delta u_y}\right) dy = 0 \tag{8}$$

(here for brevity $u(x) = u_x$). When the distribution functions are expanded in powers of $1/v$ this equation enables us to obtain them for systems with short-range interaction forces.

The actual interaction between charged particles consists of Coulomb ($r > r_0$) forces and short-range forces with potentials $\Phi_0(r)$, and $\Phi_1(r)$, respectively. However, as was noted in [1], thus far no solution has been found for the problem of constructing expansions which would enable us to obtain the correlation distribution functions for systems with interactions including both Coulomb and short-range forces and which would enable us to obtain asymptotic formulas for all approximations.

We wish here to describe a method of obtaining distribution functions of this "complex" interaction character:

$$\Phi(r) = \Phi_0(r) + \Phi_1(r). \tag{9}$$

Let the total interaction energy of a system of N particles with the potential (9) be given by

$$U = U_0 + \sum_{1 \leqslant i < j \leqslant N} \Phi_1(|x_i - x_j|),$$

where U_0 is the portion of the interaction energy of the particle system which corresponds to the potential $\Phi_0(r)$.

If, moreover, our system is in an external field $\varphi(x)$ the configuration integral and the free energy of the system are

$$\begin{gathered} Q = \int \exp\left\{-\frac{1}{\theta} U - \frac{1}{\theta} \sum_{1 \leqslant i \leqslant N} \varphi(x_i)\right\} dx_1 \ldots dx_N = \\ = \int \exp\left\{-\frac{1}{\theta} U_0 - \frac{1}{\theta} \sum_{1 \leqslant i \leqslant N} \varphi(x_i)\right\} \prod_{1 \leqslant i < j \leqslant N} (1 + f(x_i, x_j))\, dx_1 \ldots dx_N, \\ F = -\theta \ln Q, \end{gathered} \tag{10}$$

where $f(x_i, x_j) = \exp\left\{-\frac{1}{\theta} \Phi_1(|x_i - x_j|)\right\} - 1$. Both Q and F are functionals of the external field $\varphi(x)$ and of the interaction energy $f(x_i, x_j)$.

The distribution functions $F_1(x|\varphi|f)$, $F(x, y|\varphi|f)$, etc. are expressed in terms of the variational derivatives of the functional $F(\varphi|f)$ with respect to $\varphi(x)$ by the Formulas (3) and (4). However, unlike the previous cases, where the distribution functions were obtained by solving the corresponding equations with the variational derivative by means of the expansions indicated above, these functions can now be obtained differently. We shall now show that the functional $F(\varphi|f)$ can be expressed in terms of the correlation distribution functions of the system with the potential $\Phi_0(r)$, so that in order to obtain the variational derivatives of F with respect to φ and, consequently, the functions $F_s(x_1, \ldots, x_s|\varphi|f)$, it is not necessary to set up and solve their differential equations but only to know $F_s(x_1, \ldots, x_s|\varphi)$ for the potential $\Phi_0(r)$ as defined above.

For this purpose we expand the functional $F(\varphi|f)$ in a series:

$$\begin{gathered} F(\varphi|f) = F_{f=0} + \int f(x, y)\left(\frac{\delta F}{\delta f_{xy}}\right)_{f=0} dx\, dy + \\ + \frac{1}{2}\int f(x, y) f(x', y')\left(\frac{\delta^2 F}{\delta f_{xy}\delta f_{x'y'}}\right)_{f=0} dx\, dy\, dx'\, dy' + \ldots \end{gathered} \tag{11}$$

and obtain expressions for the variational derivatives $(\delta F/\delta f_{xy})_{f=0}$, $(\delta^2 F/\delta f_{xy}\delta f_{x'y'})_{f=0}$, etc.

From (10) we obtain

$$(1+f_{xy})\frac{\delta Q}{\delta f_{xy}} = \frac{\theta^2}{2}\left\{\frac{\delta^2 Q}{\delta\varphi_x\delta\varphi_y} - \frac{\delta(x-y)}{\theta}\frac{\delta Q}{\delta\varphi_x}\right\}$$

or

$$(1+f_{xy})\frac{\delta F}{\delta f_{xy}} = \frac{\theta^2}{2}\left\{\frac{\delta^2 F}{\delta\varphi_x\delta\varphi_y} - \frac{1}{\theta}\frac{\delta F}{\delta\varphi_x}\frac{\delta F}{\delta\varphi_y} + \frac{\delta(x-y)}{\theta}\frac{\delta F}{\delta\varphi_x}\right\} \tag{12}$$

and from (3) and (4):

$$(1+f_{xy})\frac{\delta F}{\delta f_{xy}} = -n^2\frac{\theta}{2}F_\alpha(x, y)\,|\,\varphi\,|\,f).$$

Assuming now $f_{xy} = 0$, we obtain

$$\left(\frac{\delta F}{\delta f_{xy}}\right)_{f=0} = -n^2\frac{\theta}{2}F_2(x, y\,|\,\varphi),$$

that is, the variational derivative $(\delta F/\delta f_{xy})_0$ is expressed in terms of the binary distribution function with the potential $\Phi_0(r)$. Therefore in first approximation, according to (11), the free energy of a system with potential (9) is

$$F(\varphi\,|\,f) = F_{f=0} - n^2\frac{\theta}{2}\int f(x, y)\,F_2(x, y\,|\,\varphi)\,dx\,dy. \tag{13}$$

Using (12) we can obtain $(\delta^2 F/\delta f_{xy}\delta f_{x'y'})_0$ and thus determine $F(\varphi|f)$ in second approximation. Knowing $F_2(x,y\,|\varphi)$, by taking the functional derivative of (13) with respect to $\varphi(x)$ we can obtain the distribution functions $F_1(x\,|\,\varphi|f)$ and $F_2(x,y\,|\,\varphi|f)$, etc., and then assuming $\varphi = 0$ we can also obtain $F_1(x|f)$ and $F_2(x,y|f)$, etc., for our system.

I consider it an obligation to express my sincere thanks to Academician N. N. Bogoliubov, who directed this work.

LITERATURE CITED

[1] N. N. Bogoliubov, Problems of Dynamical Theory and Statistical Physics (1946).

[2] H. Falkenhagen, Electrolytes (1935).

Received April 12, 1956

M. V. Lomonsov Moscow State University

PSEUDOSCALAR INTERACTION IN NONLINEAR MESON THEORY

A. Borgardt

(Presented by Academician N. N. Bogoliubov April 12, 1956)

A nonlinear meson field theory can be constructed rigorously on the basis of a first order Lagrangian

$$\mathcal{L}^{(1)} = C\left(\psi^+\left(\beta_\lambda \frac{\partial}{\partial x_\lambda} + k_0\right)\psi + \frac{\Lambda}{2}\,\psi^+\beta'\psi\cdot\psi^+\beta''\psi\right), \tag{1}$$

where

$$\beta_\mu\beta_\nu\beta_\rho + \beta_\rho\beta_\nu\beta_\mu - \delta_{\mu\nu}\beta_\rho - \delta_{\rho\nu}\beta_\mu = 0; \tag{2}$$

$\Lambda = \Lambda(k_0)$ is the self energy constant. The self energy is taken to be of the third order, which is apparently of most importance [1].

The Lagrangian [1] must satisfy the following requirements:

I. Relativistic covariance of the field equations.

II. Energy-momentum conservation (for nonlinear fields this is not guaranteed by satisfaction of I).

III. The possibility of the transition to the limit $k_0 \to 0$ without divergences in the field equations.

Thus the operators β', β'', can be represented as

$$\beta' = R'\beta,\ \beta'' = R''\beta,$$

where β belongs to G_{126} and R', R" are reflection operators which are expanded on the basis I, R_5 [2].

The operator β can be of two types:

$$\begin{aligned}&(A)\ {}^1/_2(I \pm R_5)\,\beta\cdot{}^1/_2(I \mp R_5) = 0,\\ &(B)\ {}^1/_2(I \pm R_5)\,\beta\cdot{}^1/_2(I \pm R_5) = 0.\end{aligned} \tag{3}$$

To (A) there belong I, $[\beta_\mu\beta\nu]$, $\{\beta_\mu\beta\nu\}$ and β_5; to (B) β_μ, $\beta_5\beta_\mu$.

For a pseudoscalar field we are not interested in cases where $\beta = [\beta_\mu\beta\nu]$, $\beta = \beta_5\beta_\mu$ and β_5, since the corresponding eigenvalues are zero. The self energy disappears for a neutral field with R = I and $\beta = \beta_\mu$. There remains β = I, R_5 and $\beta = R_5\beta_\mu$.

With respect to R' and R" we confine ourselves to the variants: 1) R' = R" = I; 2) R' = R" = $\frac{1}{2}(I + R_5)$; 3) R' = R" = $\frac{1}{2}(I - R_5)$; 4) R' = $\frac{1}{2}(I \pm R_5)$, R" = $\frac{1}{2}(I \mp R_5)$.

Then in the static case and for small distances ($k_0 \rightarrow 0$) the equations of the pseudoscalar field are reduced to the following five types:

$$-\nabla\psi + \vec{\psi} + \lambda\vec{\psi}\cdot\vec{\psi}^2 = 0, \quad \nabla, \vec{\psi} = 0 \quad (A_1, A_2); \tag{4}$$

$$\nabla^2\psi - \lambda\psi^3 = 0 \quad (A_3); \tag{5}$$

$$\nabla^2\psi - \lambda\psi(\nabla\psi)^2 = 0 \quad (B_3); \tag{6}$$

$$\nabla^2\psi + \lambda\psi(\nabla\psi)^2/(1-\lambda\psi^2) = 0 \quad (A_4, B_1, B_4); \tag{7}$$

$$\nabla^2\psi - 2\lambda\psi(\nabla\psi)^2/(1+\lambda\psi^2) = 0 \quad (B_2). \tag{8}$$

Eq. (4) is very complicated for integration; (5) has been examined by many authors [3-6]; Eqs. (6 - 8) are easily integrated since, according to a theorem proved in [7], their solution is always a function of the solution of the corresponding linear Laplace equation. The solution reduces to the integration of the equation (where $\psi_L(\mathbf{x}) = f\vec{\sigma}, \quad (\mathbf{x}-\mathbf{x}')^0/|\mathbf{x}-\mathbf{x}'|^2$):

$$d^2\psi(\psi_L(\mathbf{x}))/d\psi_L^2(\mathbf{x}) = \lambda f(\psi)(d\psi(\psi_L(\mathbf{x}))/d\psi_L(\mathbf{x}))^2, \tag{9}$$

the integral of which [$\psi(\mathbf{x} \rightarrow \infty) \rightarrow 0$] is

$$\int_0^\psi d\xi \exp\left(-\lambda\int_0^\xi f(\xi')\,d\xi'\right) = \psi_L(\mathbf{x}). \tag{10}$$

The solutions of (6 - 8) are

$$\int_0^\psi d\xi \exp(-\lambda\xi^2/2) = \psi_L(\mathbf{x}), \tag{11}$$

$$\psi = (1/\sqrt{\lambda})\sin(\sqrt{\lambda}\,\psi_L(\mathbf{x})), \tag{12}$$

$$\psi = (1/\sqrt{\lambda})\tan(\sqrt{\lambda}\,\psi_L(\mathbf{x})). \tag{13}$$

From these formulas it can be seen that all three Equations (6 - 8) have for $\lambda > 0$ a movable singular point at $x = x_0(\lambda)$. All of the potentials obtained are singular except (13) for $\lambda < 0$.

The applicability of these results to nuclear theory must be examined with regard to the following:

1) The nonlinear potential must lead to saturation of nuclear forces; the necessary condition for this is

$$\psi(\psi_{L1} + \psi_{L2} + \dots) < \psi(\psi_{L1}) + \psi(\psi_{L2}) + \dots, \tag{14}$$

this is satisfied for (11) and (13) with $\lambda < 0$ and for (12) with $\lambda > 0$.

2) Nonlinearity must eliminate the dipolar difficulty. This means that the interaction energy of a pair of nucleons,

$$U_{12}(\mathbf{x}_1, \mathbf{x}_2) = \int \mathcal{E}_{12}(\mathbf{x}, \mathbf{x}_1, \mathbf{x}_2)\,\mathcal{E}_1(\mathbf{x}, \mathbf{x}_1) - \mathcal{E}_2(\mathbf{x}, \mathbf{x}_2))\,(d\mathbf{x}), \tag{15}$$

where $\mathcal{E}_{12}$ is the energy density of the field created by the two nucleons [$\psi_{12} = \psi(\psi_{L_1} + \psi_{L_2})$] and $\mathcal{E}_1$, $\mathcal{E}_2$ are the energy density of the individual fields of the first and second nucleons, should not diverge when $\mathbf{x}_1 \rightarrow \mathbf{x}_2$ as $|\mathbf{x}_1 - \mathbf{x}_2|^{-3}$.

The absence of the dipolar difficulty has been shown rigorously for the field with the potential (11).

LITERATURE CITED

[1] B. Malenka, Phys. Rev. 85, 686 (1952).

[2] A. Borgardt, J. Exptl.-Theoret. Phys. (U.S.S.R.) 24, 284 (1953).

[3] L. Schiff, Phys. Rev. 84, 1 (1951).

[4] W. Thirring, Z. Naturforsch. 7a, 63 (1952).

[5] W. Thirring, Helv. Phys. Acta 26, 33 (1953).

[6] N. Mitskevich, J. Exptl.-Theoret. Phys. (U.S.S.R.) 29, 354 (1955).

[7] K. Bechert, Math. Nachrichten 6, 271 (1952).

Received April 11, 1956

Dnepropetrovsk State University
(On the 300th Anniversary of the Union of the Ukraine and Russia)

X-RAY EMISSION SPECTRA OF Mn AND Cu IN A HEUSLER ALLOY AT TEMPERATURES AROUND THE CURIE POINT

E. E. Vainshtein and B. I. Kotliar

(Presented by Academician A. P. Vinogradov April 6, 1956)

The effect of the magnetic state of a substance on the x-ray spectra of its consitutent elements has been mentioned in the literature [1, 2]. The causes of this effect have been examined theoretically [3, 4] on the basis of ideas which are similar or identical with those developed by S. V. Vonsovskii and his school [5] for the explanation of various properties of ferromagnetic materials. However, this problem has not been studied sufficiently either experimentally or theoretically. Therefore in our study of the x-ray spectra of Heusler alloys [6] we paid special attention to this question. We investigated the shape and position of the lines of the Kβ group of Mn and Cu in an alloy which was close in composition to Cu_2Mn Al and the corresponding characteristics of the K$\alpha_{1,2}$ lines of the same elements in a broad temperature range. The alloy was made of electrolytic Mn, Cu and Al and after heat treatment at 800° was quenched.

The x-ray structural analysis of the alloy, in agreement with previous investigators [7, 8], confirmed the existence after quenching of a body-centered β-phase with a superlattice and lattice constant of 5.950 A. A test showed that the structure and magnetic properties of the alloy remain practically unchanged after prolonged heating (for many tens of hours) in a temperature range which is close to the magnetic transformation point of the alloy. These properties of the alloy also remain unchanged after exposure for a few hours on the anode of a spectrograph x-ray tube while x-ray spectra are obtained.

The spectra were obtained with a Johann vacuum focusing x-ray spectrograph. A quartz reflecting crystal was used: $13\bar{4}0$ planes with constant $d = 1.174$ A. The dispersion was 2-3.8 Xu/mm. In our study of the fine structure of the K$\alpha_{1,2}$ line of the elements we used a secondary method of exciting the spectra. In studying the lines of the Kβ group we used a primary method. The construction of the x-ray fluorescence tube is shown schematically in Fig. 1. The substance under investigation (the radiator) and the heater were placed in a special holder at a distance of 3-4 mm from the anode. The temperature of the sample was controlled by a thermocouple. The transfer from secondary excitation of spectra to primary excitation was accomplished in a few minutes. This required only rotation (by 180°) and raising (by 4 mm) of the anode.

In the primary method the Heusler alloy in the form of wedges 1-2 mm thick was set into the removable head of the anode and exposed under two different modes of operation of the x-ray tube, with the temperature of the alloy either clearly below (~ 220°) or above (~ 330°) the Curie point. In order to prevent systematic errors which may result from the action on the alloy of the stream of electrons bombarding the anode of the x-ray tube, during parallel experiments we used a different order of change of the alloy temperature.

During the secondary method of exciting the spectra the temperature of the alloy near the magnetic transition point (300-340°) was changed 5° at a time.

The data which characterize the change of the asymmetry index of the K$\alpha_{1,2}$ lines of Mn in the Cu_2MnAl alloy with change of temperature from 300 to 340° are given in Fig. 2. Outside this temperature range the asymmetry index of the K$\alpha_{1,2}$ lines of the elements remains constant. The sample was not heated above 370° in order to avoid breakdown of the β-phase. The changes of shape of the Kα_1 and Kα_2 lines of manganese was analogous. The widths of both lines and the location of their peaks is independent of the change of magnetic state of the alloy. For copper we observed approximately the same change of the asymmetry index of the K$\alpha_{1,2}$ lines on both sides of the Curie point as for manganese. The widths of these lines are also constant.

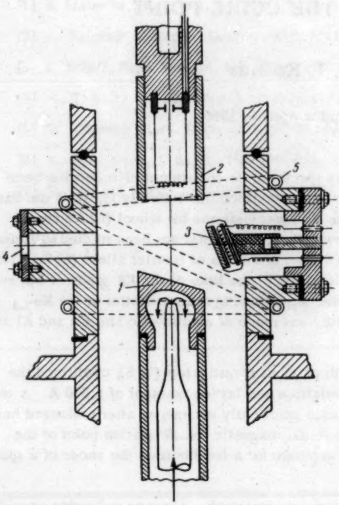

Fig. 1. Sectional view of x-ray fluorescence tube. 1) Anode; 2) heater cathode; 3) secondary anode and sample heater; 4) exit window for rays; 5) water cooling.

The data on the location of the Kβ_1 and Kβ_5 lines of Mn and Cu in the Cu_2MnAl alloy with the change of magnetic state are shown in Table 1. In measuring the wave lengths of these lines, iron and zinc lines were used for comparison.

As can be seen, a change of the magnetic state of the alloy has practically no effect on the location of the Kβ_1 lines of manganese and copper. The shape of these lines also remains unchanged within the limits of experimental accuracy. On the other hand, in the transition from the ferromagnetic to the paramagnetic state of the alloy there is considerable change in the position and shape of the Kβ_5 lines of both components. The peak of the Kβ_5 line of manganese is shifted in the long wave direction by ~ 1.2 ev and the Kβ_5 line of copper is shifted in the short wave direction by ~ 0.9 ev. There is an analogous shift in the short wave edges of these lines. There is also an appreciable change in the shape of the emission bands. In the transition from the ferromagnetic to the paramagnetic state the half width of the Kβ_5 line of manganese is reduced (by 0.8 ev) and for the Kβ_5 line of copper it is increased (by 1.7 ev). At the same time the intensity of the Kβ_5 lines is reduced, by a factor of 1.6 in the case of manganese but relatively little (by the factor 1.1) for copper.

TABLE 1

Lines of the Kβ Group of Mn and Cu for the Heusler Alloy in the Paramagnetic and Ferromagnetic States

Magnetic state	Spectral lines							
	Mn Kβ_1		Cu Kβ_1		Mn Kβ_5		Cu Kβ_5	
	λ, Xu	energy, ev	λ, Xu	energy, ev	λ, Xu	energy, ev	λ, Xu	energy, ev
Ferromagnetic	1906.12	6463.48	1389.42	8867.15	1892.93	6508.52	1378.55	8937.22
Paramagnetic	1906.15	6463.37	1389.38	8867.41	1893.30	6507.30	1378.48	8938.09

The behavior of the manganese Kβ' line in general repeats the behavior of its Kβ_5 band. Thus the alloy transition from the ferromagnetic to the paramagnetic state is accompanied by a shift of the manganese Kβ' peak of ~ 1.8 ev in the long wave direction and by a change of shape (see Fig. 3) whose exact determination involves considerable difficulty because of insufficiently accurate methods of distinguishing this line against the background of the long-wave "tail" of the strong Kβ_1 line of the same element. Under these conditions it may be assumed that the agreement in direction and closeness in value of the Kβ_5 and Kβ' line shifts of the elements is satisfactory fulfillment of predictions based on theoretical concepts [9] concerning the origin of the Kβ' satellite in the x-ray spectrum.

It seems to us that our experimental results leave no doubt regarding the fact that the magnetic state of the alloys considerably affects the x-ray spectra of the elements. Certain of our observations concerning the intensity of the Kβ_5 lines in the ferromagnetic and paramagnetic states are in good qualitative agreement with the theory [4] based on the s-d exchange interaction in ferromagnetics. This indicates that when interpreting data on x-ray

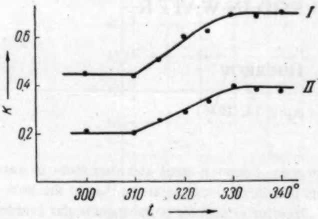

Fig. 2. Asymmetry index k for Kα_1 (I) and Kα_2 (II) lines of manganese in a Cu$_2$MnAl alloy as a function of temperature near the Curie point.

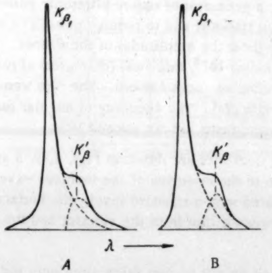

Fig. 3. Kβ_1 and Kβ' lines of manganese in a Heusler alloy in the ferromagnetic (A) and paramagnetic (B) states.

spectra of atoms in ferromagnetic metals and alloys the concepts which are derived from the single-electron zone theory of metals may be unsatisfactory. The change which we observed in certain characteristics of the spectral lines of copper atoms in the Cu$_2$MnAl alloy upon passage through the Curie point provides a clear additional experimental basis for the assumption that the copper atoms in Heusler alloys do not only play a passive role in the formation of an alloy with a lattice which possesses an optimum parameter for the appearance of magnetism in the Mn atoms, but that the electrons of the copper also participate in the ferromagnetism of the alloy as a whole.

In order to obtain a more complete understanding of the nature of ferromagnetic alloys which consist of nonferromagnetic components it would be desirable, however, to broaden the scope of the investigation and to include other Heusler alloys as well as similar alloys, particular Cu-Mn-In and Cu-Mn-Sn alloys.

LITERATURE CITED

[1] E. E. Vainshtein, X-Ray Spectra of Atoms and Molecules in Chemical Compounds and Alloys (Acad. Sci. USSR Press, 1950).

[2] V. A. Kazantsev, Doklady Akad. Nauk SSSR 101, 477 (1955).

[3] E. E. Vainshtein, Doklady Akad. Nauk SSSR 40, 117 (1943).

[4] A. V. Sokolov and S. M. Tsipis, J. Exptl.-Theoret. Phys. (U.S.S.R.) 28, 323, 326 (1955).

[5] S. V. Vonsovskii, Modern Theory of Magnetism (Moscow, 1952).

[6] B. L. Kotliar, X-Ray Spectra of Heusler Alloys, Dissertation, Odessa Univ. (1956).

[7] S. Walentiner and G. Becker, Z. Physik 83, 371 (1933).

[8] O. Heusler, Ann. Physik 19, 155 (1939).

[9] M. A. Blokin, J. Exptl.-Theoret. Phys. (U.S.S.R.) 9, 1315 (1939).

Received March 30, 1956

V. I. Vernadskii Institute of Geochemistry and Analytical Chemistry,
and
K. D. Ushinskii Odessa Pedagogical Institute

SOUND REFLECTION BY A THIN ROD IN WATER

L. M. Liamshev and S. N. Rudakov

(Presented by Academician N. N. Andreev April 14, 1956)

1. A detailed investigation of sound reflection by thin finite* rods of copper, steel and aluminum in water has shown that at certain angles of incidence strong reflection occurs in a direction opposite to that of the incident wave; this is called nonmirror reflection since the reversal of direction occurs for nonperpendicular incidence.

A similar effect was previously observed in the investigation of sound reflection by thin plates and shells [1-2], where it was shown that nonmirror reflection in the case of thin finite plates (or shells) is associated with the generation of flexural and longitudinal waves in the plates (shells), under the action of the incident wave, which are propagated along the plates (shells). It has been suggested that nonmirror reflection in thin finite rods is also caused by flexural and longitudinal waves in the rods. This hypothesis has been tested experimentally.

2. The measurements of nonmirror reflection by rods were carried out with apparatus [3], which consisted of a water-filled 200 x 60 x 60 cm^3 tank with sound-absorbing walls; a generator of square ultrasonic pulses; a quartz vibrator with an x-cut quartz plate (the vibrator was used both to transmit and to receive pulses); a receiving amplifier; and, finally, a pulse oscilloscope which served to register the amplitudes of the echoes. The pulse duration was 30 μ sec, pulse repetition rate 50 per second, duty factor 10^{-3}, thickness (diameter) of rods less than 1 mm**, usual rod length 30 mm and distance of rods from vibrator about 150 cm. The rods were fastened by filaments to a rectangular rotating frame which bore an angle dial. The accuracy of angular readings was not worse than 0.2° and relative error of reflection amplitude measurements did not exceed 10%.

3. Polar diagrams of reflection by a few copper, aluminum and steel rods are shown in Figs. 1, 2, 3 and 4. In accordance with the above they refer to reflection directed opposite to the direction of the incident wave. The vertical axis gives the magnitude of reflection in decibels compared with a standard level; the horizontal axis shows the incident angle of the sound wave, that is, the angle between a line from the vibrator and the perpendicular to the rod axis.

Nonmirror reflection associated with flexural waves was observed for a 0.95 mm thick aluminum rod at 44° (see Fig. 1), for a 0.71 mm thick copper rod at 72° (see Fig. 2) and for a 0.95 mm thick steel rod at 43° (see Fig. 3); for a brass rod of 0.39 mm thickness the velocity of the flexural waves is below the velocity of sound in water and nonmirror reflection associated with flexural waves does not appear (see Fig. 4). Nonmirror reflection associated with longitudinal waves is prominent in all four polar diagrams; for the brass rods at about 24-27° and for the aluminum and steel rods at 18°.

4. We shall now consider the problem of scattering of a plane sound wave by a thin rod immersed in water with consideration of flexural and longitudinal vibrations of the rod. The initial equations are a wave equation describing the propagation of vibrations in an ideal liquid and the equations of motion of the rod for transverse and longitudinal vibrations. It is assumed that the flexural vibrations of the rod obey the well-known 4th order differential equation and that the longitudinal vibrations are described by a wave equation which can be replaced by the equivalent equation for transverse compression waves given by

---

* The thickness of the rods is considerably smaller than the wave length in water and therefore also than the longitudinal wave in the rod.

** All rods used in the experiments were circular.

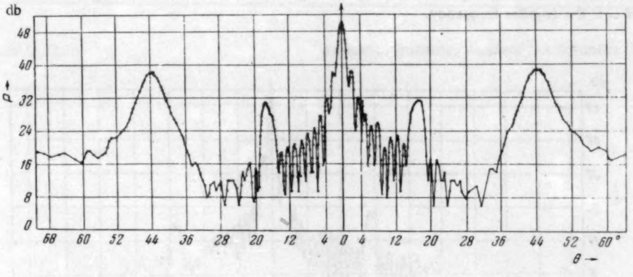

Fig. 1.

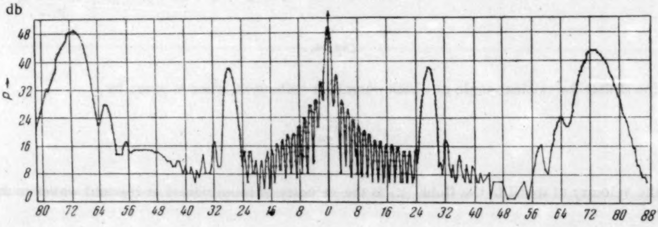

Fig. 2.

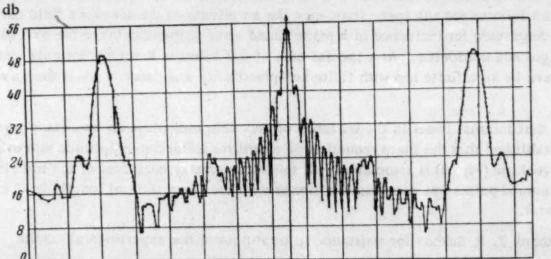

Fig. 3.

$$c_1^2 \frac{\partial^2 v}{\partial x^2} + \omega^2 v = \frac{i\omega^3 a (1-\sigma)}{E} \left[\left(1 - \frac{2\sigma^2}{1-\sigma} \right) p + \frac{c_1^2}{\omega^2} \frac{\partial^2 p}{\partial x^2} \right]_{r=a}, \tag{1}$$

where E is Young's modulus; σ is Poisson's coefficient; $\underline{a}$ is the radius; $\underline{v}$ is the velocity of normal symmetrical displacements of the rod surface; c_1 is the velocity of longitudinal waves in the rod; $\underline{p}$ is the sound pressure in the liquid and ω is the angular frequency.

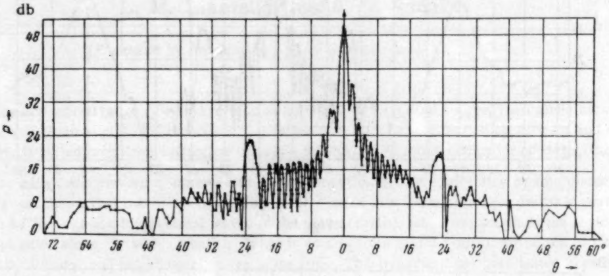

Fig. 4.

It is found that the critical angle at which nonmirror reflection arises is given by

$$\sin\vartheta = \frac{c}{c_x}, \qquad (2)$$

where $\underline{c}$ is the velocity of sound in the fluid; c_x is the velocity of longitudinal or flexural waves in the rod within the fluid.

Nonmirror reflection in finite rods is due to the effect of free longitudinal (or flexural) waves reflected from the ends of the rod.

It is found that when Condition (2) is satisfied space resonance takes place in which the amplitude of the longitudinal or flexural vibrations of the rod, excited by the external sound field, increases sharply. It was shown that in the case of an infinite rod and space resonance the amplitude of the scattered field can be very much greater than the scattering amplitude for incidence of a plane sound wave perpendicular to the axis of a rod which is considered perfectly rigid and motionless. As a special case of this solution Raleigh's formula was found for scattering of a plane sound wave by an infinite rod with finite compressibility and density, when the wave falls perpendicular to the rod axis.

It was shown that internal losses in the material of very thin rods plays an important part in the scattering of sound. It was established that the sharp reduction of nonmirror reflection amplitude due to longitudinal waves in the case of the steel rod (Fig. 3) is associated with the nonstationary character of the rod vibrations, since the duration of the ultrasound pulses was considerably shorter than the setup time of longitudinal vibrations in the steel rod immersed in water.

The authors thank Z. P. Sukhov for assistance in treatment of the experimental results.

LITERATURE CITED

[1] W. Finney, J. Acoust. Soc. Amer. 20, 5, 625 (1948).

[2] L. M. Liamshev, Doklady Akad. Nauk SSSR 99, 5, 719 (1954).

[3] L. M. Liamshev, The Reflection of Sound by Thin Plates and Shells in a Liquid (Acad. Sci. USSR Press, Moscow, 1955).

Received March 16, 1956

Acoustics Institute, Academy of Sciences USSR

DIAMAGNETIC RESONANCE IN STRONGLY MAGNETIC BODIES

Ia. G. Dorfman

(Presented by Academician A. F. Ioffe April 19, 1956)

Recent investigations have confirmed the hypothesis [1] that diamagnetic resonance* is a powerful means of studying electronic conductors [2-6]. However, thus far only weakly magnetic materials have been investigated both theoretically and experimentally. We therefore considered it of interest to determine what characteristics of diamagnetic resonance can be expected in strongly magnetic bodies.

It is known that magneto-optical and galvanomagnetic phenomena in strongly magnetic bodies are due to spin-orbit interaction, which is equivalent to the action on the conduction electrons (or holes) of a certain effective magnetic field H_i that is proportional to the spontaneous magnetization [7, 8].

The presence of the field H_i should be manifested on the diamagnetism of conduction electrons (or holes). However, this effect is practically nonexistent and can hardly be observed. In addition, we should expect diamagnetic resonance when a sample is acted on by electromagnetic radiation of frequency ν_0 given by

$$\nu_0 = \frac{eH_i}{2\pi m^* c},$$

where m^* is the effective mass of the current carriers (electrons or holes).

Since H_i in each individual domain is determined by the magnitude of spontaneous magnetization, ν_0 (for not too strong external fields H) should be independent of the macroscopic (technological) magnetization I of the body. The diamagnetic resonance frequency ν_0 in these materials should decrease with rising temperature as the spontaneous magnetization decreases. At temperatures considerably below the Curie point diamagnetic resonance should be observed here (for $H_i \cong 10^6$ oerst) in the optical frequency region $10^{12}-10^{13}$. As the Curie point is approached we must expect a shift of the resonance peak in the long wave direction and its transition (above the Curie point) to the radio frequency region. The external field H and the macroscopic magnetization I will determine only the polarization of the absorbed waves and the sharpness of the resonance peak. Resonance absorption in the $10^{12}-10^{13}$ region can evidently be observed at ordinary temperatures if the time between collisions of current carriers is $\tau \geq 1/\nu_0$.

The foregoing considerations can be applied both to ferromagnetic substances and to substances possessing uncompensated antiferromagnetism. They clearly apply, first of all, to strongly magnetic semiconductors (ferrites, manganites, etc.) with small numbers of current carriers. It is possible that the investigation of magneto-optical or galvanomagnetic phenomena and of diamagnetic resonance in the same sample would enable us to determine both H_i and m^* in strongly magnetic bodies. We should expect anisotropy of these quantities in crystals.

We do not here consider the characteristics of diamagnetic resonance which are associated with the technological magnetization curve and with the possible presence of a large number of current carriers.

---

* Diamagnetic resonance is often called "cyclotron resonance" in the American literature. In our opinion this expression cannot serve as the scientific name.

LITERATURE CITED

[1] Ia. G. Dorfman, Doklady Akad. Nauk SSSR 81, 765 (1951).

[2] G. Dresselhaus, A. F. Kip and C. Kittel, Phys. Rev. 92, 827 (1953).

[3] B. Lax, H. J. Zeiger, C. Dexter and E. S. Rosenblum, Phys. Rev. 93, 1418 (1954).

[4] R. N. Dexter, H. J. Zeiger and B. Lax, Phys. Rev. 95, 557 (1954).

[5] G. Dresselhaus, A. F. Kip and C. Kittel, Phys. Rev. 98, 368 (1955).

[6] J. K. Gait, W. A. Vager, F. R. Merritt, B. B. Cetling and H. W. Dail, Phys. Rev. 100, 748 (1955).

[7] A. G. Samoilovich and V. L. Kon'kov, J. Exptl.-Theoret. Phys. (U.S.S.R.) 20, 783 (1950).

[8] S. V. Vonsovskii, Modern Theory of Magnetism, III, §17, 1952.

Received April 12, 1956

INFRARED ASYMPTOTIC FORM OF THE GREEN'S FUNCTION FOR ELECTRONS TO ORDER e^4

L. D. Solov'ev

(Presented by Academician N. N. Bogoliubov April 20, 1956)

1. An approximate formula for the infrared asymptotic form of the Green's function for electrons can be obtained by various methods. Among these only the renormalization group method [1] permits an easy evaluation of the degree of the approximation and the obtaining of the following approximations. In this note the renormalization group is used to calculate the infrared asymptotic Green's function for an electron up to the order e^4.

For Green's functions corresponding to an electromagnetic potential of arbitrary gauge:

$$A_\mu = \mathfrak{A}_\mu + \omega \frac{\partial f}{\partial x^\mu}, \tag{1}$$

where $\langle T(\mathfrak{A}_\mu, \mathfrak{A}_\nu)\rangle_0$ is transverse and ω = const, the renormalization group equations are [2]:

$$\begin{gathered} G_2(e_2^2, \omega_2^2) = z^{-1} G_1(e_1^2, \omega_1^2); \quad \mathcal{D}_2(e_2^2, \omega_2^2) = z_3^{-1} \mathcal{D}_1(e_1^2, \omega_1^2); \\ e_2^2 = z_3 e_1^2; \quad \omega_2^2 = z_3^{-1}\omega_1^2. \quad \Gamma_2(e_2^2, \omega_2^2) = z\Gamma_1(e_1^2, \omega_1^2); \end{gathered} \tag{2}$$

2. Representing the G functions and $\mathcal{D}$ in the form

$$G(p, e^2, \omega^2) = i\,\frac{\hat{p}a(p^2, e^2, \omega^2) + mb(p^2, e^2, \omega^2)}{p^2 - m^2}, \tag{3}$$

$$\mathcal{D}_{mn}(p, e^2, \omega^2) = \frac{1}{ip^2}\left(g_{mn} - \frac{p_m p_n}{p^2}\right) d(p^2, e^2) + \frac{1}{ip^2}\,\frac{p_m p_n}{p^2}\,\omega^2 d_l(p). \tag{4}$$

by using (2) we obtain for the infrared asymptotic forms of the functions a̲ and b̲ (denoted by the same symbol s̲) the following equation [1]:

$$\ln\frac{s(x, 1, e'^2, \omega'^2)}{s(x_0, 1, e'^2, \omega'^2)} = \int_{x_0}^{x} \frac{dz}{z-1}\left[\frac{\partial}{\partial \xi}\ln S(\xi, 1-z, e'^2 d(z, 1, e'^2), \omega'^2 d^{-1})\right]_{\xi=1}, \tag{5}$$

where

$$s(x, y, e'^2, \omega'^2) = s\left(\frac{p^2}{\lambda^2}, \frac{m^2}{\lambda^2}, e'^2, \omega'^2\right) = S\left(\frac{m^2 - p^2}{m^2 - \lambda^2}, \frac{m^2 - \lambda^2}{m^2}, e'^2, \omega'^2\right);$$

$$a(1, y, e'^2, \omega'^2) = A(1, u, e'^2, \omega'^2) = a_0; \; d(1, y, e'^2) = 1;$$

$e'^2 = e^2 d\left(\frac{\lambda^2}{m^2}, e^2\right);\quad \omega'^2 = \omega^2 d^{-1}\left(\frac{\lambda^2}{m^2}, e^2\right);$ $\underline{e}$ is the experimentally observed charge.

For $\xi \to 0$ ($m^2-p^2 \to 0$) a perturbation theory series for the function S on the right-hand side of (5) would have no meaning. Measuring $m^2-p^2 \to 0$ in the units $m^2-\lambda^2 \to 0$ we do not leave the region $\xi \sim 1$ in which successive terms of this series decrease rapidly. Therefore (5) reduced the problem of obtaining the asymptotic form of $\underline{s}$ to the usual perturbation calculation of the asymptotic form of S. It is then evident that the asymptotic form of $\underline{s}$ contains a contribution from only the zeroth term of the series expansion of $d(z, 1, e'^2)$ in terms of $z-1$; this equals 1.

The calculation is continued for $d_l(p) = d_l$ = const. Turning in (5) to the experimental charge e^2 and $\omega^2 = 1$, which in the calculation of S requires the use of the function $d(p^2/m^2, e^2)$ normalized to $p^2 = 0$, and denoting the corresponding functions by $s(x, 1, e^2, d_l)$, we obtain instead of (5):

$$\ln\frac{s(x, 1, e^2, d_l)}{s(x_0, 1, e^2, d_l)} = \int_{y_0}^{x}\frac{dz}{z-1}\left[\frac{\partial}{\partial\xi}\ln S(\xi, 1-z, e^2, d_l)\right]_{\xi=1}. \tag{6}$$

3. We shall calculate the asymptotic form of the function $S(\xi, u, e^2, d_l) = s$ by perturbation theory with accuracy up to the order e^4. Comparing (3) with

$$G(p) = i\,\frac{\hat{p}+m}{p^2-m^2}\left(1+\frac{\Sigma}{\hat{p}-m}\right), \tag{7}$$

where $\Sigma(\hat{p}) = (p-m)\,[\hat{p}F_1(p^2) + mF_2(p^2)]$ is the sum of all electron self energy diagrams normalized to the experimental mass $\underline{m}$, we obtain for $p^2 = m^2$:

$$a = b = s = 1 + mF_1 + mF_2 = 1 + \left.\frac{\Sigma}{\hat{p}-m}\right|_{\hat{p}=m}. \tag{8}$$

With accuracy up to the order e^4

$$\Sigma = \Sigma^{(2)} + \Sigma^{(2)}\frac{1}{\hat{p}-m}\Sigma^{(2)} + \Sigma_1^{(4)} + \Sigma_2^{(4)} + \Sigma_3^{(4)} \tag{9}$$

or, graphically:

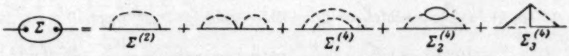

We shall proceed with the calculation as follows. An exact expression can easily be obtained for $\Sigma^{(2)}$. We shall use this as well as the 2nd order polarization (Π) and vertex (Γ) operators for the calculation of $\Sigma^{(4)}$. It is necessary to consider only those terms in $\Sigma^{(4)}(\hat{p})$ whose derivative with respect to $\hat{p}$ with $p^2 = m^2$ can be expressed by an integral over $\underline{k}$ which diverges for $k \to 0$. Only these terms make a logarithmic contribution to the asymptotic form of $\underline{a}$ and $\underline{b}$ in (8).

In order to determine the convergence of the integrals it is sufficient to compute the power of $\underline{k}$ in the numerator and denominator of the integrand, neglecting k^2 compared with pk.

Eq. (6) does not depend on the normalization factor of $\underline{s}$. Therefore the calculational procedure for Σ must correspond to normalization to the experimental mass $\underline{m}$: $\Sigma\big|_{\hat{p}=m} = 0$, but $\frac{\partial \Sigma}{\partial \hat{p}}\big|_{\hat{p}=m}$ may be undetermined (with Γ normalized in accordance with Ward's identity).

4. Using the α representation for coupling [3] we easily obtain for $\Sigma^{(2)}(p)$:

$$\Sigma^{(2)}(\hat{p}) = \frac{e^2}{16\pi^2}\left\{\frac{-\delta}{p^2}\left[d_l\frac{p^2+m^2}{p^2}\hat{p} - (d_l+3)\,m\right]\ln\frac{\delta}{m^2} + d_l\frac{-\delta}{p^2}\hat{p} + c(\hat{p}-m)\right\}. \tag{10}$$

Here and in the following $\delta = m^2 - p^2, |\delta| \ll m^2$.

Inserting $\Sigma^{(2)}(\hat{p}+\hat{k})$ in the integral over $\underline{k}$ for $\Sigma_1^{(4)}$ and dropping all terms which make a finite contribution to $\frac{\partial \Sigma_1^{(4)}}{\partial \hat{p}}\Big|_{p^2=m^2}$, we obtain two integrals, one of which can be calculated in elementary fashion, while the calculation of the other is essentially simplified if we replace the term $\ln\frac{k^2+2pk-\delta}{-m^2}$ by $\ln\frac{k^2+2pk-\delta}{k^2+2pk-\delta-m^2}$ and use for the logarithm the following α representation:

$$\ln\frac{X}{Y} = \int\limits_0^\infty \frac{d\alpha}{\alpha}e^{-\varepsilon\alpha}\left(e^{i\alpha Y} - e^{i\alpha X}\right), \quad \varepsilon \to +0. \tag{11}$$

Finally, for $\delta \to 0$ we obtain

$$\Sigma_1^{(4)} = (\hat{p}-m)\left(\frac{e^2}{4\pi}\right)^2\left[\frac{(3-d_l)^2}{8\pi^2}\ln^2\frac{\delta}{m^2} - \frac{(3-d_l)(6+c)}{8\pi^2}\ln\frac{\delta}{m^2} + c^{(1)}\right]. \tag{12}$$

The diagram of $\Sigma_2^{(4)}$ with normalization to the experimental charge in (6) makes only a finite contribution to the infrared asymptotic form of S, since the integral for $\Sigma_2^{(4)}$ contains in the integrand the polarization operator $\Pi(k, e^2)$, which for small $\underline{k}$ is of the order of k^4.

5. We shall finally consider the overlapping diagram of $\Sigma_3^{(4)}(p)$. This corresponds to an integral over $\underline{k}$ containing the vertex part $\Gamma^n(p, k)$.

Unlike $\Sigma^{(2)}$, $\Gamma^n(p, k)$ can only be expressed in terms of single integrals. But it is easily shown that with accuracy up to terms which make a finite contribution to $\frac{\partial \Sigma_3^{(4)}}{\partial \hat{p}}\Big|_{p^2=m^2}$:

$$\begin{aligned}\Gamma^n(p,k) = \frac{e^2}{16\pi^2}\Big\{&-2d_l\frac{p^n}{m} - c\gamma^n + 2(3-d_l)\frac{p^n}{m}\frac{k^2+2pk-\delta}{k^2+2pk}\ln\frac{k^2+2pk-\delta}{-m^2} + \\ &+\frac{1}{k^2+2pk}\left[2(3-d_l)\frac{p^n}{m} + \frac{1+d_l}{2m^2}\gamma^\sigma(\hat{p}+m)\gamma^n\hat{k}\gamma_\sigma - \frac{2(d_l-1)}{m^2}\gamma^n\hat{k}\hat{p}\right]\delta\ln\frac{\delta}{m^2}\Big\},\end{aligned} \tag{13}$$

whence for $\Sigma_3^{(4)}$ with $\delta \to 0$ we obtain

$$\Sigma_3^{(4)} = (\hat{p}-m)\left(\frac{e^2}{4\pi}\right)^2\left[-\frac{(3-d_l)^2}{4\pi^2}\ln^2\frac{\delta}{m^2} + \frac{(3-d_l)(3+c+d_l)}{4\pi^2}\ln\frac{\delta}{m^2} + c^{(3)}\right]. \tag{14}$$

6. From (8), (9), (10), (12) and (14), inserting $\frac{m^2-p^2}{m^2} = \xi u$, we finally obtain:

$$\begin{aligned} S(\xi, u, e^2, d_l) = s = \Big\{1 - \frac{e^2}{4\pi}\Big[\frac{3-d_l}{2\pi}\ln u - \frac{2d_l + c}{4\pi}\Big] + \\ + \left(\frac{e^2}{4\pi}\right)^2\Big[\frac{(3-d_l)^2}{8\pi^2}\ln^2 u - \frac{(3-d_l)(4d_l+c)}{8\pi^2}\ln u + c_1\Big] + \ldots\Big\} \times \\ \times \Big\{1 - \frac{e^2}{4\pi}\frac{3-d_l}{2\pi}\ln\xi + \left(\frac{e^2}{4\pi}\right)^2\frac{(3-d_l)^2}{8\pi^2}\ln^2\xi - \left(\frac{e^2}{4\pi}\right)^2 0 \ln\xi + \ldots\Big\}. \end{aligned} \quad (15)$$

For any $u \neq 0$ the arbitrary constants $\underline{c}$, $c_1, \ldots$, can be selected in such a way that the first bracket, which represents $S(1, \underline{u}, e^2, d_l)$, becomes a_0. The dots in the second bracket indicate unimportant terms of the form $u(\xi - 1) \times [e^2 f_1(\xi, u) + e^4 f_2(\xi, u)]$ and all higher terms in $\underline{e}$.

Substituting

$$\left[\frac{\partial}{\partial\xi}\ln S(\xi, 1-z, e^2, d_l)\right]_{\xi=1} = -\frac{e^2}{4\pi}\frac{3-d_l}{2\pi} - \ldots = -\alpha(e^2) \quad (16)$$

in (6), we obtain the asymptotic Green's function for an electron:

$$G(p) = i\,\frac{\hat{p} + m}{p^2 - m^2}\left(1 - \frac{p^2}{m^2}\right)^{-\alpha(e^2)}, \quad (17)$$

where with accuracy up to the order e^4

$$\alpha(e^2) = \frac{e^2}{2\pi}\frac{3-d_l}{4\pi} + \ldots; \quad \frac{e^2}{4\pi} = \frac{1}{137}.$$

Thus there is no term of the order e^4 in $\alpha(e^2)$ and the previously obtained formula for α is correct to the order e^4.

The function S on the right-hand side of (6) is represented through perturbation theory in a series which contains a logarithm to the 1st, 2nd, etc., powers. From (6) it follows at once that $\alpha(e^2)$ is a series in e^2 constituted by the coefficients of the logarithm in the first power. The coefficients of the higher logarithms from

$\left[\frac{\partial}{\partial\xi}\ln S(\xi, u, e^2, d_l)\right]_{\xi=1}$ drop out. Consequently, all are given in terms of $\alpha(e^2)$.

Expanding $\left(1 - \frac{p^2}{m^2}\right)^{-\alpha} = (u\xi)^{-\alpha} = u^{-\alpha}e^{-\alpha\ln\xi}$ in a series with respect to $\alpha\ln\xi$, we obtain $u^{-\alpha}(1 - \alpha(e^2)\ln\xi + \frac{1}{2}\alpha^2(e^2)\ln^2\xi - \ldots)$, whence, in particular, it follows that the fourth-order coefficient of $\ln^2\xi$ must be $\frac{1}{2}\alpha_1^2$, hwere α_1 is the first term in $\alpha(e^2)$. This is also what occurs in (15), which was calculated directly from perturbation theory.

In conclusion I wish to express my deep appreciation to D. V. Shirkov for his direction of this work.

LITERATURE CITED

[1] N. N. Bogoliubov and D. V. Shirkov, Doklady Akad. Nauk SSSR 103, 203, 391 (1955).

[2] A. A. Logunov, J. Exptl.-Theoret. Phys. (U.S.S.R.) 30, 4, 793 (1956) [Soviet Physics – J.E.T.P., p. 766].

[3] N. N. Bogoluibov and D. V. Shirkov, Progr. Phys. Sci. (U.S.S.R.) 55, 149; 57, 3 (1955).

Received April 18, 1956

M. V. Lomonosov Moscow State University

ON A MACROSCOPIC THEORY OF SUPERCONDUCTIVITY FOR ALL TEMPERATURES

V. L. Ginzburg, Corresponding Member of the Academy of Sciences USSR

The macroscopic theory of superconductivity developed by Ginzburg and Landau [1] is based on the equations

$$\frac{1}{2m}\left(-i\hbar\nabla-\frac{e}{c}\mathbf{A}\right)^2\Psi+\frac{\partial F_{s0}}{\partial\Psi^*}=0, \tag{1}$$

$$\Delta\mathbf{A}=-\frac{4\pi}{c}\mathbf{j}_s,\ \ \operatorname{div}\mathbf{A}=0,\ \ \mathbf{j}_s=-\frac{ie\hbar}{2m}(\Psi^*\nabla\Psi-\Psi\nabla\Psi^*)-\frac{e^2}{mc}\Psi^*\Psi\mathbf{A}, \tag{2}$$

where $|\psi|^2$ is the concentration of "superconducting electrons", $\vec{A}$ is the vector potential and $F_{s0}(|\psi|^2)$ is the free energy density in the superconducting state in the absence of a field.

The form of the function $F_{s0}(|\psi|^2)$ is not known in general, but for small values of $|\psi|^2$ it can be assumed that

$$F_{s0}=F_{n0}(T)+\alpha(T)\,|\,\Psi\,|^2+\frac{\beta(T)}{2}\,|\,\Psi\,|^4, \tag{3}$$

where F_{n0} is the free energy density in the normal state and close to the critical temperature T_k:

$$\alpha(T)=\left(\frac{d\alpha}{dT}\right)_k(T-T_k),\quad \beta=\beta_k=\beta(T_k). \tag{4}$$

In [1] and a number of other articles referred to in [2] only (3) was used, which is clearly correct near T_k since at T_k we have $\psi=0$.

However, we have the problem of generalizing the theory of [1] to cover all temperatures in the range $0\le T\le T_k$. For this purpose Bardeen [3] used the expression

$$F_{s0}^{(\delta)}=F_{n0}(t)+\frac{H_0^2}{8\pi}\{2t^2(1-\sqrt{1-|\chi|^2})-|\chi|^2\}, \tag{5}$$

where $t=\frac{T}{T_k}$; H_0 is the critical magnetic field for T = 0; $\chi=\psi/\psi_p(0)$ and $\psi_p(t)$ is the equilibrium value of ψ in the absence of a field (at temperature t) that is obtained from the condition $\frac{\partial F_{s0}}{\partial\psi^*}=0$. According to (5) we have*:

---

* The general expressions of (6) for δ_0 and H_{KM} in [6] follow from the definitions of these quantities [1] and thus from (5) there follow specifically only the expressions in (6) which contain t explicitly.

$$\delta_0^2 = \frac{mc^2}{4\pi e^2 \mid \Psi_p(t) \mid^2} = \frac{mc^2}{4\pi e^2 \mid \Psi_p(0) \mid^2 \mid \chi_p(t) \mid^2} = \frac{\delta_{00}^2}{\mid \chi_p(t) \mid^2} = \frac{\delta_{00}^2}{1-t^4}, \tag{6}$$

$$H_{\text{KM}}^2 = 8\pi \{F_{n0}(t) - F_{s0}(\mid \chi_p \mid^2)\} = H_0^2 (1-t^2)^2,$$

where δ_0 is the depth of penetration of a weak magnetic field, H_{KM} is the critical magnetic field and, obviously, $\chi_p = \psi_p(t)/\psi_p(0)$.

On the other hand, as was indicated in [2] and [4], we can arrive at (6), as a first approximation to experiment, from (3) by assuming

$$\alpha = -\frac{H_0^2}{4\pi \mid \Psi_p(0) \mid^2} \frac{1-t^2}{1+t^2}, \quad \beta = \frac{H_0^2}{4\pi \mid \Psi_p(0) \mid^4} \frac{1}{(1+t^2)^2}. \tag{7}$$

Then (3) becomes:

$$F_{s0}^{(a)} = F_{n0}(t) + \frac{H_0^2}{8\pi} \left\{ 2 \frac{t^2-1}{1+t^2} \mid \chi \mid^2 + \frac{1}{(1+t^2)^2} \mid \chi \mid^4 \right\}. \tag{8}$$

The agreement of $H_{KM}(t)$ and $\delta_0(t)$ as obtained from (5) and (8) is certainly no guarantee that the two variants of the theory are equivalent, and we can in principle choose between them on the basis of experimental information [4] concerning, of course, some quantities other than H_{KM} and δ_0. However, although variant (8) seems to us for certain reasons [4] preferable to (5) it is impossible to reach any reliable conclusions regarding the function $F_{s0}(t, |\chi|^2)$ from general considerations, and in this sense (5) and (8) are not the only possibilities. Therefore the most correct procedure would not give in advance the dependence of F_{s0} on $|\chi|^2$ and would determine it from experiment. The present article deals with the possibilities which arise in this connection.*

We assume

$$F_{s0}(t, \mid \chi \mid^2) = F_{n0}(t) + \frac{H_0^2}{8\pi} f(t, \mid \chi \mid^2). \tag{9}$$

Then, clearly, $f(t, |\chi_p|^2) = -\frac{H_{KM}^2(t)}{H_0^2}$ and $f(t, 0) = 0$, where the value of χ_p corresponding to thermodynamic equilibrium is obtained from the condition $\frac{\partial f}{\partial \chi} = 0$. The magnitude of $|\chi_p|^2$ is determined experimentally from the measured depth δ_0 [see (6)] and thus two points on the curve of $f(t, |\chi|^2)$ can be regarded as known for all t for which the values of H_{KM} and δ_0 are measured.

Just as was done in [1] we shall confine ourselves below to the one-dimensional case in which the vectors $\vec{A}$ and $\vec{j}_s$ are taken along the x axis, the field $\vec{H}$ along the y axis and $\nabla\psi$ along the z axis. The function ψ and thus also χ can be regarded as real and the set of equations equivalent to (1) becomes

$$\frac{d^2\chi}{d\xi^2} = \varkappa_0^2 \left\{ \frac{1}{4} \frac{\partial f(t, \chi^2)}{\partial \chi} + a^2\chi \right\}, \quad \frac{d^2 a}{d\xi^2} = \chi^2 a, \tag{10}$$

---

* Generally speaking, it can also be assumed in (1 - 2) that $m = m(|\chi|^2)$. We shall not consider this possibility here.

where the following notation is used:

$$\xi = \frac{z}{\delta_{00}},\ a = \frac{A}{\sqrt{2}H_0\delta_{00}},\quad \varkappa_0^2 = \frac{2e^2}{\hbar^2c^2}H_0^2\delta_{00}^4,\quad \delta_{00}^2 = \frac{mc^2}{4\pi e^2\Psi_p^2(0)},$$

$$\chi = \Psi / \Psi_p(0),\ H = dA/dz = \sqrt{2}H_0\,da/d\xi = \sqrt{2}H_0 h. \tag{11}$$

In the presence of an external field H_B the function $\chi(\xi)$ decreases near the boundary between the superconductor and the vacuum, and at the boundary

$$\chi(0) = \chi_p + \varphi(0) = \chi_p\left\{1 - \frac{\varkappa_0\left(\frac{H_{KM}}{H_0\chi_p}\right)^2\left(\frac{H_B}{H_{KM}}\right)^2}{8\chi_p^2\eta(1+\varkappa_0\eta)}\right\},\qquad \eta = \frac{1}{4\chi_p}\left(\frac{\partial^2 f}{\partial\chi^2}\right)^{1/2}_{\chi_p}. \tag{12}$$

This expression was obtained by the perturbation method already used in [1], which is applicable when $|\varphi| \ll \chi_p$. Under these conditions the depth of penetration into the superconductor by an additional weak field depends on H_B and is given by δ_1, where

$$\frac{\delta_1 - \delta_0}{\delta_0} = \frac{3\varkappa_0(2+\varkappa_0\eta)}{16\chi_p^2\eta(1+\varkappa_0\eta)^2}\left(\frac{H_{KM}}{H_0\chi_p}\right)^2\left(\frac{H_B}{H_{KM}}\right)^2. \tag{13}$$

In cases a) and b) [see (8) and (5)] we have:

$$\eta^{(a)} = [\sqrt{2}(1+t^2)]^{-1},\ \eta^{(b)} = [2\sqrt{2}t^2]^{-1},$$

and for t → 0 we obtain entirely different results. Thus, in case a) for all t and $\kappa_0 \ll 1$ we have $\frac{\delta_1-\delta_0}{\delta_0} = \frac{3\varkappa_0}{4\sqrt{2}(1+t^2)}\left(\frac{H_B}{H_{KM}}\right)^2$, whereas in case b) for $t \ll 1$ we have $\frac{\delta_1-\delta_0}{\delta_0} = \frac{3}{2}t^4\left(\frac{H_B}{H_{KM}}\right)^2$.

The surface energy on the interface between the superconducting and normal phases expressed in the variables (11) is $\left(h_{KM} = \frac{H_{KM}}{\sqrt{2}H_0}\right)$:

$$\sigma_{ns} = \frac{H_0^2}{2\pi}\delta_{00}\int_{-\infty}^{+\infty}\left\{\frac{1}{\varkappa_0^2}\left(\frac{d\chi}{d\xi}\right)^2 + h^2 - hh_{KM}\right\}d\xi =$$

$$= \frac{H_0^2}{2\pi}\delta_{00}\int_{-\infty}^{+\infty}\left\{\frac{f(\chi^2)}{2} + \chi^2a^2 + h_{KM}^2 - hh_{KM}\right\}d\xi. \tag{14}$$

Since σ_{ns} is given in integral form it naturally depends slightly on the form of $f(\chi^2)$; in particular, the difference between variants (8) and (5) with respect to σ_{ns} is less than 20% (regarding cases in which $\kappa_0 \ll 1$; see [3, 4]).

In order to determine $f(\chi^2)$ from experimental data it is best, at least in principle, to use small samples. Very thin samples enable us to neglect the dependence of χ on the coordinates, so that all calculations are very much simplified [5]. Proceeding in this manner, in the case of films of thickness 2d in a field H_B for the equilibrium value of χ_0 we obtain (for $H_B = 0$ we, of course, have $\chi_0 = \chi_p$)*

$$\left(\frac{H_B}{H_0}\right)^2 = \frac{\frac{\partial f(\chi_0^2)}{\partial \chi_0}\,\chi_0\,\mathrm{ch}^2\left(\chi_0 \frac{a}{\delta_{00}}\right)}{1 - \frac{\delta_{00}}{2\chi_0 d}\,\mathrm{sh}\,\frac{2\chi_0 d}{\delta_{00}}} \tag{15}$$

χ_0 can be determined from the magnetic moment of the film, which is

$$\mu = -\frac{H_B d}{2\pi}\left(1 - \frac{\delta_{00}}{\chi_0 d}\,\mathrm{th}\,\frac{\chi_0 d}{\delta_{00}}\right), \tag{16}$$

where the moment is given per unit area [5]. Knowing $\chi_0(H_B)$, $\underline{d}$, δ_{00}, we from (15) now obtain $\frac{\partial f(\chi_0^2)}{\partial \chi_0}$. For the critical field H_K of the film we obtain

$$\left(\frac{H_K}{H_0}\right)^2 = -\frac{f(\chi_0^2)}{1 - \frac{\delta_{00}}{\chi_0 d}\,\mathrm{th}\,\frac{\chi_0 d}{\delta_{00}}}. \tag{17}$$

Having determined H_K for the films, for which a transition of the first kind occurs [5], and having measured the corresponding value of χ_0 at the transition point from the film moment, from (17) we now obtain $f(\chi_0^2)$. If $f(\chi_0^2)$ is given and we wish to check the theory, instead of measuring the moment we can for the determination of χ_0 in (17) use (15) with $H_B = H_K$.

In practice the measurement of the film moment is difficult and it may be more convenient to measure the moments of small spheres or cylinders. In this case we can also obtain formulas analogous to (15 - 17) by a suitable generalization of the results in [6] for the special case of Eqs. (3 - 4), which was investigated in [1]. Thus in order to make a transition to expressions analogous to (15), on the left-hand side of (8), (16) and (21) of reference [6] it is necessary to replace $\psi_0^2(1-\psi_0^2)$ by $-\frac{1}{4}\left(\frac{H_0}{H_{KM}}\right)^2 \frac{\partial f(\chi_0^2)}{\partial \chi_0}\,\chi_0$, and on the right-hand side of the same equations to replace $\psi_0 r_0$ by $\chi_0 \frac{r_0}{\delta_{00}}$, where r_0 is the radius of the cylinder or sphere in ordinary units.

We thus see that experiment offers certain possibilities of obtaining $f(\chi^2)$ and, in particular, of deciding whether (5) or (8) is closer to reality.

The author is indebted to Academician L. D. Landau and B. M. Bolotovskii for discussion and comments.

Note added in proof: The author has been informed by Professor D. Shenberg that unpublished work by Whitehead, which is also mentioned in [7], contains experimental information that favors the correctness of (8).

LITERATURE CITED

[1] V. L. Ginzburg and L. D. Landau, J. Exptl.-Theoret. Phys. (U.S.S.R.) 20, 1064 (1950).

[2] V. L. Ginzburg, J. Exptl.-Theoret. Phys. (U.S.S.R.) 29, 748 (1955).

[3] J. Bardeen, Phys. Rev. 94, 554 (1954).

[4] V. L. Ginzburg, J. Exptl.-Theoret. Phys. (U.S.S.R.) 30, 593 (1956) [Soviet Physics – J.E.T.P., p. 621].

[5] V. L. Ginzburg, Doklady Akad. Nauk SSSR 83, 3, 385 (1952).

---

* [In this article, 'sh' ≡ 'sinh', 'ch' ≡ 'cosh', 'th' ≡ 'tanh' – editor's note].

[6] V. P. Silin, J. Exptl.-Theoret. Phys. (U.S.S.R.) 21, 1330 (1951).

[7] A. B. Pippard, Phil. Trans. Roy. Soc. 248, 97 (1955).

Received April 25, 1956

P. N. Lebedev Physics Institute, Academy of Sciences USSR

EXCHANGE INTERACTION IN SOME PARAMAGNETICS

S. -Kh. G. Kashaev

(Presented by P. L. Kapitsa April 27, 1956)

S. A. Al'tshuler, E. K. Zavoiskii and B. M. Kozyrev [1, 2] have shown that magnetic dipole interactions between particles of a paramagnetic substance must induce broadening of paramagnetic resonance lines. It follows that magnetic dilution of a paramagnetic must result in reduced half widths.

In a number of instances disagreement is found between the theoretical half widths which are to be expected on the basis of magnetic dipole interactions alone and the experimental values, which these authors have explained as a possible effect on line width resulting from exchange interaction and electrical fields in the crystal lattice.

Van Vleck [3] later showed theoretically that exchange interaction should narrow the centers of absorption lines and broaden the wings. He supported his deductions by comparison with the experimental data of E. K. Zavoiskii,et al.

It is clear from the above that by comparing experimental half widths with theoretical predictions based only on magnetic interaction and by studying the dependence of the experimental half width on the concentration of magnetic ions it is possible to arrive at a decision regarding exchange interactions in a particular paramagnetic; such is the purpose of the present work. A change in the concentration of magnetic ions while preserving the parameters of the lattice was possible through the preparation of several solid solutions of a paramagnetic salt in a suitable diamagnetic.

The principal investigations of the author were carried through by the grid current method of E. K. Zavoiskii [4] at a frequency of 2.00×10^8 cycles.

The apparatus enables us to obtain absorption lines whose half widths in the same material did not differ by more ± 5%. We took this figure as the error in determining the half widths of the curves.

Measurements were made on crystalline powders of two systems of solid solutions: MnS, ZnS and $Mn(NH_4)_2(SO_4)_2 \cdot 6H_2O$, $Zn(NH_4)_2(SO_4)_2 \cdot 6H_2O$, which contain the same paramagnetic ion Mn^{++} but which differ with regard to their lattices. In manganous sulfide the Mn^{++} ions form a face-centered cubic lattice but the lattice of $Mn(NH_4)_2(SO_4)_2 \cdot 6H_2O$ is monoclinic. The latter is characterized by the presence of two Mn^{++} ions per unit cell.

It was the purpose of our measurements to show in what way the difference in the lattice influences the experimental dependence of the half width on the magnetic ion concentration and how the character of the variation of exchange interaction is affected. It was also of interest to determine at what average distances between the paramagnetic ions in both cases investigated there is a limit for the observable influence of the exchange interaction on line shape.

The dependence of the experimental half width δ on the relative concentration $\underline{f}$ of magnetic ions for the indicated systems of solid solutions is shown in Fig. 1. Curve I refers to the system of solid solutions of MnS, ZnS; Curve II refers to $Mn(NH_4)_2(SO_4)_2 \cdot 6H_2O$, $Zn(NH_4)_2(SO_4) \cdot 6H_2O$. Here f = 1 corresponds to undiluted MnS and $Mn(NH_4)_2(SO_4)_2 \cdot 6H_2O$. Similar curves were obtained in further investigations at $9.194 \cdot 10^9$ cycles.

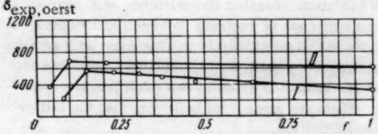

Fig. 1.

These curves show that with magnetic dilution the half width of paramagnetic absorption lines, contrary to the theory which considers only magnetic interactions, increases at first, reaches a maximum and then begins to decrease. Such behavior could be explained as resulting from different rates of decrease of the magnetic and exchange interactions during dilution. The maximum half width clearly corresponds to a magnetic concentration at which the rates of decrease of exchange and magnetic interaction are identical; at higher magnetic concentrations the exchange interaction decreases more rapidly than the magnetic; at lower concentrations this is reversed.

The concentration corresponding to the maximum half width was taken as an arbitrary limit for the influence of the exchange interaction. This arbitrary limit for the solid solutions of MnS, ZnS corresponds to an average distance between Mn^{++} ions of 6.2 A (f = 0.151) and for $Mn(NH_4)_2(SO_4)_2 \cdot 6H_2O$, $Zn(NH_4)_2(SO_4)_2 \cdot 6H_2O$ to 15.1 A (f = 0.103). Since the volumetric concentration of Mn^{++} ions in the second system of solid solutions is lower than in the first it could be expected that for MnS, ZnS the arbitrary limit would correspond to a smaller f. Yet the experiments yield the opposite result. This is due to the presence of two Mn^{++} ions in a unit cell of $Mn(NH_4)_2(SO_4)_2 \cdot 6H_2O$, $Zn(NH_4)_2(SO_4)_2 \cdot 6H_2O$ and to considerable exchange interaction between them.

A computation of the theoretically expected half width for undiluted MnS, considering only magnetic interaction, showed that in pure manganous sulfide the exchange interaction is very large, as the experimental half width was smaller than the theoretical prediction by an entire order of magnitude. We note that at the concentration which corresponds to the arbitrary limit the exchange interaction is reduced by a factor of 4 compared with pure MnS, while the magnetic dipole interaction is reduced by only the factor 2.5.

Comparison of the results obtained for these two systems of solid solutions containing Mn^{++} shows that a study of the exchange interaction dependence on the average distance between magnetic particles is possible only when we compare substances with identical lattices (i. e., the same type of solid solution); the comparison of data from the investigations of paramagnetics with different lattices is inadmissible and can lead to false conclusions.

Reference [5] describes an investigation of the effect of exchange interaction on the width of paramagnetic resonance lines through study of the dependence of the width on the interionic distance for a number of different salts with different volumetric concentrations of the same paramagnetic Mn^{++} ion. It was assumed that the lattices of all the salts under investigation have simple cubic symmetry. This assumption resulted in an extremely doubtful conclusion regarding the reduction of the exchange interaction in especially dense lattices. Our experiments show that this conclusion cannot be considered well-founded. The results in [5] indicate only that when exchange interactions in highly concentrated salts are studied any possible departure of the lattice from the assumed type is very important. In this range of concentrations it is meaningless to employ average interionic separations without considering the nature of the specific lattices.

In this connection it is appropriate to mention the hypothesis [6] that exchange interactions in $CuCl_2 \cdot 2H_2O$ are very much stronger than in CuF_2 by virtue of the possible additional exchange between 3d shells of copper ions through chlorine 3d shells.

We have investigated $CuF_2 \cdot 2H_2O$, which is of greater magnetic dilution than CuF_2. However, for $CuF_2 \cdot 2H_2O$, which lacks the possibility of exchange interaction through 3d shells, we obtained spectral lines that are much narrower than for CuF_2 and indistinguishable in width from lines of $CuCl_2 \cdot 2H_2O$. These experiments showed the unsuitability of the hypothesis mentioned. Indeed, from crystallographic data it follows that exchange interactions in $CuCl_2 \cdot 2H_2O$ and $CuF_2 \cdot 2H_2O$ must be stronger than in CuF_2 since in the latter substance the separation between nearest Cu^{++} ions is greater than in the hydrated salts mentioned.

We shall finally discuss measurements on Nd_2O_3 and the solid solutions Nd_2O_3, La_2O_3. Neodymium oxide is one of the few rare earth compounds which show considerable paramagnetic absorption at room temperature [7]. Even magnetostatic investigations [8] of Nd_2O_3, La_2O_3 solid solutions revealed the existence of exchange interaction between Nd^{+++} ions. Our experiments confirmed the existence of exchange between 4f electrons, although this exchange interaction is very weak and vanishes with the slightest dilution. Thus even with an average distance of 4.3 A between Nd^{+++} ions the absorption curve becomes so wide that it becomes impossible to evaluate its width. In the investigation of Nd_2O_3 we noted that this substance exists in two modifications (pink and lilac) in which the exchange interactions differ somewhat. There are grounds for believing that the lattice of the pink modification is denser than the lattice of the lilac modification.

In conclusion the author sincerely thanks B. M. Kozyrev for directing this work.

LITERATURE CITED

[1] S. A. Al'tshuler, E. K. Zavoiskii and B. M. Kozyrev, J. Exptl.-Theoret. Phys. (U.S.S.R.) 17, 1122 (1947).

[2] S. A. Al'tshuler, Doctoral Dissertation, Phys. Inst., Acad. Sci. USSR (Moscow, 1954).

[3] J. H. van Vleck, Phys. Rev. 74, 1168 (1948).

[4] E. K. Zavoiskii, Doctoral Dissertation, Phys. Inst., Acad. Sci. USSR (Moscow, 1944).

[5] H. Kumagai, K. Ono, et al., Phys. Rev. 83, 1077 (1951).

[6] F. W. Lancaster and W. Gordy, J. Chem. Phys. 19, 1181 (1951).

[7] N. S. Garif'ianov, Dissertation, Kazan State University (Kazan, 1952).

[8] P. Selwood, Magnetochemistry (For. Lit. Press, 1949).

Received March 22, 1955

Physico-Technical Institute, Kazan Affiliate,
Academy of Sciences USSR

ON THE ISOTOPE SHIFT IN THE SPECTRUM OF NEODYMIUM

F. A. Korolev and Iu. I. Osipov

(Presented by Academician A. A. Lebedev April 25, 1956)

In this work we have investigated the isotope shift in a natural mixture of neodymium isotopes in the spectral region from 4450 to 6500 A. The light source was a water-cooled tube with hollow cathode. Argon with a small admixture of helium was used as the excited gas. A current of ~ 150 ma was sent through the tube. The optical scheme consisted of an ISP-51 triple prism glass spectrograph with UF-84 camera (focal length 800 mm) and a silver-coated Fabry-Perot interferometer (of GOI – State Optical Institute – design). "Isopanchrom" film was used, whose sensitivity is 90 units GOST (All-Union State Standard). A series of photographs were taken for different widths of the interferometer rings: h = 3, 8, 10, 15, 30 mm. The best results were obtained for h = 10 mm.

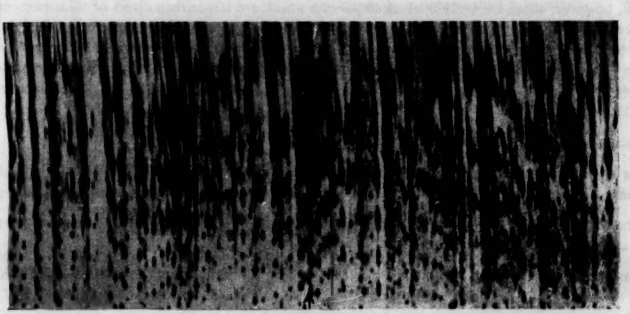

Fig. 1.

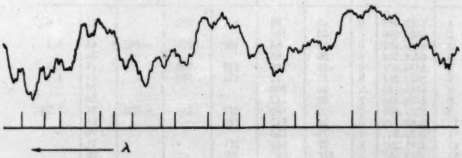

Fig. 2.

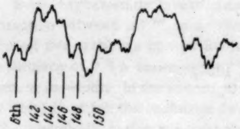

Fig. 3.

The spectrograms were measured with an IZA-2 comparator and some lines were measured photometrically with a MF-4 photoelectric recording microphotometer. 17 lines were measured altogether, although more than 40 lines had clear structure. The structure of the lines was not identical with regard to either location and number of components or intensity distribution (see Fig. 1). With sufficient resolution (h = 8 mm) the majority of the lines divided into 3-6 components (see Fig. 2, which is a microphotogram of the structure of λ = 5291.665 A).

Five components were ascribed to five even neodymium isotopes. The origin of the sixth component, which was observed in three lines, is not entirely clear. However, from its position it can be ascribed to the hyperfine structure of the odd isotope 143 [1, 2, 4]. The location of the components is shown in Fig. 3. Our results are given in Table 1.

The separations of the components due to the first four even Nd isotopes, whose mass numbers are 142, 144, 146 and 148, are approximately equal and will be denoted by $\delta\tilde{\nu}$. The separation of the isotopes Nd^{148} and Nd^{150} is considerably greater. This so-called anomalous isotope shift ($\delta\tilde{\nu}_{\mathrm{an}}$) was discovered for Nd by Klinkenberg [2]. As can be seen from Table 1, $\delta\tilde{\nu}$ decreases with increasing wave length (against the over-all background of decreasing $\delta\tilde{\nu}$, however, there are individual discrepancies which are larger than errors of measurement and cannot be ascribed to the latter). This relationship can also be seen in the results of other authors, although it has not been noted by them. In this connection we considered it useful to reproduce portions of other articles [2, 3], which are given in Tables 2 and 3. The behavior of $\delta\tilde{\nu}_{\mathrm{an}}$ is of the greatest interest. In [2] $\delta\tilde{\nu}_{\mathrm{an}}$ was measured for lines from 4569 to 4688 A; the value obtained for $\delta\tilde{\nu}_{\mathrm{an}}/\delta\tilde{\nu}$ was about 1.7. In [3] $\delta\tilde{\nu}_{\mathrm{an}}$ was measured from 4600 to 5125 A.

As can be seen from Table 3, $\delta\tilde{\nu}_{\mathrm{an}}/\delta\tilde{\nu} \approx 1.5$.

In our work we were able to measure $\delta\tilde{\nu}_{\mathrm{an}}$ for lines from 5291 to 6485 A. The values of $\delta\tilde{\nu}_{\mathrm{an}}/\delta\tilde{\nu}$ are given in Table 1.

For the red end of the neodymium spectrum, i. e., for $\lambda > 6000$ A, $\delta\tilde{\nu}_{\mathrm{an}}/\delta\tilde{\nu}$ has an average value of 1.3, which is lower than for the blue-violet end, where its value is 1.5-1.7.

It is an interesting fact that $\delta\tilde{\nu}_{\mathrm{an}}/\delta\tilde{\nu}$ for certain lines in the red portion (λ = 6310.4 and 6070.2 A) is almost unity, that is, $\delta\tilde{\nu}_{\mathrm{an}} \approx \delta\tilde{\nu}$, and, consequently, for these lines there is no anomaly in the shift of Nd^{148} and Nd^{150} lines.

TABLE 1

Separation of Components in 0.001 cm^{-1}

	λ, A	142	144	146	148	150	6-th component	$\delta\tilde{\nu}$	$\frac{\delta\tilde{\nu}_{\mathrm{an}}}{\delta\tilde{\nu}}$
1	6485.687	0	45	88	131	192		44	1.4
2	6319.686	0	63	109				54	
3	6310.487	0	45	84	131	176	—183	44	1.1
4	6226.502	0	36	68				34	
5	6178.591	0	46	89	133	193		44	1.4
6	6073.267	0	35	70	134	183		44	1.1
7	5815.442	0	50	100				50	
8	5470.410	0	61	117				58	
9	5291.665	0	70	139	219	346	—109	74	1.78
10	5269.778	0	74	147	184			61	
11	5022.6	0	77	153				76	
12	4981.283	0	75	144	214			71	
13	4688.557	0	101	195	297			99	
14	4678.908	0	99	195	282			94	
15	4659.373	0	96	196	285			95	
16	4616.68	0	113	216				108	
17	4569.849	0	113	206	295		—130	103	

TABLE 2

Klinkenberg's Data [2]

λ, A	142	144	146	148	150	$\delta\tilde{\nu}$
6619.39	0	36	69			36
6504.92	0	55	105			55
6321.22	0	53	103			52
6307.02	0	67	134			67
6230.20	0	50	100			50
6223.38	0	41	81	123		41
6178.59	0	47	88	127		45
6074.43	0	68	131			67
6006.44	0	49	102			50
5876.34	0	30	60			30
5837.15	0	55	115			56
5653.55	0	46	86			45
5640.50	0	38	76			38
5575.50	0	91	181	254		90
5314.35	0	76	158	233		77
5198.45	0	93				93
5149.78	0	74	142			73
5073.84	0	108	200			102
4966.15	0	102	206			103
4966.68	0	67	133			67
4940.30	0	93	181			92
4688.547	0	93	183	276		93
4678.95	0	98	195	297		98
4618.061	0	107	208	325		104
4442.49	0	100	200			100

TABLE 3

Data of Nõldeke and Steudel [3]

λ, Å	144	146	148	150	$\delta\tilde{\nu}$	$\delta\tilde{\nu}_{an}$	$\delta\tilde{\nu}_{an}/\delta\tilde{\nu}$
4599.3	−95	−180	−289	−429	96	140	1.46
4659.4	−102	−192	−294	−444	98	150	1.53
4678.9	−101	−190	−298	−450	99	152	1.54
4688.6	−101	−192	−297	−446	99	149	1.51
4871.4	−71	−137	−216	−322	72	106	1.46
4926.7	−72	−140	−218	−326	73	108	1.48
4965.3	−70	−134	−208	−324	69	116	1.68
4966.7	−73	−138	−216	−327	72	111	1.53
4996.1	−109	−213	−331	−492	110	161	1.46
5022.7	−78	−145	−233	−348	78	115	1.43
5125.9	−79	−148	−227	−346	76	119	1.57

The above results are of interest for the theory of the isotope shift; thus further experimental study of the anomalous isotope shift is required.

LITERATURE CITED

[1] K. Murakawa and J. S. Ross, Phys. Rev. 82, 967 (1951).

[2] P. F. A. Klinkenberg, Physica 11, 327 (1945).

[3] G. Nõldeke and A. Steudel, Z. Physik 137, 632 (1954).

[4] K. Murakawa, Phys. Rev. 96, 1543 (1954).

Received April 24, 1956

M. V. Lomonosov Moscow State University

DISPERSION RELATIONS FOR THE PHOTOPRODUCTION OF PIONS

A. A. Logunov and B. M. Stepanov

(Presented by Academician N. N. Bogoliubov April 27, 1956)

We are familiar with the dispersion relations formulated by Kramers and Kronig [1] in optics, which relate the real and imaginary parts of the refractive index of a medium. In a number of recent articles, and especially by Goldberger [2] it has been shown that analogous dispersion relations can be established for the Hermitian and anti-Hermitian parts of the pion-nucleon scattering amplitude based on the causality principle and without the use of perturbation theory. The formulas of [3] have been employed by Anderson et al. [4] to obtain a correct set of phase shifts for meson-nucleon collisions. But Goldberger's method cannot be applied to reactions of the photoproduction type, where the initial and final states contain bosons of different masses. N. N. Bogoliubov* has developed general principles for constructing dispersion relations applicable to the most diverse scattering processes. His method is based on theorems concerning analytic functionality which are proved with the aid of the causality principle. In the present note Bogoliubov method is used to set up dispersion relations for photoproduction.

We shall denote the absorption operator for a meson of type ρ ($\rho = 1, 2, 3$) by $\overset{(-)}{\varphi_{\rho}}(q)$, and the photon creation operator by $a_{\nu}^{(+)}(k)$ ($\nu = 0, 1, 2, 3$). Then the matrix element for processes of photoproduction reactions can be written in the S matrix formalism as

$$S(k, \alpha; q', \omega) = (2\pi)^3 \langle \Phi^{*}_{p's'} \varphi^{(-)}_{\rho'} (q') S a^{(+)}_{\nu} (k) \Phi_{ps} \rangle. \tag{1}$$

Here Φ designates the state amplitude of the scatterer, and the composite indices α and ω, which refer to the initial and final states, respectively, include all quantum numbers that characterize the system except the photon and meson momenta. It is easily seen that

$$S(k, \alpha; q', \omega) = \sum_{(m)} \eta^{m}_{\nu} \Lambda_{\xi, \omega}, \tag{2}$$

where

$$\Lambda_{\xi, \omega} = \frac{1}{\sqrt{4k^0 q'^0}} \int e^{i(q'x - ky)} \langle \Phi^{*}_{p's'} \frac{\delta^2 S}{\delta A_m (y)\, \delta \varphi_{p'} (x)} S^{+} \Phi_{ps} \rangle \, dx\, dy,$$

and the η^{m}_{ν} are polarization vectors.

In our investigation all components of the vector potential of the electromagnetic field $A_m(x)$ are independent. From considerations of translational invariance

---

* Presented by N. N. Bogoliubov at a number of seminars during January 1956 in the V. A. Steklov Mathematics Institute of the Academy of Sciences USSR.

$$\langle \overset{*}{\Phi}_{p's'} \frac{\delta^2 S}{\delta A_m(y)\,\delta\varphi_{\rho'}(x)} S^+ \Phi_{ps}\rangle = e^{i\frac{p'-p}{2}(x+y)} V_{\xi,\omega}(x-y),$$

consequently:

$$\Lambda_{\xi,\omega} = \frac{i(2\pi)^4}{\sqrt{4k^0 q'^0}}\,\delta(k+p-q'-p')\,T_{\xi,\omega}\left(\frac{k+q'}{2}\right),$$

where

$$T_{\xi,\omega}\left(\frac{k+q'}{2}\right) = -i\int e^{i\frac{k+q'}{2}x} V_{\xi,\omega}(x)\,dx. \tag{3}$$

Eq. (3) is too complicated. However, following Goldberger, it is possible to introduce a new amplitude $M_{\xi,\omega}$ which is of considerably simpler structure and coincides with the amplitude $T_{\xi,\omega}$ for actual momenta:

$$M_{\xi,\omega}\left(\frac{k+q'}{2}\right) = i\int e^{i\frac{k+q'}{2}x}\,\theta(x^0)\,\{F_{\xi,\omega}(x) - PF_{\xi,\omega}(-x)\}\,dx, \tag{4}$$

$$F_{\xi,\omega}(x) = \left(\frac{1}{2\pi}\right)^3 \sum_{(n)} \int d\mathbf{l}\ \langle \dot{\Psi}_{p's'} J_{\rho'}(0)\,\Psi_{\mathbf{l},n}\rangle \langle \dot{\Psi}_{\mathbf{l},n} I_m(0)\,\Psi_{p,s}\rangle \times \\ \times \exp\left\{-il_n x + \frac{i}{2}(p'+p)x\right\}. \tag{5}$$

Here $\Psi_{\mathbf{l},n}$ is a complete set of eigen-amplitudes of states of the energy-momentum operator of the system in the real particle representation; $J_{\rho'}(0)$ and $I_m(0)$ are the meson and electromagnetic currents in the same representation; and P is the permutation operator of these currents.

Let us separate the amplitude $M_{\xi,\omega}$ into a Hermitian part $D_{\xi,\omega}$ and an anti-Hermitian part $A_{\xi,\omega}$. Then

$$A_{\xi,\omega}\left(\frac{k+q'}{2}\right) = \frac{1}{2}\int e^{i\frac{k+q'}{2}x}\{F_{\xi,\omega}(x) - PF_{\xi,\omega}(-x)\}\,dx, \tag{6}$$

$$A_{\xi,\omega}\left(\frac{k+q'}{2}\right) = -PA_{\xi,\omega}\left(-\frac{k+q'}{2}\right).^{*} \tag{7}$$

We shall now use the analytic functionality theorem. In the reference system where $\vec{p} + \vec{p}' = 0$ the scattering amplitude $M_{\xi,\omega}$ will have a cut in the upper half plane of E. With the aid of (7) and invariance of the spatial components of the vectors $\vec{p}$, $\vec{k}$, $\vec{q}'$ with respect to reflection we have deduced that the combinations

$$A^{(\pm)}_{\xi,\omega}(E,\lambda\mathbf{e}) = A_{\xi,\omega}(E,\lambda\mathbf{e}) \pm P_{s,s'}\dot{A}_{\xi,\omega}(E,\lambda\mathbf{e}) \tag{8}$$

---

* In deriving (6) we used the causality condition in the form $\delta j_\rho(x)/\delta A_m(y) = 0$ for x ~ y. However, the same formula can be obtained, following Bogoliubov, without resorting to a causality condition at this stage.

are odd (even) functions of E. It is easy to construct combinations $A^{(\pm)}_{\xi,\omega}$ which do not have a cut in the upper half plane of E:

$$S_e A^{(\pm)}_{\xi,\omega}(E,\lambda\mathbf{e}) = A^{(\pm)}_{\xi,\omega}(E,\lambda\mathbf{e}) + A^{(\pm)}_{\xi,\omega}(E,-\lambda\mathbf{e}),$$
$$\mathfrak{A}_e A^{(\pm)}_{\xi,\omega}(E,\lambda\mathbf{e}) = \frac{1}{\lambda}\left\{A^{(\pm)}_{\xi,\omega}(E,\lambda\mathbf{e}) - A^{(\pm)}_{\xi,\omega}(E,-\lambda\mathbf{e})\right\}. \tag{9}$$

These combinations are analytic functions in the entire upper half plane of E. This provides the possibility of using the generalized Cauchy theorem and writing the following dispersion relations for photoproduction processess:

$$S_e\left(D^{(+)}_{\xi,\omega}(E,\mathbf{p}) - D^{(+)}_{\xi,\omega}(E_0,\mathbf{p})\right) = \frac{\mathcal{P}}{\pi}\int_0^\infty \frac{2E'(E^2-E_0^2)}{(E'^2-E^2)(E'^2-E_0^2)} S_e A^{(+)}_{\xi,\omega}(E',\mathbf{p})\,dE'$$
$$\mathfrak{A}_e\left(D^{(+)}_{\xi,\omega}(E,\mathbf{p}) - D^{(+)}_{\xi,\omega}(E_0,\mathbf{p})\right) = \frac{\mathcal{P}}{\pi}\int_0^\infty \frac{2E'(E^2-E_0^2)}{(E'^2-E^2)(E'^2-E_0^2)} \mathfrak{A}_e A^{(+)}_{\xi,\omega}(E',\mathbf{p})\,dE',$$
$$S_e\left(D^{(-)}_{\xi,\omega}(E,\mathbf{p}) - \frac{E}{E_0} D^{(-)}_{\xi,\omega}(E_0,\mathbf{p})\right) = \frac{\mathcal{P}}{\pi}\int_0^\infty \frac{2E(E^2-E_0^2)}{(E'^2-E^2)(E'^2-E_0^2)} S_e A^{(-)}_{\xi,\omega}(E',\mathbf{p})\,dE', \tag{10}$$
$$\mathfrak{A}_e\left(D^{(-)}_{\xi,\omega}(E,\mathbf{p}) - \frac{E}{E_0} D^{(-)}_{\xi,\omega}(E_0,\mathbf{p})\right) = \frac{\mathcal{P}}{\pi}\int_0^\infty \frac{2E(E^2-E_0^2)}{(E'^2-E^2)(E'^2-E_0^2)} \mathfrak{A}_e A^{(-)}_{\xi,\omega}(E',\mathbf{p})\,dE'.$$

In the deduction of the basic Formulas (10) we have assumed that the scattering amplitude has a pole at infinity which is not above the first order. For the practical application of the relations which have been derived, a phase analysis must be carried through; this will be considered in subsequent articles.

In conclusion we consider it our pleasant duty to express our deep gratitude to Academician N. N. Bogoliubov, who directed this work, and to B. V. Medvedev for discussions.

LITERATURE CITED

[1] R. Kronig, J. Opt. Soc. Amer. 12, 547 (1926); H. A. Kramers, Atti congr. interfisici Como 2, 545 (1927); R. Kronig, Physica 12, 543 (1946).

[2] M. L. Goldberger, Phys. Rev. 99, 979 (1955).

[3] M. L. Goldberger, H. Miyazawa and R. Oehme, Phys. Rev. 99, 986 (1955).

[4] H. L. Anderson, W. C. Davidon and U. E. Kruse, Phys. Rev. 100, 339 (1955).

Received April 25, 1956

V. A. Steklov Mathematics Institute,
Academy of Sciences USSR

ON THERMAL AGITATION IN DISTRIBUTED SYSTEMS

S. M. Rytov

(Presented by Academician M. A. Leontovich March 7, 1956)

1. In a series of articles by Callen and others the familiar Nyquist theorem [1] concerning the intensity of thermal agitation of electric charge in a conductor was extended to thermal fluctuations in any dissipative system. At first the generalized theorem was formulated for the case of one fluctuating parameter and the proof was given both on the basis of quantum mechanics [2, 3] and by a macroscopic "thermodynamical" procedure [4]. Subsequently the result was extended to cover a few fluctuating parameters, also in two ways – the quantum mechanical [5] and the "thermodynamical" [6].*

In the present article the theorem is generalized for distributed systems in which fluctuations are described by random functions of time and a spatial point. In the terminology of the theory of random functions we here pass from stationary random processes to uniform random fields which from the nature of the problem are also isotropic.

2. The content of the "fluctuation-dissipation" theorem of Callen et al. can be summed up as follows. Let x_j be equilibrium values of the parameters of interest and F_j the corresponding generalized forces, so that the change of energy of the system due to the action of these forces is $\sum_j F_j dx_j$. Let the random deviations from x_j and F_j, which we denote by $\xi_j(t)$ and $f_j(t)$, be expanded in harmonic spectra:

$$\xi_j(t) = \int_{-\infty}^{+\infty} \xi_{j\omega} e^{i\omega t}\, d\omega, \qquad f_j(t) = \int_{-\infty}^{+\infty} f_{j\omega} e^{i\omega t}\, d\omega,$$

where we know the linear equations which relate the harmonic amplitudes $\xi_{j\omega}$ and $f_{j\omega}$:

$$\xi_{j\omega} = \sum_k \alpha_{jk}(\omega) f_{k\omega}, \qquad f_{j\omega} = \sum_k \alpha_{jk}^{-1}(\omega)\, \xi_{k\omega}\,.^{**} \tag{1}$$

Then the correlation matrix of the harmonic amplitudes $\xi_{j\omega}$ is

$$\overline{\xi_{j\omega}\xi^*_{k\omega'}} = C(\omega)\, i\, (\alpha_{jk} - \alpha^*_{kj})\, \delta(\omega - \omega'), \tag{2}$$

---

* The correlation matrix for the harmonic spectral amplitudes of fluctuating parameters was obtained by M. A. Leontovich in 1941, but its relation to the dissipative properties of a system (with admittance) was not fully investigated.

** α_{jk}^{-1} is the matrix which is the reciprocal of α_{jk}. The matrix $Y_{jk} = i\omega\alpha_{jk}$ is designated in [5, 6] as the admittance matrix of the considered dissipative system.

where

$$C(\omega)=\frac{\hbar}{4\pi}\operatorname{cth}\frac{\hbar\omega}{2\Theta} \tag{2'}$$

and $\Theta = kT$ is the energetic temperature.*

The matrix α_{jk} satisfies certain symmetry relations [5] which generalize Onsager's reciprocity theorem [8, 9] for kinetic coefficients.

The Theorem (2) can also be formulated differently if we use the concept of "extraneous" fluctuation forces which act in a closed system to induce the observed fluctuations $\xi_j(t)$. The spectral amplitudes of these equivalent fictitious forces must be related to $\xi_{j\omega}$ by the same Equations (1), and we can therefore understand further by $f_j(t)$ just the equivalent "extraneous" forces. The rate of change of the average energy of the system due to the work of the "extraneous" forces is

$$\frac{d\overline{E}}{dt}=\sum_j\overline{f_j^*\frac{d\xi_j}{dt}}=-\sum_j\overline{\xi_j\frac{df_j^*}{dt}}. \tag{3}$$

From (1) and (2) it follows that the correlation matrix of the harmonic amplitudes $f_{j\omega}$ is

$$\overline{f_{j\omega}f^*_{k\omega'}}=C(\omega)\,i\,(\alpha^{-1*}_{kj}-\alpha^{-1}_{jk})\,\delta(\omega-\omega'). \tag{4}$$

3. We now proceed to our problem. Let the fluctuations in the distributed system occupying volume V be described by the uniform random field $\xi(t, \mathbf{r})$. For simplicity we take the case of a one-dimensional (scalar) field. Generalization to a system of fields $\xi^{(\alpha)}(t, \mathbf{r})$ $(\alpha = 1, 2, \ldots)$ offers no difficulty and the corresponding result will be given below. Let $f(t, \mathbf{r})$ be the spatial density of the equivalent "extraneous" force, with the harmonic amplitudes $\xi_\omega(\mathbf{r})$ and $f_\omega(\mathbf{r})$ related among themselves by the linear spatial operators A and A^{-1}:

$$\xi_\omega(\mathbf{r})=Af_\omega(\mathbf{r}),\quad f_\omega(\mathbf{r})=A^{-1}\xi_\omega(\mathbf{r}). \tag{5}$$

In applications the reciprocal operator A^{-1} is usually given; this is a differential operator. Let us, finally have available a complete orthonormalized set of functions $\varphi_j(\mathbf{r})$ defined for the region V:

$$\int_V\varphi_j(\mathbf{r})\,\varphi_k^*(\mathbf{r})\,dV=\delta_{jk}. \tag{6}$$

We expand $\xi(t, \mathbf{r})$ and $f(t, \mathbf{r})$ in terms of the functions $\varphi_j(\mathbf{r})$:

$$\xi(t,\mathbf{r})=\sum_j\xi_j(t)\,\varphi_j(\mathbf{r}),\quad f(t,\mathbf{r})=\sum_j f_j(t)\,\varphi_j(\mathbf{r}), \tag{7}$$

---

* The double coefficient of $\delta(\omega-\omega')$ in (2) is the matrix of harmonic spectral intensity (for positive frequencies) which was obtained in [5, 6] but which is written here in the form given by L. D. Landau and E. M. Lifshits in the part of their "Course in Theoretical Physics" which is devoted to macroscopic electrodynamics. I take this opportunity to thank the authors for their kindness in enabling me to become acquainted with the manuscript of their work.

or in the spectral form

$$\xi_\omega(\mathbf{r}) = \sum_j \xi_{j\omega}\varphi_j(\mathbf{r}), \quad f_\omega(\mathbf{r}) = \sum_j f_{j\omega}\varphi_j(\mathbf{r}). \tag{8}$$

We note that, according to (6) and (7) the mean power developed by the "force" $f(t, \mathbf{r})$ can be written in the form of (3):

$$\int_V \overline{f\frac{\partial \xi}{\partial t}}\, dV = -\int_V \overline{\xi\frac{\partial f}{\partial t}}\, dV = -\sum_j \overline{\xi_j \frac{\partial f_j^*}{\partial t}} = \frac{d\bar{E}}{dt}. \tag{9}$$

Taking the $\xi_j(t)$ as the discrete variables which describe the fluctuations in the system under consideration, Theorems(2) and (4) can naturally be extended to the amplitudes $\xi_{j\omega}$ and $f_{j\omega}$.* This permits us to obtain spatial correlation functions for $\xi_\omega(\mathbf{r})$ and $f_\omega(\mathbf{r})$.

We note first that from (1), (5) and (8) it is easy to obtain the relations

$$A\varphi_k(\mathbf{r}) = \sum_j \alpha_{jk}\varphi_j(\mathbf{r}), \quad A^{-1}\varphi_k(\mathbf{r}) = \sum_j \alpha_{jk}^{-1}\varphi_j(\mathbf{r}), \tag{10}$$

according to which α_{jk} and α_{jk}^{-1} are Fourier coefficients of the expansions of $A\varphi_k$ and $A^{-1}\varphi_k$ in terms of the functions φ_j.

Using (8), (2) and (10) we obtain

$$\begin{aligned}\overline{\xi_\omega(\mathbf{r})\,\xi^*_{\omega'}(\mathbf{r}')} &= \sum_{j,k} \overline{\xi_{j\omega}\,\xi^*_{k\omega'}}\,\varphi_j(\mathbf{r})\,\varphi_k^*(\mathbf{r}') = \\ &= C(\omega)\, i\delta(\omega-\omega') \sum_{j,k} (\alpha_{jk} - \alpha^*_{kj})\,\varphi_j(\mathbf{r})\,\varphi_k^*(\mathbf{r}') = \\ &= C(\omega)\, i\delta(\omega-\omega') \sum_j \{\varphi_j^*(\mathbf{r}')\, A\varphi_j(\mathbf{r}) - \varphi_j(\mathbf{r})\, A^*\varphi_j^*(\mathbf{r}')\}.\end{aligned}$$

But the operator A is taken here with respect to the coordinates of the point $\mathbf{r}$ and A^* with respect to the coordinates of the point $\mathbf{r}'$ so that both can be taken outside the summation sign; the summation is then the expansion of the δ function of $\mathbf{r}-\mathbf{r}'$ in terms of the $\varphi_j(\mathbf{r})$ [or the $\varphi_j^*(\mathbf{r}')$]: $\sum_j \varphi_j(\mathbf{r})\varphi_j^*(\mathbf{r}') = \delta(\mathbf{r}-\mathbf{r}')$. As a result

$$\overline{\xi_\omega(\mathbf{r})\,\xi^*_{\omega'}(\mathbf{r}')} = C(\omega)\, i\delta(\omega-\omega')\,(A - A^*)\,\delta(\mathbf{r}-\mathbf{r}'). \tag{11}$$

Since the δ function depends only on the vector $\vec{\rho} = \mathbf{r}-\mathbf{r}'$ (the field $\xi(t, \mathbf{r})$ is spatially uniform) both operators A and A^* can be expressed in terms of the components of $\bar{\rho}$.

In a completely analogous manner (8), (4) and (10) are used to give the correlation function for $f_\omega(\mathbf{r})$:

$$\overline{f_\omega(\mathbf{r})\, f^*_{\omega'}(\mathbf{r}')} = C(\omega)\, i\delta(\omega-\omega')\,(A^{-1*} - A^{-1})\,\delta(\mathbf{r}-\mathbf{r}'), \tag{12}$$

---

* It is, of course, necessary to assume that (2) and (4) remain in force for a denumerable set of variables.

where in the differential operators $A^{-1}(\nabla)$ and $A^{-1*}(\nabla')$ we have $\nabla = -\nabla' = \nabla_\rho$.

4. Equations (11) and (12), which now in no way show the shape and size of the region V, can naturally be extrapolated to the case which is suitable for calculation in which V is regarded as an infinite space and the functions φ are taken in the form $e^{i\mathbf{kr}}$, that is, the fields are represented as spatial Fourier integrals*:

$$f(t, \mathbf{r}) = \int_{-\infty}^{+\infty} f_{\mathbf{k}}(t)\, e^{i\mathbf{kr}}\, d\mathbf{k}, \quad f_\omega(\mathbf{r}) = \int_{-\infty}^{+\infty} f_{\omega\mathbf{k}} e^{i\mathbf{kr}}\, d\mathbf{k}. \tag{13}$$

It is easily shown that

$$\overline{f_{\omega,\mathbf{k}} f^*_{\omega',\mathbf{k}'}} = \frac{C(\omega)\, i}{(2\pi)^3}\, \delta(\omega - \omega')\, \delta(\mathbf{k} - \mathbf{k}')\, [A^{-1*}(-i\mathbf{k}) - A^{-1}(i\mathbf{k})]. \tag{14}$$

The generalization of these results to the case of a system of homogeneous fields $\xi^{(\alpha)}(t, \mathbf{r})$ which are homogeneously related among themselves is almost obvious. Instead of (5) we now have the set of equations

$$f_\omega^{(\alpha)}(\mathbf{r}) = \sum_\beta A^{-1}_{\alpha\beta}\, \xi_\omega^{(\beta)}(\mathbf{r}), \tag{15}$$

and the correlations Functions (12) and (14) are replaced by the correlation matrices:

$$\overline{f_\omega^{(\alpha)}(\mathbf{r})\, f_{\omega'}^{(\beta)*}(\mathbf{r}')} = C(\omega)\, i\delta(\omega - \omega')\, (A^{-1*}_{\beta\alpha} - A^{-1}_{\alpha\beta})\, \delta(\vec{\rho}), \tag{16}$$

$$\overline{f^{(\alpha)}_{\omega,\mathbf{k}} f^{(\beta)*}_{\omega',\mathbf{k}'}} = \frac{C(\omega)\, i}{(2\pi)^3}\, \delta(\omega - \omega')\, \delta(\mathbf{k} - \mathbf{k}')\, [A^{-1*}_{\beta\alpha}(-i\mathbf{k}) - A^{-1}_{\alpha\beta}(i\mathbf{k})]. \tag{17}$$

5. We shall now consider as an example the thermal fluctuations of the electromagnetic field in a uniform medium which is described by the tensors of the dielectric and magnetic constants $\hat{\varepsilon}$ and $\hat{\mu}$.** The equivalent fluctuation forces are introduced in the form of the "extraneous" inductions $\mathfrak{D}$ and $\mathfrak{B}$, so that the equations for the harmonic spectral amplitudes of the field strengths will be

$$\mathfrak{D}_j = -\varepsilon_{jk} E_k + \frac{c}{i\omega} \operatorname{curl}_j \mathbf{H}, \quad \mathfrak{B}_j = -\mu_{jk} H_k - \frac{c}{i\omega} \operatorname{curl}_j \mathbf{E}. \tag{18}$$

The increase of electromagnetic energy associated with the action of the "forces" $\mathfrak{D}$ and $\mathfrak{B}$ is

$$\frac{dE}{dt} = -\frac{1}{4\pi} \int_V \left(\mathbf{E} \frac{\partial \mathfrak{D}}{\partial t} + \mathbf{H} \frac{\partial \mathfrak{B}}{\partial t} \right) dV.$$

Consequently, if for the parameters $\xi^{(\alpha)}$ we take $\mathbf{E}/4\pi$ and $\mathbf{H}/4\pi$, then in accordance with (9) $\mathfrak{D}$ and $\mathfrak{B}$ will be generalized forces. It then follows from (18) that the matrix of the operators A^{-1} is

---

* For the sake of brevity we shall hereinafter write only the formulas for the field of the "extraneous" force $f(t, \mathbf{r})$.

** This example was considered in the above-quoted (see footnote on p. 557) "Course in Theoretical Physics" by L. D. Landau and E. M. Lifshits using the "discrete" Formulas (1) and (4), for which purpose the somewhat artificial procedure was followed of dividing space into cells ΔV and replacing the differential operators with difference operators.

$$A^{-1}_{\mathfrak{D}_j\mathfrak{D}_k} = -4\pi\varepsilon_{jk}, \qquad A^{-1}_{\mathfrak{D}_j\mathfrak{B}_k} = A^{-1}_{\mathfrak{B}_k\mathfrak{D}_j} = -\frac{4\pi c}{i\omega}\begin{pmatrix} 0 & \nabla_3 & -\nabla_2 \\ -\nabla_3 & 0 & \nabla_1 \\ \nabla_2 & -\nabla_1 & 0 \end{pmatrix}.$$
$$A^{-1}_{\mathfrak{B}_j\mathfrak{B}_k} = -4\pi\mu_{jk},$$

As a result, from (16) and (2') we have for the matrix of the spectral intensity of the "extraneous" forces

$$\overline{\mathfrak{D}_j\mathfrak{D}_k^{\bullet}} = \hbar\coth\frac{\hbar\omega}{2\Theta}\, i\,(\varepsilon_{jk} - \varepsilon_{kj}^{\bullet})\,\delta(\vec{\rho}), \qquad \overline{\mathfrak{D}_j\mathfrak{B}_k^{\bullet}} = 0,$$
$$\overline{\mathfrak{B}_j\mathfrak{B}_k^{\bullet}} = \hbar\coth\frac{\hbar\omega}{2\Theta}\, i\,(\mu_{jk} - \mu_{kj}^{\bullet})\,\delta(\vec{\rho}) \qquad (\vec{\rho} = \mathbf{r} - \mathbf{r}').$$

These formulas were obtained by F. V. Bunkin [10], who from indirect physical considerations generalized the formulas for an isotropic medium which I had previously obtained [11].

LITERATURE CITED

[1] H. Nyquist, Phys. Rev. 29, 614 (1927); 32, 110 (1928).

[2] H. B. Callen and T. A. Welton, Phys. Rev. 83, 34 (1951).

[3] J. L. Jackson, Phys. Rev 87. 471 (1952).

[4] H. B. Callen and R. F. Greene, Phys. Rev. 86, 702 (1952).

[5] H. B. Callen, M. L. Barash and J. L. Jackson, Phys. Rev. 88, 1382 (1952).

[6] R. F. Greene and H. B. Callen, Phys. Rev. 88, 1387 (1952).

[7] M. A. Leontovich, J. Phys. USSR 4, 499 (1941).

[8] L. Onsager, Phys. Rev. 37, 405 (1931); 38, 2265 (1931).

[9] H. B. G. Casimir, Rev. Mod. Phys. 17, 343 (1945).

[10] F. V. Bunkin, Thermal Emission of an Anisotropic Medium, Cand. Dissert., Phys. Inst., Academy of Sciences USSR (1955).

[11] S. M. Rytov, Theory of Electrical Fluctuations and Thermal Emission (Acad. Sci. USSR Press, Moscow, 1953).

Received February 23, 1956

P. N. Lebedev Physics Institute,
Academy of Sciences USSR

ON THE DEPARTURE FROM WEAK COUPLING IN THE DOUBLY-CHARGED MESON FIELD THEORY

I. F. Ginzburg

(Presented by Academician N. N. Bogoliubov May 4, 1956)

1. The renormalization group method has been used by Shirkov [1] to show that in a doubly-charged pseudoscalar meson field theory with a certain relationship between the coupling constants, even when these are small it is impossible to use the weak coupling theory consistently, since one must go outside of this theory for large momenta. In [2] a similar result was obtained by summing a certain class of Feynman diagrams for the single-charge theory.

In the present article it is shown that the result mentioned above is obtained in the doubly-charged theory with an arbitrary relation between the charges. The asymptotic forms of the Green's functions of the doubly-charged theory are also obtained for large momenta.

These results apply both to the neutral theory and to the symmetrical charged theory.

2. In the notation of [1] the equations for the Green's functions in the large momentum region $|p^2| \gg m^2$ and the initial conditions are written as:

$$\frac{d\sigma}{dz} = \sigma\Psi(\sigma, \rho), \quad \frac{d\rho}{dz} = \rho\Phi(\rho, \sigma), \quad \sigma(0) = g^2, \; \rho(0) = h, \tag{1}$$

where

$$\Psi(\sigma, \rho) = \psi_1\sigma + \psi_2\rho^2 + \psi_3\rho\sigma + \dots \tag{2}$$

$$\rho\Phi(\sigma, \rho) = \varphi_1\sigma^2 + \varphi_2\rho\sigma + \varphi_3\rho^2 + \dots \tag{3}$$

and in addition for any Green's function Δ

$$\ln \Delta(x, g^2, h) = \int\limits_0^{\ln x} dz \left\{\frac{d}{d\xi} \ln \Delta[\xi, \sigma(z, g^2, h), \rho(z, g^2, h)]\right\}_{\xi=1}. \tag{4}$$

The power Series (2) and (3) for Φ and Ψ were obtained by perturbation theory from a consideration of lowest order diagrams. The coefficients φ_i, ψ_i which are required hereinafter are given in Table 1.

The investigation is conveniently carried through in the (ρ, σ) phase plane. Each integral curve $\rho(\sigma)$ of Equations (1) corresponds to some pair of values of the constants g and h. Passage from one point of a curve to another is the passage from one value of z to another or the transition from one pair of charges g and h to another by a transformation of the renormalization group. From (1 - 3) it is seen that in the neighborhood of the singular point at the coordinate origin in the phase plane there are no other singular points. One of the integral curves must contain a point which corresponds to the experimental values of g and h. Only this curve possesses real physical meaning. But since the experimental values of g and h have thus far not been determined it is necessary to investigate all possible curves $\rho(\sigma)$.

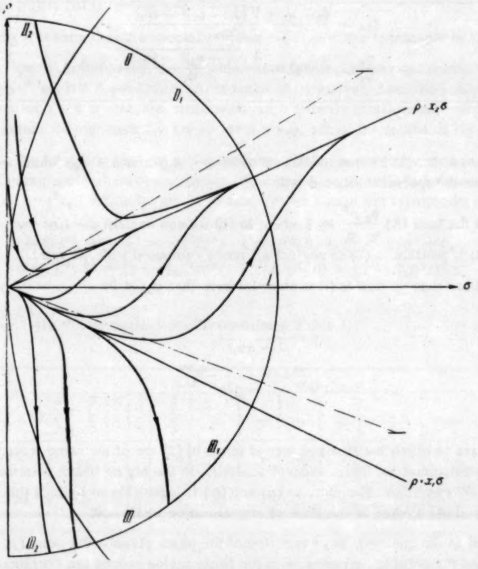

Fig. 1. Integral curves of Equations (1) in the phase plane around the coordinate origin $\rho, \sigma \ll 1$ for the neutral theory.

Figure 1 will serve as an illustration for what follows.

3. We shall first consider the case $(\alpha)\ \frac{\psi_2}{\psi_1}\frac{\rho^2}{\sigma} \ll 1$ where in (2) the second term can be neglected by comparison with the first.*

The solutions of (1) can then be written as

$$\sigma = \frac{g^2}{1 - \psi_1 g^2 z} = \frac{g^2}{1 - \dfrac{5g^2 z}{16\pi^2}}, \tag{5}$$

$$\frac{\rho}{\sigma} = x_2 + \frac{x_1 - x_2}{1 - \dfrac{h - g^2 x_1}{h - g^2 x_2}\left(\dfrac{\sigma}{g^2}\right)^{-x}}, \tag{6}$$

---

* It is always permissible to neglect the remaining terms for weak coupling.

where

$$x_{1,2} = \frac{\psi_1 - \varphi_2 \pm \sqrt{(\psi_1 - \varphi_2)^2 - 4\varphi_1\varphi_3}}{2\varphi_3},$$

$$\alpha = \frac{\varphi_3}{\psi_1}(x_1 - x_2) = \frac{\sqrt{(\psi_1 - \varphi_2)^2 - 4\varphi_1\varphi_3}}{\psi_1} > 0. \tag{7}$$

From (6) it is also seen that (1) has the special solutions $\rho = x_1\sigma$ and $\rho = x_2\sigma$ which were investigated in [1]. In addition Eq. (1) has the special solution $\sigma = 0$.

Let us now consider the case (β) $\frac{\psi_2}{\psi_1}\frac{\rho^2}{\sigma} \gg 1$ where in (2) we can neglect the first term by comparison with the second. In this case it is possible in (3) to neglect all terms compared with the third.

The solutions of (1) are then written as (it is essential here that $\varphi_3 < 0$):

$$\rho = \frac{h}{1 - h\varphi_3 z}, \tag{8}$$

$$\sigma = g^2 e^{\frac{\psi_2}{\varphi_3}(\rho - h)} = g^2 e^{\frac{\psi_2 h^2 z}{1 - h\varphi_3 z}}. \tag{9}$$

The intermediate case in which the first and second terms of (2) are of the same order is shown by a detailed calculation to be unimportant for the subsequent analysis. In the region which corresponds to this case the integral curves of (6) and (9) combine. Therefore in (α) and (β) it is possible to replace the sign ≫ by > without altering the results. (α) and (β) altered in this manner are said to be weakened.

4. We are interested in the question, to what region of the phase plane is the point (ρ, σ) shifted when z changes from 0 to ∞.* When the point (ρ, σ) remains in the finite region around the coordinate origin, $\rho, \sigma \ll 1$, then for all momenta the weak coupling theory (A) can be used. If the point (ρ, σ) does not remain close to the origin the weak coupling theory ceases to be applicable for very large momenta (B). It is shown below that in actuality the second possibility (B) occurs.

5. Let us now divide the portion of the phase plane close to the origin into three regions: $x_2 > \frac{\rho}{\sigma} > x_1$ (I); $\frac{\rho}{\sigma} < x_2$ (II); $x_1 > \frac{\rho}{\sigma}$ (III). Regions (II) and (III) are each divided into two subregions: (II_1) and (III_1), where the weakened case (α) applies, and (II_2) and (III_2) for the weakened case (β).

We shall first consider the integral curves in regions (I) and (II). Let the initial point (g^2, h) first lie in subregion (II_2). Then from (8) and (9) with $h > 0$ it follows that as z increases from 0 at some value of z instead of weakened (β) weakened (α) begins to be satisfied. We now choose the initial point (g^2, h) to be in region (I) or (II). Then from (5 – 7) it follows that if $\frac{h}{g^2} - x_1 > 0$, then $\frac{\rho}{\sigma} > x_1$, and that

$$\lim_{z \to \infty} \frac{\rho}{\sigma} = x_2, \tag{10}$$

that is, the problem is reduced to that considered in [1]. From (5) we see that in this case possibility (B) is realized.

We further consider the integral curves in region (III). Let the initial point (g^2, h) first lie in subregion (III_1). From (5 – 7) with the condition $0 > x_1 > \frac{h}{g^2}$ it follows that as z increases from 0 at some value of z, instead of weakened (α), weakened (β) begins to be satisfied. We now take the initial point (g^2, h) in subregion (III_2). Then from (8) and (9) with $h < 0$ it follows that when (β) holds for h^2/g^2, (β) also holds for ρ^2/σ. From (8) it is seen that in this case also possibility (B) is realized.

---

* Since we have used the condition $|p^2| \gg m^2$, the region $z < 0$ is not under consideration.

From the foregoing it is seen that the special solution of (1) $\rho = x_1\sigma$ is unstable but that $\rho = x_2\sigma$ is stable.

In the case of the special Solution (1), $\sigma = 0$, which corresponds to nonlinear meson theory with nonlinearity in the Lagrangian $L = \frac{1}{4}h\varphi^4$, for $h > 0$ possibility (A) is realized. However, from the analysis given above it can be seen that this solution for $h > 0$ is unstable, since when an arbitrarily small meson-nucleon interaction is allowed for a large momentum we approach the asymptote $\rho = x_2\sigma$, where the results of [1] are valid.

6. It is seen from the foregoing that for sufficiently large momentum (but remaining within the conditions for the applicability of perturbation theory) the asymptotic form of the Green's functions depends essentially on the sign of the expression $h-g^2x_1$. When $h-g^2x_1 \geq 0$ from (4) we obtain the asymptotic form of the Green's functions*

$$\begin{gathered} s(z, g^2, h) = (1-\psi_1 g^2 z)^{\alpha_s},\ \Gamma(z, g^2, h) = (1-\psi_1 g^2 z)^{\alpha_\Gamma}, \\ d(z, g^2, h) = (1-\psi_1 g^2 z)^{\alpha_d},\ \square(z, g^2, h) = (1-\psi_1 g^2 z)^{\alpha_\square}, \end{gathered} \tag{11}$$

where α_s, α_Γ, α_d, $\alpha_\square$ are the numerical coefficients from Table 1.

TABLE 1

Theory	$(2\pi)^2\psi_1$	$(2\pi)^4\psi_2$	$(2\pi)^2\varphi_1$	$(2\pi)^2\varphi_2$	$(2\pi)^2\varphi_3$	α_s	α_d	α_Γ	$\alpha_\square$	x_1	x_2	α
Neutral	$^5/_4$	$^3/_{16}$	1	1	$-^9/_2$	$-^1/_{10}$	$-^2/_5$	$-^1/_5$	$-^1/_5$	$-^1/_2$	$^4/_9$	$-^{17}/_5$
Symmetrical	$^5/_4$	$^5/_{16}$	2	2	$-^{11}/_2$	$-^3/_{10}$	$-^4/_5$	$+^1/_5$	$+^3/_5$	$\frac{3-\sqrt{713}}{44}$	$\frac{3+\sqrt{713}}{44}$	$-\frac{\sqrt{713}}{5}$

When $h-g^2x_1 < 0$ we obtain a different asymptotic form of the Green's functions

$$\begin{gathered} s(z, g^2, h) = 1;\ \Gamma(z, g^2, h) = e^{\frac{\psi_2 h^2 z}{1-h\varphi_3 z}}, \\ d(z, g^2, h) = 1;\ \square(z, g^2, h) = \frac{e^{-\frac{2\psi_2 h^2 z}{1-h\varphi_3 z}}}{1-h\varphi_3 z}. \end{gathered} \tag{12}$$

In conclusion I wish to express my sincere thanks to D. V. Shirkov, who directed this work.

Note added in proof: After the present article went to press we became acquainted with [3]. Here by the same method as in [2] an expression was obtained for the four-vertex factor □ in the doubly-charged theory. Such an expression is easily obtained from (4) by the use of (5) and (6). This expression is valid only in regions (I), (II_1) and (III_1) and cannot be applied to regions (II_2) and (III_2). Therefore for the case $h-g^2x_1 < 0$ the asymptotic form of the function □ obtained in [3] is incorrect. The result in [3] is thus a special case of our result. Moreover [3] uses a calculation for the meson self energy in the h^2 approximation which gives half the correct value.

---

* Obtained for the neutral theory in [1]; for the symmetrical theory (except □) in [2].

LITERATURE CITED

[1] D. V. Shirkov, Doklady Akad. Nauk SSSR 105, 5, 972 (1955).

[2] A. D. Galanin, B. L. Ioffe and I. Ia. Pomeranchuk, J. Exptl.-Theoret. Phys. (U.S.S.R.) 29, 1, 51 (1955).

[3] I. T. Diatlov and K. A. Ter-Martirosian, J. Exptl.-Theoret. Phys. (U.S.S.R.) 30, 2, 416 (1956); I. T. Diatlov, V. V. Sudakov and K. A. Ter-Martirosian, Abstracts of Reports at the All-Union Conference on the Physics of High-Energy Particles (Moscow, 1956), p. 225.

Received April 23, 1956 M. V. Lomonosov Moscow State University

TOTAL p - d CROSS SECTION FROM 390 TO 650 MEV

V. P. Dzhelepov and V. I. Moskalev

(Presented by Academician L. A. Artsimovich May 8, 1956)

In the present article total cross section measurements are given for proton-deuteron interactions from 390 to 650 Mev, which were obtained in experiments with the synchrocyclotron of the Institute for Nuclear Problems of the Academy of Sciences USSR. These cross sections were obtained from measurements of the attenuation of a collimated proton beam in samples of light and heavy water, with "good" geometry. The general experimental scheme and method of measurement (Fig. 1) is similar to that used in [1], where the total cross section of the p-p interaction was measured from 410 to 660 mev.

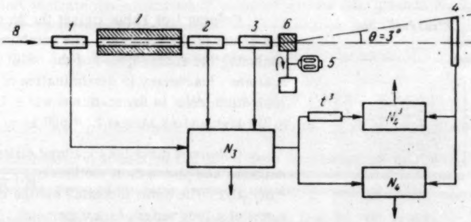

Fig. 1. Block diagram of the experiment. 1, 2 and 3) Telescope consisting of three proportional counters; 4) liquid scintillation counter, 10 cm diameter; 5) device for automatic switching of scatterers; 6) light and heavy water containers; 7) brass collimater, inside diameter 10 mm; 8) proton beam; N_3, N_4 and N_4^3) schemes of triple, quadruple and delayed quadruple coincidences; t_3) 2.5 μsec delay line.

The samples of light and heavy water used in the experiment were held in cylindrical plastic thin-walled (1 mm) containers. The diameter of the containers was 60 mm. In order to determine the scattering of protons by the container walls measurements were also made with empty containers that were identical with the two filled containers. At this time besides scattering from the walls a number of other effects were measured (scattering from the end of the counter 3, in air, etc.) which affected the "efficiency" of the scintillation counter 4 that registered the attenuated beam. This "efficiency" was usually not below 98%. All three containers (H_2O, D_2O and empty) were successively placed in the operating position automatically. The automatic device was remotely controlled; this permitted rapid exchange of scatterers without turning off the accelerator. The experimental arrangement enabled us to reduce to a minimum the possible influence of drift of the electronic apparatus as the duration of a single measurement did not usually exceed 10 minutes, and in treating the results we used only the ratios of attenuation due to H_2O and D_2O and the immediately succeeding measurements of attenuation with the empty container.

Scintillation counter 4 was placed at such a distance from the center of the scatterer that it recorded all protons that were scattered by not more than 3° from the original direction of the beam. With this geometry Coulomb scattering of protons by the samples of H_2O and D_2O had practically no effect on the magnitude of the measured attenuation.

At the same time as the count of triple and quadruple coincidences (N_3 and N_4 refer to measurements with the water samples; N_3^0 and N_4^0 refer to measurements with the empty container) a separate circuit measured the number of delayed quadruple coincidences N_4^3, which under our experimental conditions did not exceed 2% of the number of triple coincidences. The number of random quadruple coincidences for each measurement with the H_2O and D_2O samples was estimated from the formula

$$N_4^r = \left(1 - \frac{N_3^0 N_4}{N_4^0 N_3}\right) N_4^3. \tag{1}$$

This did not exceed 0.2% since in our experiments $N_3 = N_3^0$ and $N_4/N_4^0 \simeq 0.9$. Random triple coincidences in the telescope did not affect the measured attenuation as the beam intensity and, consequently, the number of these random coincidences during the course of the experiment, remained approximately constant.

TABLE 1

E_p Mev	$\sigma_{p(d-p)}$	σ_{pd}	$(\sigma_{pp}+\sigma_{np})^{*}-\sigma_{pd}$
	in 10^{-27} cm^2		
390	32.0±1.5	58.9±1.6	2.0±2.5
490	31.8±2.9	61.1±3.0	3.2±3.5
580	30.7±2.2	66.3±2.3	5.3±3.0
620	31.1±3.0	69.7±3.1	5.9±5.0
650	31.7±1.8	72.3±1.9	5.3±4.4

The results of the measurements are given in Table 1.

Column 1 of Table 1 gives the proton energies at the center of the scatterers. The combined energy spread, including the energy spread of the beam striking the scatterer, inaccuracy in determination of its energy and ionization losses in the scatterers was ± 15 Mev at E_p = = 390 Mev and ±8 Mev at E_p = 650 Mev.

Column 2 gives the measured differences of the deuteron and proton cross sections $\sigma_{p(d-p)} = \frac{1}{2}[\sigma(D_2O) - \sigma(H_2O)]$. The errors indicated are the root mean square errors of a long series of measurements. The deviations of individual measurements did not exceed the deviations to be expected from only statistical considerations. Corrections to $\sigma_{p(d-p)}$ associated with recording by the scintillation counter 4 of charged particles leaving the scatterer at angles less than 3° are negligibly small.

As our measurements show $\sigma_{p(d-p)}$ in the range 390-650 Mev remains constant within the limits of experimental error, which is in agreement with the previous data of Shapiro, Chen and Leavitt [3]. $\sigma_{p(d-p)}$ at 390 Mev is in practical agreement with $\sigma_{p(d-p)} = (31.6 \pm 2)\cdot 10^{-27}$ cm^2 obtained with 408 Mev protons in [4].

The total cross sections of the p-d interaction are given in Column 3; to determine these we used the total p-p cross sections which we obtained jointly with S. V. Medved' [1]. When the proton energy increases from 390 to 650 Mev σ_{pd} increases by about 25%. This increase is evidently associated with increase of the cross section for meson production in elementary nucleon-nucleon collisions. A comparison of our results with the total n-d cross sections in [2] supports the assumption of charge symmetry of nuclear forces at high energies.

Column 4 gives the difference between the sum of the total cross sections for free p-p and n-p collisions and the total p-d cross section. It can be seen that at proton energies of 580-650 Mev the sum of the cross sections for free nucleons and the deuteron cross section differ by an amount which somewhat exceeds the limits of experimental error and comprises about 8% of the deuteron cross section. This difference was observed more clearly at 1400 Mev [5,6], where the differences $(\sigma_{pp} + \sigma_{np}) - \sigma_{pd}$ and $(\sigma_{pp} + \sigma_{np}) - \sigma_{nd}$ are, $9 \cdot 10^{-27}$ and $6 \cdot 10^{-27}$ cm^2 (errors about $\pm\ 2 \cdot 10^{-27}$ cm^2) and also comprise about 10% of the total cross sections σ_{pd} and σ_{nd}. An analogous effect was observed in the interaction of pions with nucleons and deuterons at 200 Mev [7], 170 Mev [8], 800 Mev [9] and 1 Bev [10]. On the other hand, both our experiments at 400-500 Mev and data from several other sources [2, 4, 11] show that the difference between the total deuteron cross section and the sum of the interaction cross sections for free nucleons is not outside the limits of experimental error.

---

* Data from [1] and [2]; at 650 Mev we used $\sigma_{np} = (37 \pm 4)\cdot 10^{-27}$ cm^2.

Several more or less significant causes of the observed decrease of the deuteron cross section can be mentioned. These clearly can include "screening" of one nucleon in the deuteron by the other, interference effects, forbidding of some final nucleonic states by the Pauli principle, and simultaneous interaction of all three particles participating in the collision. In [6] an attempt is made to calculate this effect quantitatively on the basis of "screening" of one nucleon by the other. The calculation used the methods of the diffraction theory which is usually employed to calculate scattering in the presence of strong absorption. For the total deuteron cross section the following formula was obtained:

$$\sigma_d = \sigma_1 + \sigma_2 - \frac{\sigma_1\sigma_2}{4\pi}\left(\frac{1}{r^2}\right)_d. \qquad (2)$$

where σ_1 and σ_2 are the cross sections for free nucleons, and $r_d = 1.7 \cdot 10^{-13}$ cm is the deuteron radius in the triplet state. The third term in this formula, which corrects for "screening", at 1.4 Bev is equal to $6 \cdot 10^{-27}$ cm^2. Since for 600-650 Mev the meson-production cross sections in nucleon-nucleon collisions comprise a considerable portion of the total cross sections (30-40%), Formula (2) can also be used for these energies; then for the "screening" term we obtain $4 \cdot 10^{-27}$ cm^2. Thus within the limits of the assumptions made for the calculation and the relatively large experimental error we have obtained satisfactory agreement between calculations and experimental results; this may indicate the correctness of proposed explanations given in [6] for the departure from additiveness of the nucleon cross sections in the deuteron.

We wish to thank S. V. Medved' for assistance with the measurements.

LITERATURE CITED

[1] V. P. Dzhelepov, V. I. Moskalev and S. V. Medved', Doklady Akad. Nauk SSSR 104, 380 (1955).

[2] V. P. Dzhelepov, V. I. Satarov and B. M. Golovin, Doklady Akad. Nauk SSSR 104, 717 (1955).

[3] C. P. Leavitt, Proc. of the Fifth Annual Rochester Conference, 1955.

[4] J. Marshall, L. Marshall and V. A. Nedzel, Phys. Rev. 91, 767 (1953).

[5] T. Coor, D. A. Hill, et al., Phys. Rev. 98, 1369 (1955).

[6] R. J. Glauber, Phys. Rev. 100, 242 (1955).

[7] A. E. Ignatenko, A. I. Mukhin, E. B. Ozerov and B. M. Pontecorvo, Doklady Akad. Nauk SSSR 103, 209 (1955); J. Exptl.-Theoret. Phys. (USSR) 30, 7 (1956) [Soviet Physics – J.E.T.P., p. 10].

[8] J. Ashkin, J. P. Blaser, et al., Phys. Rev. 96, 1104 (1954).

[9] O. Piccioni, cited in [6].

[10] R. L. Cool, L. Madansky and O. Piccioni, Phys. Rev. 93, 637 (1954).

[11] V. A. Nedzel, Phys. Rev. 94, 174 (1954).

Received May 4, 1956

Institute for Nuclear Problems, Academy of Sciences USSR

AN EXPERIMENTAL INVESTIGATION OF THE ANGULAR DISTRIBUTION AND POLARIZATION OF OPTICAL RADIATION FROM ELECTRONS IN A SYNCHROTRON

F. A. Korolev, V. S. Markov, E. M. Akimov and O. F. Kulikov

(Presented by Academician A. A. Lebedev April 25, 1956)

The purpose of the present work was the experimental test of the theory of the radiating electron which was expounded by D. D. Ivanenko and A. A. Sokolov [1]. The work was done in 1955 on the electron synchrotron in the laboratory of V. I. Veksler.

The first calculations of emission from an electron in uniform circular motion were those of Schott [2] and were related to atomic models that were abandoned upon the appearance of the Bohr theory. D. D. Ivanenko and I. Ia. Pomeranchuk [3] were the first to show that electrons which move in circular orbits in cyclical accelerators will radiate and thus limit the maximum energy obtainable in a betatron. L. Artsimovich and I. Pomeranchuk [4], Schiff [5] and others have further developed the theory of radiation by electrons in cyclical accelerators. In [1, 6-11] the classical theory of the radiating electron was perfected and the quantum theory was developed.

This emission was detected experimentally by Blewett [12] as well as by Pollack and his associates [13, 14]. In [14, 15] the spectrum of the radiation was studied as well as the change in intensity in the accelerating cycle. No special work was done on the polarization effects and the angular distribution. Only [13, 14] contain indications of qualitative observation of linear polarization. These authors observed only one polarization component and did not detect the existence of the other component whose electric vector is parallel to the magnetic field.

Since the angular intensity distribution and polarization of the radiation are fundamental results of the theory [1] their experimental investigation is of very great interest. For this purpose we constructed optical apparatus which enabled us to study the angular distribution of radiation from sychrotron electrons both with respect to the polarization component whose electric vector is parallel to the plane of the orbit (σ-component) and the component whose electric vector is perpendicular to the electric vector of the first component (π-component). For this purpose the apparatus included suitable polarizing devices. The radiation was recorded photographically and the photographs were studied by photographic photometry. Radiation from the synchrotron chamber passed through a special window. The work was performed on the visible spectrum, individual portions of which were singled out by interference light filters with a broad transmission band of the order 100 A.

We obtained a large number of photographs of the angular intensity distribution for the different polarization components from electrons accelerated to different energies. The left side of Fig. 1 is a photograph of the π-component; the right side is the σ-component. The numerals over the photographs are the serial numbers of the photographs taken in the experimental work. Figure 2 contains microphotograms of the same photographs. Figure 3 gives graphs of the intensity distribution for the π-and σ-components. λ 4080 A is the maximum wave length of the transmission band of the light interference filter. The circles represent experimental data; the theory is given by the solid curves. The curves were drawn on the basis of the theory in [1] for 250 Mev and λ 4000 A. Experimental curves were constructed from the photometric study of photographs obtained by the summation of radiation over the entire accelerating cycle. Considering the slight dependence of the angular intensity distribution on the energy of the accelerated electrons > 100 Mev, where basically all of the ra-

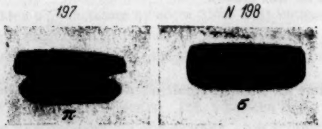

Fig. 1. Photographs of the π component and the σ component of polarized radiation from an electron.

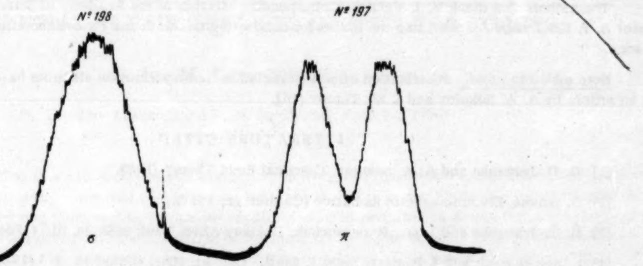

Fig. 2. Microphotograms of the photographs of radiation from electrons which are reproduced in Fig. 1.

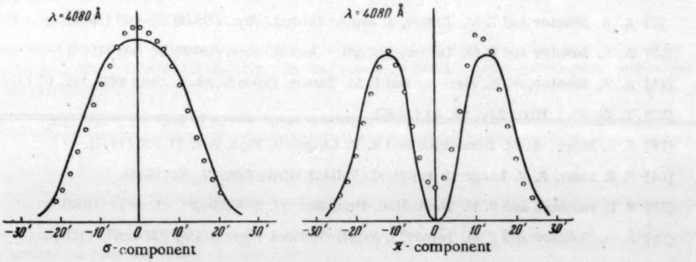

σ-component

π-component

Fig. 3. Angular intensity distribution of the π- and σ-polarization components of radiation from electrons.

diation occurs, it is possible to compare the experimental results with the theoretical calculations given above.

Figure 3 shows very satisfactory agreement of experiment and theory. The nonzero intensities between the peaks of the π-component can be attributed to betatron oscillations and imprecise adjustment of the optical system.

From the comparison of the exposures required to obtain identical darkening on the photographic plates it follows that the π-component is several times weaker in intensity than the σ-component, which is in agreement with theory. Photographs obtained for electrons accelerated to different energies showed the slight energy dependence of the angular intensity distribution which is predicted by theory.

We also detected qualitatively the presence of elliptical polarization, but this was not studied in detail. At the present time a more thorough investigation is being made of the above-mentioned effects over a broad spectral range.

The authors are deeply grateful to Professor D. D. Ivanenko for initiating the investigation and for assistance with the work, and to Professor A. A. Sokolov and Instructor I. M. Ternov for communicating experimental results and for assistance in the comparison of the experiment with theory.

The authors also thank V. I. Veksler, Corresponding Member of the Academy of Sciences USSR and Professor A. P. Cherenkov for providing the means for conducting this work and for collaboration during its performance.

Note added in proof. Polarization effects in radiation from synchrotron electrons have also been treated in an article by A. A. Sokolov and I. M. Ternov [16].

LITERATURE CITED

[1] D. D. Ivanenko and A. A. Sokolov, Classical Field Theory (1949).

[2] G. Schott, Electromagnetic Radiation (Cambridge, 1912).

[3] D. D. Ivanenko and I. Ia. Pomeranchuk, Doklady Akad. Nauk SSSR 44, 315 (1944).

[4] L. Artsimovich and I. Pomeranchuk, J. Exptl.-Theoret. Phys. (USSR) 16, 379 (1946).

[5] R. J. Schiff, Rev. Sci. Instr. 17, 6 (1946).

[6] D. D. Ivanenko and A. A. Sokolov, Doklady Akad. Nauk SSSR 59, 1551 (1948).

[7] A. A. Sokolov, N. P. Klepikov and I. M. Ternov, J. Exptl.-Theoret. Phys. (USSR) 23, 632 (1952).

[8] A. A. Sokolov, N. P. Klepikov and I. M. Ternov, J. Exptl.-Theoret. Phys. (USSR) 25, 249 (1953).

[9] A. A. Sokolov and I. M. Ternov, J. Exptl.-Theoret. Phys. (USSR) 25, 698 (1953).

[10] A. A. Sokolov and I. M. Ternov, J. Exptl.-Theoret. Phys. (USSR) 28, 431 (1955).

[11] A. A. Sokolov, A. N. Matveev and I. M. Ternov, Doklady Akad. Nauk SSSR 102, 65 (1955).

[12] T. Blewett, Phys. Rev. 69, 87 (1946).

[13] F. R. Elder, A. M. Gurewitsch and R. V. Langmuir, Phys. Rev. 71,829 (1947).

[14] F. R. Elder, R. V. Langmuir and H. C. Pollack, Phys. Rev. 74, 52 (1948).

[15] P. L. Hartman and P. H. Tombulian, Phys. Rev. 87, 233 (1952); 91, 1577 (1953).

[16] A. A. Sokolov and I. M. Ternov, J. Exptl.-Theoret. Phys. (USSR) 31, 3, 473 (1956).

Received April 24, 1956

M. V. Lomonosov Moscow State University

THE POTENTIAL IN PAIR THEORIES OF NUCLEAR FORCES

Iu. M. Lomsadze

(Presented by Academician N. N. Bogoliubov April 12, 1956)

It is known [1-3] that in a pair theory of the interaction between two (quantized) spinor fields, the nucleon and meson fields, the interaction potential of the two nucleons as calculated in nonrelativistic approximation for these nucleons and neglecting their recoils, in first nonvanishing order of perturbation theory (second order in the field coupling constant) has a singularity at the origin of the form $1/r^5$ (r is the distance in three dimensions between the nucleons).* As is also quite well known, such a strong singularity of the potential – stronger than $1/r^2$ – theoretically leads to the denial of the possibility of stationary bound states of the two-nucleon system, which is in clear contradiction, for example, with the fact that the deuteron exists.

The question arises, cannot this unsatisfactory situation be changed by a consistent relativistic theory of nucleons which takes their recoil into consideration? It is known, for instance [4], that for relativistic electrons the singularity of the electromagnetic potential is reduced in higher orders to $1/r$ (to within a logarithmic factor) while for nonrelativistic electrons the potential in the fourth order with respect to the charge e, for example, reveals an unsuitable singularity of the form $1/r^3$.

It is the purpose of the present article to answer this question, for which purpose we had to suitably solve the new problem, for pair theory, of eliminating infinities that appear in the first nonvanishing order, unlike the case in ordinary nonpair theories.

Let us consider specifically the case of pseudoscalar coupling:

$$\mathcal{H}_g(x) = g\bar{\Psi}(x)\gamma_5\Psi(x)\cdot\bar{\psi}(x)\gamma_5\psi(x), \tag{1}$$

where $\Psi(x)$ and $\psi(x)$ are the operators of the nucleon and meson** (spinor) fields, respectively; $\bar{\Psi}(x) \equiv \Psi^H(x)\gamma_4$ and the index H denotes the Hermitian conjugate operator.

The character of the singularity at the origin for the interaction potential of two nucleons is most clearly seen [4] by investigating the asymptotic behavior for large momenta of the scattering S matrix of these nucleons, for the calculation of which (by the perturbation method) we use the obvious extension to pair theory of the Feynman-Dyson diagram method.

In a pair theory of the form (1), unlike ordinary nonpair theories, to every point of the diagram there will be attached not three but four lines: two nucleon (solid) lines – an ingoing and an outgoing, and two meson (dotted) lines – also an ingoing and an outgoing. Each diagram point in pair theory may be regarded as split into two points, one belonging to the succession of nucleon lines (with the operator $\sqrt{g}\gamma_5$ introduced correspondingly into the S matrix) the other to the succession of meson lines (with the same operator introduced). All other rules for the calculation of an S matrix are carried over into pair theory without alteration.

---

* When the interaction part of the Hamiltonian does not contain derivatives of the operator fields, as will be assumed hereinafter; in the contrary case the singularity becomes even stronger.

** Of a muon, for example.

The scattering of two nucleons in first nonvanishing (second in g) order is represented by a single diagram (I) accurate apart from "exchange":

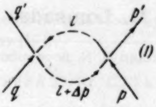

($\Delta p \equiv \Delta p_{\mu} \equiv p'_{\mu} - p_{\mu}$, $p^2 = q^2 = p'^2 = -m^2$, m is the nucleon rest mass), the S matrix element of which is by an already known procedure [4] put into "relativistically covariant" form (in "natural" units):

$$S_g(\Delta p^2) = g^2 A \tilde{S}_g(\Delta p^2),$$

$$A \equiv \overline{\Psi}_{p'}\gamma_5\Psi_{p} \cdot \overline{\Psi}_{q'}\gamma_5\Psi_{q} \cdot \delta(p'_{\mu} - p_{\mu} + q'_{\mu} - q_{\mu}), \tag{2}$$

$$\tilde{S}_g(\Delta p^2) \equiv 4\int_0^1 dx \int d^4l \, \frac{-l^2 + \Delta p^2\alpha - \mu^2}{(l^2 + \Delta p^2\alpha + \mu^2)^2},$$

$$\alpha \equiv x(1-x), \ \mu^2 \equiv \mu^2 - i\epsilon,$$

where Ψ_p, Ψ_q are the amplitudes of plane waves with the indicated momenta; μ is the meson rest mass; $\epsilon > 0$ after integration approaches zero.

In order to avoid possible ambiguity of the final results we shall here and hereinafter follow a rule requiring preliminary conversion of all initial and generally divergent ℓ-integrals to "relativistically covariant" form. By this we mean the form of the ℓ-integrals in which the integrand depends on $\ell \equiv \ell_{\mu}$ only through ℓ_{μ}^2. The method of converting the integrals to this form follows from general considerations of relativistic covariance.

It may be found that $\tilde{S}_g(\Delta p^2)$ in (2), diverging quadratically for large ℓ, contains an (infinite) part which can (and in accordance with the general concept of renormalization must) be included in the constant κ of a "contact" term of the form $\kappa\,[\overline{\Psi}(x)\gamma_5\Psi(x)]^2$. For this purpose the Hamiltonian contains an additional term:

$$\mathscr{H}'_g(x) = \mathscr{H}_g(x) + \delta\kappa\,[\overline{\Psi}(x)\gamma_5\Psi(x)]^2, \tag{3}$$

in which the constant $\delta\kappa$ is found, as usual, from the vanishing of the S matrix of a "self-energy" process, in this case for two nucleons. In the first nonvanishing order with respect to g and $\delta\kappa$ this process is represented by two diagrams (II):

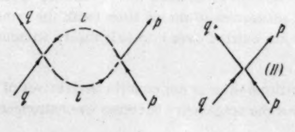

We obtain

$$\delta\varkappa = -\frac{g^2}{(2\pi)^4}\widetilde{S}_g(\Delta p^2 = 0) + O(g^4). \tag{4}$$

If we now operate with the Hamiltonian not in the form (1) but in the form (3), then for the scattering of two nucleons in the second order with respect to g, to diagram (I) another diagram (III) is added:

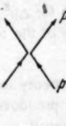

(III)

The sum of the elements of the S matrix which correspond to diagrams (I) and (III):

$$\begin{aligned} S_g(\Delta p^2) = g^2 A\widetilde{S}'_g(\Delta p^2),\ \widetilde{S}'_g(\Delta p^2) &\equiv \widetilde{S}_g(\Delta p^2) - \widetilde{S}_g(\Delta p^2 = 0) = \\ &= 4\Delta p^2\int_0^1 dx\,\alpha\int d^4l\,\frac{3l^2 + \Delta p^2 x + 3\mu^2}{(l^2+\mu^2)(l^2+\Delta p^2\alpha+\mu^2)}, \end{aligned} \tag{5}$$

now diverges only logarithmically.

This last divergence can be included in the constant k of the "contact" term

$$k\left\{\frac{\partial}{\partial x_\mu}\left[\overline{\Psi}(x)\gamma_5\Psi(x)\right]\right\}^2 \tag{6}$$

of somewhat different form. Considerations identical with the above lead to the expression

$$\delta k = -\frac{g^2}{(2\pi)^4}\lim_{\Delta p^2\to 0}\frac{\widetilde{S}'_g(\Delta p^2)}{\Delta p^2} + O(g^4), \tag{7}$$

as a result of which the term (6) in which we set k → k + δk also contributes to our S matrix for the scattering of two nucleons, of the second order in g, thus converting it into the final and now finite form

$$\begin{aligned} S''_g(\Delta p^2) &= g^2 A\widetilde{S}''_g(\Delta p^2), \\ \widetilde{S}''_g(\Delta p^2) &\equiv \widetilde{S}'_g(\Delta p^2) - \Delta p^2\lim_{\Delta p^2\to 0}\frac{\widetilde{S}'_g(\Delta p^2)}{\Delta p^2} = \\ &= -12\pi^2 i\Delta p^4\int_0^1 dx\int_0^1 dy\int_0^y dz\,\alpha^2 z^2\left[\frac{5}{\lambda} + \frac{3\Delta p^2\alpha + 10\mu^2}{3\lambda^2} + \frac{(\Delta p^2\alpha+\mu^2)\mu^2}{3\lambda^3}\right], \\ \lambda &\equiv \Delta p^2\alpha(1-z) + \mu^2. \end{aligned} \tag{8}$$

For our purposes it is unnecessary to perform any further calculations with (8).

It should be emphasized that (8) could perhaps be obtained more simply by applying to (2) the two "regularizations" of Pauli and Villars [5]:

$$\sum_i C_i = 0, \quad \sum_i C_i \mu_i^2 = 0, \tag{9}$$

but just this possibility of reducing our "subtraction" method to renormalizations is evidence of its internal consistency.

It is easily found directly from (8) that $\tilde{S}_g''(\Delta p^2)$ for $\Delta p^2 \to \infty$ behaves as $\Delta p^2 \ln \Delta p^2$; this indicates that the corresponding potential has at the origin a singularity of the form $\ln r/r^5$, that is, the singularity is also a little stronger than obtained previously.

We have confined our examination of the pair theory to pseudoscalar coupling. But the examination of other possible forms of field coupling (scalar, vector, pseudovector and tensor) as well as of the additional variants of the pair theory suggested in [3] leads to the same result.

Consideration of relativity and nucleon recoil thus does not eliminate the unsatisfactory aspects of the pair theory of interactions between spinor fields.

It is also not superfluous, especially in view of the interest shown lately in theories with so-called "nonlinear interaction", to determine the character of the singularity of the potential in the other forms of pair theory, such as the pair theory of the interaction of a spinor nucleon field $\psi(x)$ with a scalar (or pseudoscalar) meson field $\varphi(x)$:

$$\mathscr{H}_f(x) = f\overline{\Psi}_\varsigma(x)\,\Psi(x)\,\varphi^H(x)\,\varphi(x). \tag{10}$$

Analogous calculations* lead to the following expression for an element of the S matrix for scattering of two nucleons:

$$S_f''(\Delta p^2) = f^2 A \tilde{S}_f''(\Delta p^2),$$

$$\tilde{S}_f''(\Delta p^2) = \frac{\pi i \Delta p^4}{\mu^2} \int_0^1 dx \, \frac{(x^2 - \alpha)\,\alpha}{\Delta p^2 \alpha + \mu^2}, \tag{11}$$

which, as is easily seen, for $\Delta p^2 \to \infty$ behaves as Δp^2, which corresponds to a $1/r^5$ inadmissible singularity at the origin.

Summing up the above we can conclude that if the current theory adequately describes reality at very small distances, then either constants such as g and f for coupling of a nucleon field with mesons must be considered exactly equal to zero or, if they are not zero, the contradiction which arises between the theory and reality must be attributed to inadequacies of the usual perturbation method.

We note in conclusion that all of the above relates to only the first nonvanishing order of the perturbation method. The problem of the singularity of the potential in higher orders of pair theory encounters the difficulty due to the "nonrenormalizability" of pair theories. However, we have been obliged to discuss this question outside of the present article.

---

* We note here that in the theory of (10) unlike the theory of (1) our S matrix is finite after renormalization of the constant κ. However, in accordance with the general concept, it is still necessary to renormalize the constant k. This renormalization amounts to subtracting from the S matrix a certain finite part, which considerably changes its asymptotic form for $\Delta p^2 \to \infty$.

LITERATURE CITED

[1] I. Tamm and D. Ivanenko, Nature 133, 981 (1934).

[2] R. Marshak, Phys. Rev. 57, 1101 (1940).

[3] Iu. Lomsadze and M. Markov, J. Exptl.-Theoret. Phys. (USSR) 19, 178 (1949).

[4] Iu. Lomsadze, On the Electromagnetic Interaction of Two Electrons in the Higher Approximations of Perturbation Theory, Dissertation, Phys. Inst., Academy of Sciences USSR (Moscow, 1954); J. Exptl.-Theoret. Phys. (USSR) 30, 707 (1956). [Soviet Physics – J.E.T.P., p. 554].

[5] W. Pauli and F. Villars, Symp. Level Shifts of Atomic Electrons (For. Lit. Press, 1950).

Received February 27, 1956

Uzhgorod State University

A METHOD OF INVESTIGATING THE ELECTRONIC STATES OF DIATOMIC MOLECULES

THE ELECTRONIC STATES AND BOND DISTANCES OF ALKALI METALS AND THEIR HYDRIDES*

F. Sh. Shifrin

(Presented by Academician A. N. Terenin May 23, 1956)

1. Method. For homologous molecules** we have previously [1] established the rule: optical electronic terms T_k are approximately inversely proportional to the molecular bond distances ℓ: $T_k\ell = C_k$ = const. We here present a method of investigation the T_k of diatomic molecules (and probably also of polyatomic molecules [1]) – the mutual agreement of the set of electronic terms of homologous molecules by means of the said rule.

TABLE 1

Molecule	Bond	Terms [2]		$T_k l$
		Symbol	T_k	
Na_2	3.07	$A'\Sigma_u^+$	14680	45000
		$B'\Pi_u$	20319	62400
K_2	3.91	$A'\Sigma_u^+$	11684	45500
		$B'\Pi_u$	15378	60300
Rb_2	4.23	$A'\Pi$	24663	62000

We shall explain the method by means of the example given in Table 1. It can be seen here that the values of $T\ell$ for different molecules are indeed grouped close to two numbers: 45,000 and 60,000. Terms with close values of $T\ell$ are given [1] the same serial number and symbol. For $T\ell \sim 45{,}000$ we take $T = T_1$ and symbol $A'\Sigma_u^+$ ($A'\Sigma^+$ if the atoms are different), for $T\ell \sim 60{,}000$ we take $T = T_2$ and $B'\Pi_u$ ($B'\Pi$). Then for the term 14663 of Rb_2, where $T\ell = 60{,}000$ we obtain the number 2 and the symbol $B'\Pi_u$ instead of $A'\Pi$ in [2], that is, this is not the first T_1 but the second T_2 of the excited terms, and it is also odd (index u). T_1, which is absent in [2], evidently has the symbol $A'\Sigma_u^+$, $T_1\ell \sim 45{,}000$. Hence, from the knowledge that ℓ for Rb_2 is 4.23 it can be predicted that $T_1 \sim 10{,}600$.

The method is simple and clearly effective. It enables us to classify (establishing the numbers and symbols) electron terms (band systems), reveal the existence of previously unobserved terms and predict their approximate values (or with known T_k to give ℓ).

Hereafter when a new term (correcting the old term) is found for any molecule it will be possible to determine the degree of similarity and to predict (correct) this term for its homologues.

2. Alkali metals and their hydrides. The results of a review, by the indicated method, of the experimental values of T_k and ℓ of these molecules are given in Table 2 (we do not write the zero term):

1) The rule was verified and confirmed by additional data that the product $T_k\ell$ for k = 1, 2, . . ., 9 within a column is approximately constant; it changes very much less than T_k (ΔT_k and $\Delta(T_k\ell)$ in Table 2):***

---

* A preliminary report was presented at the 8th scientific meeting of the Herzen Pedagogical Institute April 12, 1955.

** Homologous molecules are diatomic molecules consisting of atoms of the same group of the periodic table. Terminology, notation, units and references to the literature are the same as in [1]. There are slight discrepancies between the different sources. For definiteness we have retained [2], where the data of interest are most full presented.

*** In [1] only k = 1, 2 have been taken and the ionization potentials ΔT_k and $\Delta(T_k\ell)$ in Table 2 refer only to data in the literature (the number of the latter differs for different columns), except Li_2 (compare [1]). The rough nature of the rule permits us to take the wave numbers ν_{00} (with the letter R) instead of T_ℓ, the half sum of the bond distances of Na_2 and K_2 as ℓ for NaK (similarly for other intermetallic molecules), etc.

TABLE 2

System of Electronic Levels of Molecules of Alkali Metals and Their Hydrides

Molecule	l	A $^1\Sigma_u^+, ^1\Sigma^+$ T_1	B $^1\Pi_u, ^1\Pi$ T_2	C $^1\Pi$ T_3	D $^1\Sigma_u^+, ^1\Sigma^+$ T_4	E $^1\Sigma$ T_5	F $^1\Pi_u, ^1\Pi$ T_6	G $^1\Sigma$ T_7	H $^1\Sigma$ T_8	I $^1\Pi$ T_9	J $^1\Sigma$ T_{10}
1. Molecules of alkali metals											
A. Molecules consisting of identical atoms											
Li_2	2.67	14068	20437	(22800)	30559	R 30886	R 31375	R 31899	34800	35800	37600
Na_2	3.07	14680	20319	(22800)	29342	R 31144	R 32241	R 33466	R 34685	R 45846	R 37613
K_2	3.91	11684	15378	(17970)	22970	R 24485	24628	26493	27571	28091	29600
Rb_2	4.23	10600^8	14663^1	(16500)	20835	22500	22777	24400	25300	26000	27300
Cs_2	4.55	9900^9	13044^2	$(15400)^{10}$	19750^{11}	21000^{12}	21500	22600	23500	24200	25400
Б. Molecules consisting of different atoms											
LiNa	2.87	15700	20900	24400	31300	(33200)	(34100)	(36000)	(37300)	(38300)	(40300)
LiK	3.29	13700	17579^3	21300	27300	(29000)	(29700)	(31300)	(32500)	(33400)	(35100)
LiRb	3.45	13000	17550^4	20300	26000	(27600)	(28400)	(29900)	(31000)	(31900)	(33500)
LiCs	3.61	12450	16477^5	19400	24900	(26400)	(27100)	(28500)	(29600)	(30500)	(32000)
NaK	3.49	12140	16991	20091	25228	(27300)	(28000)	(29500)	(30700)	(31500)	(33100)
NaRb	3.65	12300	16422^6	19200^{13}	24600	(26100)	(26800)	(28200)	(29300)	(30200)	(31600)
NaCs	3.81	11800	15750	18249	24270	$(25000)^{14}$	(25700)	(27000)	(28100)	(28900)	(30400)
KRb	4.07	11050	14750	17200	22100	(23500)	(24000)	(25300)	(26300)	(27000)	(28400)
KCs	4.23	10600	14200	16500	21200	(22500)	(23100)	(24400)	(25300)	(26000)	(27300)
RbCs	4.39	10200	13747^7	15950	20500	(21700)	(22300)	(23500)	(24400)	(25000)	(26300)
2. Molecules of alkali hydrides											
LiH	1.59	26516	37700	(44000)	(56500)	(60000)	(61500)	(64800)	(67300)	(69200)	(72600)
NaH	1.89	22719	31707^{15}	(37000)	(47500)	(50500)	(51700)	(54500)	(56700)	(58200)	(61100)
KH	2.24	19530	26800^{16}	(30600)	(40100)	(42500)	(43700)	(46000)	(47800)	(49200)	(51600)
RbH	2.37	18906	25300	(29500)	(37900)	(40200)	(41300)	(43400)	(45200)	(46400)	(48700)
CsH	2.49	18409	24100	(28100)	(36000)	(38300)	(39300)	(41400)	(43000)	(44200)	(46400)
ΔT_k, %		127	56	10	40	27	41	26.5	25	27.5	
$\Delta(T_k l)$%		9	8	1	5	0.5	2.5	0.7	1	0.2	
$[T_k l]$		45000	60000	70000	90000	95500	98000	103000	107000	110000	115500

Remarks:

1. Example. Correction of the numbers and symbols for T_2.

No. of superscript in table	1	2	3, 4, 5, 7	6
In [2]	A'Π	A'Π?	A	A'Π
In Table 2	B'Π_u	B'Π_u	B'Π	B'Π

2. To the predicted terms supplied with the superscripts 8-16 the following observed values correspond: 8. Rb_2 T ~ 11,500 [3]; 9. Cs_2 T ~ 10,000 [3]; 10. Cs_2 T−B 16,066 and C 16,176 [2]?; Cs_2 ~ 19,200 [5]? 12. Cs_2 ~ 21,200 [5]? ~ 20,500 [3]; 13. NaRb: unanalyzed system ~ 18,600 [3, 6]; 14. NaCs ν 25,400-24,800 [2]; 15. NaH ν ~ 32,000 [4]; 16. KH B'Π T−28,834 [4].

2) In some cases the numbers and symbols of terms taken from the literature [2] have been corrected (for example, those with superscripts 1-7 in Table 2); and many terms which are absent in [2] have been predicted (small type) – these apparently have not been observed, are sometimes disputed, etc.* In some cases it was possible to compare the predictions with observations and agreement was found (superscripts 8-16 in Table 2).

State B of the hydrides is evidently unstable and decays into an unexcited H atom and an excited (2^2P – excitation energy Π) alkali atom; hydride states dissociate mainly (dissociation energy D) into unexcited atoms. If such is the case then $T_2 = \Pi + D$. For the values of T_2 predicted in Table 2 this is observed roughly.

For the predictions of T_k we used the same round figure for $T_{k\ell}$ in the case of all molecules except Li_2 (denoted by $[T_{k\ell}]$); for Li_2 the numbers were divided by 1.15 since those $T_{k\ell}$ which are known for this molecule are less than the corresponding $[T_{k\ell}]$ by a factor of 1.1 to 1.2; this is presumably related to the lower effective charge of the atomic cores in the case of Li_2 (compare Slater's rules and [1]). It may be possible to improve the predictions by considering to a greater extent the gradations in similarity and taking for the prediction of T_1 for Rb_2 and Cs_2 not $[T_1\ell] = 45{,}000$ but the known value $T_1\ell = 45{,}500$ of their closest homologue κ_2 by taking the known $T_1\ell = 42{,}300$ of NaK also for other "alloys", etc.

When in the future a reliable value of the ionization potential I is found for one of the molecules it will be possible to predict I for the others. When ℓ is obtained (and preferably also some of $T_1, \ldots, T_{10}$, in order to determine the degree of similarity), for Fr_2, say, it will be possible to predict $T_1, \ldots, T_{10}$ for Fr_2, LiFr, NaFr, KFr, RbFr, CsFr, FrH, i. e., to determine as many as 70 numbers from one or a few.

Although the predictions are rough and not uniformly reliable they are useful for preliminary orientation and also for determination of the conditions under which the rule itself can be applied.

LITERATURE CITED

[1] F. Sh. Shifrin, Doklady Akad. Nauk SSSR 106, 233 (1956) [Soviet Physics – Doklady, p. 32].

[2] Landolt-Bŏrnstein, Zahlenwerte und Funktionen, Aufl. 6, 1, T. 2, 3 (1951).

[3] Donnees spectroscopiques, concernant les molecules diatomiques, Red. B. Rosen (Paris, 1951).

[4] T. Hori, Japan J. Phys. 8, 151 (1933).

[5] J. M. Walter and S. Barrat, Proc. Roy. Soc. (London) A 119, 257 (1928).

[6] G. Herzberg, Molecular Spectra and Molecular Structure 1, Spectra of Diatomic Molecules, 2 ed. (1951).

Received March 17, 1956

A. I. Herzen (Leningrad) State Pedagogical Institute

---

* Reservations. 1) It is quite possible that instead of the two terms T_5, T_6 taken here, following [2], there is only one [3, 6] (then the numbers of the following T_k are changed). 2) It is not sufficiently clear for all terms that we are justified in assuming agreement between the "pure metals" (like Na_2) and the "alloys" (like NaK) and with the hydrides. We have bracketed the more doubtful predictions. The numbers in the brackets are not actually predicted terms but only indications where they must be found if similarity is observed [1]. It is doubtful to varying degrees whether such terms actually exist. But in cases where such existence is perhaps excluded the numbers in brackets can serve in comparisons of homologous molecules. 3) It is possible, especially for "alloys" that there exists a term with $T_\ell \sim 80{,}000$.

There are other possible limitations. Table 2 will probably require correction and revision following new observations and varied analysis which will include, among other means, the above-proposed method of agreement.

A POSSIBLE EXAMPLE OF ANOMALOUS DECAY OF A HYPERFRAGMENT

A. A. Varfolomeev, R. I. Gerasimova and L. A. Karpova

(Presented by Academician L. A. Artsimovich May 25, 1956)

A stack of 56 nuclear track plates was irradiated in the stratosphere for the purpose of studying unstable particles. The plates were made of Type P emulsion with a thickness of 330 μ and 10 cm diameter each (see also [1, 2]). One of the detected secondary stars was attributed to an unstable fragment which decays with unusually small reaction energy.

The primary star was of the 18 + 4n type. Particle a (Fig. 1) is emitted, which after traversing 39 μ decays emitting two charged particles, b and c. Both of the latter are stopped in the emulsion with ranges 15.5 + 0.3 mm and 4.5 + 0.5 μ, respectively. The tracks of a, b and c are coplanar within 2°. The angle between tracks b and c is 169 ± 4°.

Track a has 3 gaps and no noticeable δ-electron tracks. This agrees with the assumption that a decayed after stopping or just before stopping. For the purpose of determining its charge a measurement was made of the darkened area in the track by a graphical photometric method [3]. At an enlargement of ~ 4500 x the track image was projected on a screen. The track was accurately traced with a pencil and for each point of the contour the micrometer screw of the microscope was adjusted to give the clearest image of the track. The track contour was then transfered to fixed x-ray film and covered with India ink. The area of the darkened track image was determined photometrically in 12 μ sections. The areas of the sections served as a measure of particle ionization at the given points of the track. Measurements along a were compared with area measurements for a few tracksof protons, alpha particles and Li nuclei. In order to reduce the possible errors the comparison employed tracks whose angle α with the plane of the emulsion was the same as that of track a ($\tan \alpha = 0.23$).

The measurements showed the charge of the particle to be $z_a \leq 3$ and presumably less than 3. On the other hand the area of track a was somewhat greater than the area of the corresponding portions of the proton tracks, from which it followed that the mass of particle a at least exceeded the proton mass.

From the grain count as well as from the count of gaps in the track it was established that track b belongs to a pion stopped in the emulsion. Since at the stopping point of the pion no muon track was detected track b must be ascribed to a π-meson. Its energy allowing for the possibility of track straggling was determined as 29.4 ± 1.2 Mev. The stopping power of the emulsion agreed to within 1 or 2% with the stopping power of the Ilford G-5 emulsion. Therefore in order to determine the energies of light particles from their tracks, tables [4] were used and energies of fragments were determined from their tracks from the data in [5].

The case under consideration cannot be interpreted as nuclear disintegration due to a Σ-hyperon since the absorption of a Σ^--hyperon by a nucleon must according to Gell-Mann's scheme give the reaction $\Sigma^- + p \rightarrow \Lambda^0 + n$. It follows from the shortness of the track that the disintegration could result from the capture of a Σ^--hyperon by a light nucleus such as C, N or O and not a heavy nucleus such as Ag or Br. The emission of a pion is then possible only if the Λ^0 particle is absorbed by the residual nucleus, which must be at rest. The Λ^0 particle must then decay inside the fragment at rest and emit a π-meson. Of course, such a process without the emission of charged particles in the primary event and without transfer of momentum to the residual nucleus which captures the Λ^0 particle is extremely improbable if at all possible.

On this basis the case was interpreted as the decay of an unstable fragment associated with an Λ^0 particle. In the analysis of the different possible decay schemes of the fragment it was assumed that the ultimate recoil

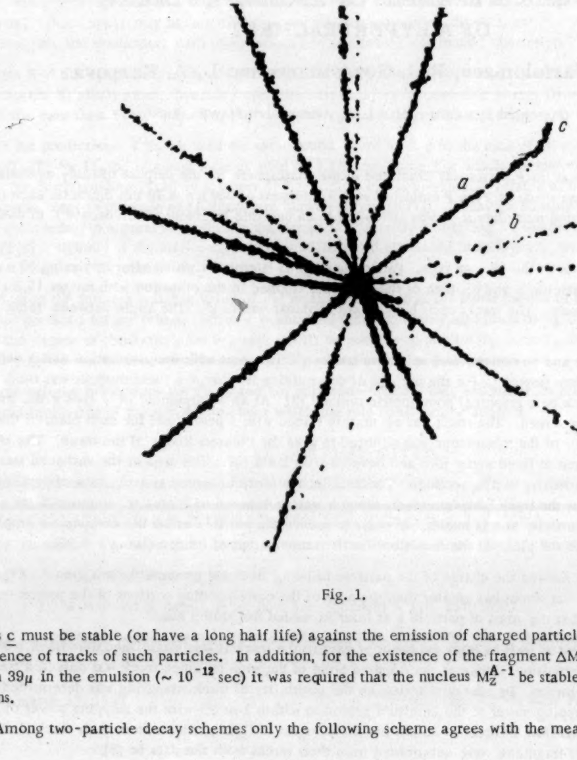

Fig. 1.

nucleus c must be stable (or have a long half life) against the emission of charged particles in accordance with the absence of tracks of such particles. In addition, for the existence of the fragment ΔM_Z^A during the flight time through 39μ in the emulsion ($\sim 10^{-12}$ sec) it was required that the nucleus M_Z^{A-1} be stable against emission of nucleons.

Among two-particle decay schemes only the following scheme agrees with the measurements:

$${}_{\Lambda}H^4 \rightarrow He^4 + \pi^- + Q,$$

where the reaction energy $Q \approx 31$ Mev. However, the value of the Λ^0 particle binding energy $B_\Lambda \approx 26$ Mev which is obtained in this case is too large and does not agree with the average value of B_Λ from the measurements of other authors (1-2 Mev). The same considerations evidently do not allow the three-particle scheme

$${}_{\Lambda}H^4 \rightarrow He^3 + \pi^- + n + Q,$$

for which, with allowance for all errors of measurement, range straggling and indeterminacy of range-energy curves, we obtain $Q = (31 \pm 1.6)$ Mev and thus $B_\Lambda = (5.1 \pm 1.8)$ Mev (assuming that $Q_\Lambda = 36.92 \pm 0.22$ Mev [6]).

Of all the three-particle decay schemes analyzed only the following three schemes cannot be eliminated for some reason:

$$ {}_{\Lambda}H^3 \to \pi^- + He^3 + \gamma + Q_1 \qquad Q_1 = 50 \pm 8 \text{ Mev} \quad B_\Lambda = -7.5 \pm 9 \text{ Mev} \tag{1} $$

$$ {}_{\Lambda}H^4 \to \pi^- + He^4 + \gamma + Q_2 \qquad Q_2 = 51 \pm 9.5 \text{ Mev} \quad B_\Lambda = -6 \pm 10 \text{ Mev} \tag{2} $$

$$ {}_{\Lambda}He^7 \to \pi^- + Li^6 + n + Q_3 \qquad Q_3 = 35.5 \pm 2.2 \text{ Mev} \quad B_\Lambda = 4.2 \pm 2.4 \text{ Mev.} \tag{3} $$

Thus the case under consideration is either the decay of the hyperfragment ${}_{\Lambda}He^7$ with relatively large $B_\Lambda = 4.2 \pm 2.4$ Mev or the radiation decay of an unstable ${}_{\Lambda}H^3$ or ${}_{\Lambda}H^4$ fragment with emission of a photon whose energy E_γ is 19 ± 8 Mev or 20 ± 9 Mev, respectively. (The indeterminacy of E_γ is basically due to errors in fixing the direction of particle c).

At present about 100 cases of hyperfragment decay are known. Thus if Scheme (1) or (2) is correct the observed case could correspond to a relative probability for radiation decay of about 1%. Clearly, the mechanism for the formation of a photon in this could be the same as in anomalous π-μ decay with short-range muons and in the radiation decay of a τ-meson according to the scheme $\tau \to 3\pi + \gamma$ (all the more so since the probability for radiation decay of the fragment can be obtained theoretically near 1% by the same formulas [7] as for the decays $\pi \to \mu + e + \gamma$, $\tau \to 2\pi + \gamma$, $K \to \mu + \nu + \gamma$).

Of the remaining prongs of the primary star 20 were tracks of stable particles stopped in the emulsion and 2 tracks did not end in the stack.

In conclusion the authors wish to thank I. I. Gurevich for his interest in this work and valuable advice, L. V. Surkova and S. A. Chueva for assistance, Iu. L. Sokolov for making us acquainted with the photometric method for short tracks and A. I. Baz' for participating in the discussion of light hyperfragments.

LITERATURE CITED

[1] V. V. Alpers, R. I. Gerasimova, I. I. Gurevich, A. M. Mishakova and L. V. Surkova, Doklady Akad. Nauk SSSR 105, 2, 237 (1955).

[2] A. A. Varfolomeev, R. I. Gerasimova, E. A. Zamchalova, M. I. Podgoretskii and M. N. Shcherbakova, J. Exptl.-Theoret. Phys. (USSR) 30, 6, 1164 (1956) [Soviet Physics – J.E.T.P., p. 986].

[3] E. A. Al'bitskaia and Iu. L. Sokolov, Report of Acad. Sci. USSR for 1954.

[4] H. Fay, K. Gottstein and K. Hain, Nuovo Cimento 11, Suppl. No. 2, 234 (1954).

[5] J. R. Lonchamp, Ann. Phys. 12-e Ser. 10, 201 (1955).

[6] M. W. Friedlander, D. Keefe, M. G. K. Menon and M. Merlin, Phil. Mag. 45, 533 (1954).

[7] T. Eguchi, Phys. Rev. 85, 943 (1952); M. Annis, L. Taffara and B. Dequal, Nuovo Cimento 12, 813 (1954); T. Eguchi, Bull. Am. Phys. Soc. 30, 3, 19 (1955).

Received April 25, 1956

EXCITON STRUCTURE OF THE SPECTRAL CURVES OF THE PHOTOCONDUCTIVE EFFECT IN CRYSTALS

E. F. Gross, Corresponding Member of the Academy of Sciences USSR
A. A. Kaplianskii and B. V. Novikov

In recent years wide prominence has been given to the important role of excited (exciton) crystal states in connection with the photoconductive effect. It is suggested [1, 2] that excitons, although neutral quasiparticles, are nevertheless able to create current carriers either through thermal dissociation or through interaction with local lattice imperfections. On the basis of experimental data V. P. Zhuze and S. M. Ryvkin have concluded that excitons participate in the production of a photocurrent in cuprous oxide [3]. Subsequently the exciton mechanism of the photoconductive effect was also proposed for several other crystals [4, 5]. The experiments of Apker and Taft are evidence of the important role of excitons also in the (external) photoelectric effect [6].

New methods of investigating excitons in connection with the photoconductive effect have enabled us to observe in a number of crystals the line structure of the long-wave absorption edge, which is assumed to be associated with the excitation of excitons. First a parallelism was noted between the presence of an exciton absorption structure in crystals and high photosensitivity [7]. This parallelism was especially clear for different crystal modifications of a single substance [8]. Further support for the proposed exciton mechanism of photoconduction may be obtained from the fact that the photosensitivity of many crystals is concentrated in a narrow spectral region at the long-wave absorption edge, i. e., just in the region of exciton absorption [5, 7]. There is therefore great interest in a detailed study of the spectral photosensitivity curve for crystals which possess a discrete exciton absorption structure. When optical excitation of excitons in a crystal leads to the appearance of a photocurrent it can be expected that the spectral curve of the photoconductive effect will have a "fine structure" together with the discrete structure at the absorption edge.

As the objects of this investigation we chose crystals of HgI_2 and CdS, which possess a line structure of the absorption edge [9-13]. Although the photoconductive effect in these crystals has been studied frequently the available experimental data on the spectral characteristics of photoconductivity in both HgI_2 [14-16] and CdS [16-20] do not enable us to establish any correspondence with the spectroscopic data regarding the structure of the absorption edge [9-13]. In the present work therefore we have carefully investigated the spectral curves of photosensitivity for HgI_2 [21] and CdS [22] crystals in the region of the spectrum close to the absorption edge, where narrow lines associated with the excitation of excitons are observed. The measurements were made at T = 77.3° K on single crystals with polarized light. The light was spectrally decomposed by a triple-prism monochromator of relatively high dispersion; the photocurrent was recorded continuously by electronic means.

The measurements of photoconduction in HgI_2 [21] were performed on single crystal plates both containing the optic axis and perpendicular to it. In the absorption spectra of the first kind of single crystals at T = 77.3° K a single line λ 5330 is observed, which is polarized with its electric vector perpendicular to the optic axis [11]. We observed that the spectral sensitivity curve as well as absorption [11] is strongly dependent on the state of polarization of the incident light and the orientation of the crystal with respect to the beam. From the great variety of photoconduction spectra obtained with different relative orientations of the light vector (E), direction of the light beam (ℓ) and optic axis ($\underline{c}$) three basic curves can be derived, which are represented in Fig. 1, where they are compared with the corresponding absorption spectra.* Curve A corresponds to the ordinary beam ($E \perp c$).

---

* The vertical axes in Figs. 1, 2 and 4 give the photocurrent per unit of incident light energy in arbitrary units for each curve.

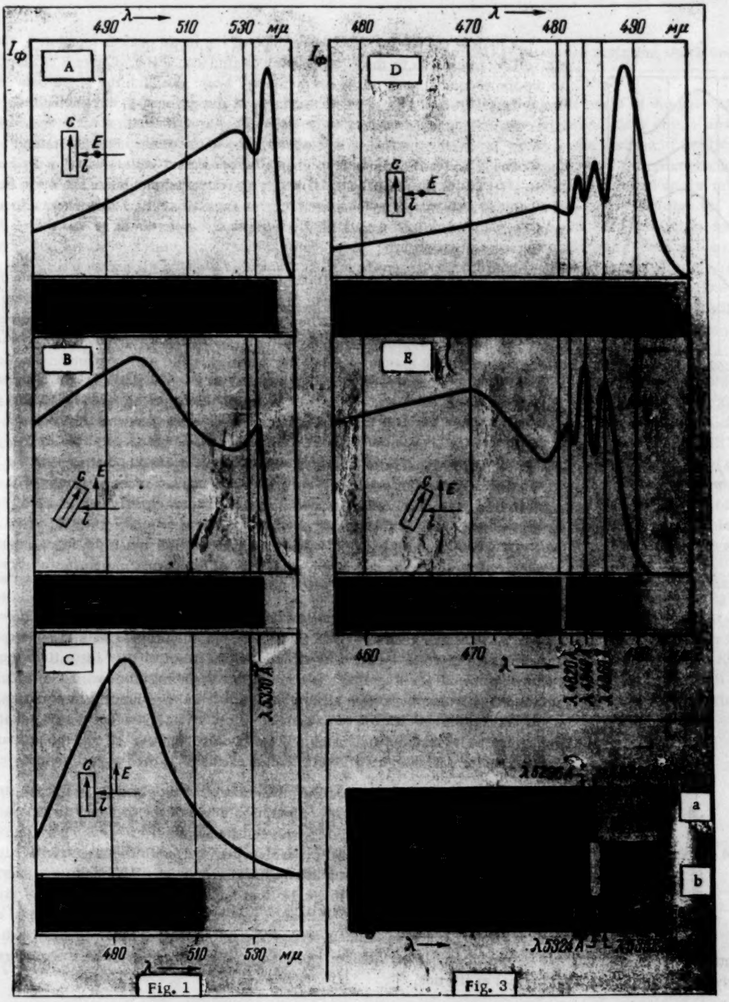

Fig. 1. Spectral sensitivity distribution of the photoconductive effect in crystals of HgI_2 (curves A, B, C) and CdS (curves D and E) compared with the absorption spectra of these crystals.

Fig. 3. Emission (b) and absorption (a) spectra of HgI_2 crystals at T = 4.2° K.

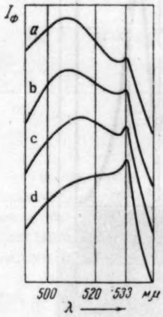

Fig. 2.

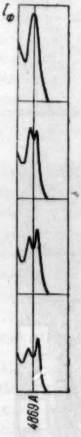

Fig. 4.

A narrow dip on the short-wave slope of the broad peak is found at λ 5330. Curve C corrpesponds to the extraordinary beam, with E ∥ c. Curve B corresponds to the more general case of the extraordinary beam in which the angle between E and c differs from 0°. In correspondence with absorption [11] the photoconduction curve shows higher sensitivity in the long-wave direction with a narrow peak at λ 5330. Figure 2 contains a few curves for the extraordinary beam obtained with increasing ∠ Ec (the corresponding change of absorption is shown in Fig. 2 of reference [11]). In the investigation of HgI_2 plates perpendicular to the optic axis it was found that the photoconduction curves for normal light incidence with any polarization, as well as natural light, have the same character as curve A of Fig. 1 for the ordinary beam.

CdS crystals were then similarly investigated [22], with measurements made on plates containing the optic axis. Figure 1 shows the photosensitivity curves of CdS (for different relative orientations of c, E and ℓ) compared with the corresponding absorption spectrograms taken from [13]. Curve E corresponds to the extraordinary beam when c makes an acute angle with E. The narrow photoconduction peak at λ 4869 coincides with the absorption line λ 4869 [12, 13], and the peaks at λ 4840 and λ 4820 coincide with the centers of the bands λλ 4836-4815 and 4809-4800 observed at T = 4.2° K [13] if we allow for the temperature shift of these bands when the crystal is heated to T = 77.3° K. Curve D corresponds to the ordinary beam. The three narrow dips in the photoconduction curve agree in position with the photoconduction peaks of the preceding curve and are located at the positions of the absorption lines. From a comparison of the photoconduction curves D and E of Fig. 1 for CdS with the curves for the corresponding relative orientations of E, c and ℓ for HgI_2 (curves A and B in Fig. 1) we find a great similarity in the fundamental character of these curves due to the similarity of the optical properties of monoaxial and dichroic HgI_2 and CdS crystals.

The presence of the photoconduction peaks λ 5330 in HgI_2 (Fig. 1, B) and λ 4869, λ 4840 and λ 4820 in CdS (Fig. 1, E), which coincide with the absorption lines for these crystals, is direct evidence that the absorption of these lines produces a photocurrent. If the hypothesis is correct that the absorption line structure of HgI_2 and CdS is due to exciton absorption, then it follows directly from our experiments that optical excitation of excitons in these crystals induces the photoconductive effect. The exciton mechanism of the photoconductive effect, the primary process of which is the optical excitation of excitons, is then experimentally proved.

The presence in the photoconduction curves of HgI_2 and CdS of broad structureless peaks in the vicinity of the absorption edges of the ordinary and extraordinary beams is probably associated with continuous absorption, which increases monotonically close to the longe-wave absorption edges in the direction of higher frequencies. Thus the photoconductive effect in these crystals occurs not only through the absorption of light in single lines but also through absorption of the continuous spectrum. It should be noted, however, that the recombination of electrons and holes, which we assume to be formed through the absorption of light in the continuous band, can proceed in part through intermediate exciton states which can produce a photocurrent similarly to excitons created by optical excitation.

The hypothesis that excitons are formed by recombination of electrons and holes is supported by experiments on the luminescence of crystals. When HgI_2 crystals were irradiated with light from the continuous absorption region we observed emission lines near the long-wave absorption edge of HgI_2 [21]. At T = 4.2° K this emission consists of two lines completely polarized with E ⊥ c, λ 5324 and λ 5352, which according to their position, relative intensity and polarization correspond to the absorption lines λ 5296 and λ 5321 which are observed at the temperature of liquid helium [11] (Fig. 3). It may be assumed that this is resonance radiation which accompanies the annihilation of excitons. Similar resonance emission is observed from CdS.*

From the form of the photoconduction curves for HgI_2 and CdS it follows that the peaks of the photoconductive effect are found at the positions of the absorption lines only for certain relative orientations of $\underline{c}$, E and ℓ (Figs. 1, B and 1, E). For other relative orientations of $\underline{c}$, E and ℓ instead of peaks at the position of the lines we observe narrow valleys of the photoconductive effect (Fig. 1, A and 1, D). We can attribute this phenomenon to the polarization of lines, as a result of which the magnitude of the absorption coefficient depends on the relative orientation of $\underline{c}$, E and ℓ. For the extraordinary beam (Figs. 1, B and 1, E) this orientation is such that the absorption coefficient in the lines is relatively small [11], as a result of which light in the lines penetrates deeply into the crystal creating a photoconduction current (in the photoconduction curves this means peaks at the positions of the lines). When $E \perp c$ (Figs. 1, A and 1, D) the absorption coefficient in lines polarized with $E \perp c$ is very large [11], so that light in the lines is practically completely absorbed in the thin surface layer. The photoconductive effect for the lines is likely to be much smaller in the surface layer than in the volume (a possible explanation is given below), so that light absorbed in the line gives almost no photocurrent (valleys of the photoconductive effect at the positions of the lines).

Figure 4 shows the change of the photoconductive peak λ 4869 (the curve of the photoconductive effect in CdS for the extraordinary beam) as $\angle Ec$ is increased. The peculiar "self-inversion" of the peak is evidently associated with the increase of the absorption coefficient for the line polarized with $E \perp c$, as a result of which light in the center of the line begins to be absorbed in the surface layer while light on the edges of the line still penetrates into the crystal. A similar self-inversion was observed by Apker and Taft in the exciton maxima of spectral yield curves for the photoelectric effect [6]. This was attributed by Hebb [24] to the destruction of excitons near the crystal surface [2]. This hypothesis concerning the destruction of excitons near the surface may be used in our case to explain the lowered photoconductive yield when lines are absorbed in the surface layer, which produces valleys in the photoconduction curves and self-inversion of a photoconduction peak as the crystal is rotated.

We also performed experiments to study the effect produced on the photoconduction curves by preliminary red and infrared irradiation, which is known [18, 25] to lower the photosensitivity of HgI_2 and CdS. For HgI_2 such irradiation was found to strongly reduce the photosensitivity in portions of the continuous absorption spectrum without affecting the photoconduction peak at λ 5330. On the other hand, in the case of CdS preliminary irradiation with red or infrared light can completely annihilate the photoconduction peak at λ 4869 while only slightly affecting the remainder of the spectral curve. Illumination in the fundamental absorption band of crystals after cessation of the preliminary irradiation results in a gradual restoration of the usual curve shape. These effects naturally require further and more thorough study.

LITERATURE CITED

[1] N. Mott, Proc. Roy. Soc. 167, 384 (1938).

[2] F. Seitz, Imperfections in Nearly Perfect Crystals (New York, 1952).

[3] V. P. Zhuze and S. M. Ryvkin, J. Exptl.-Theoret. Phys. (USSR) 20, 152 (1950); Doklady Akad. Nauk SSSR 76, 241 (1951); Bull. Acad. Sci. USSR, Phys. Ser. 16, 93 (1952).

[4] V. E. Lashkarev and G. A. Fedorus, Bull. Acad. Sci. USSR, Phys. Ser. 16, 81 (1952).

[5] W. Tyler and R. Sproull, Phys. Rev. 83, 548 (1951).

[6] L. Apker and E. Taft, Phys. Rev. 79, 964 (1950); 81, 698 (1951); 82, 814 (1951).

---

* This follows from the experiments of M. A. Iakobson in our laboratory which show that the familiar "blue" emission of CdS, that was discovered and investigated by Kröger [23] and later by Klick [19], corresponds to the line absorption of CdS [13]. As was shown by V. A. Arkhangel'skaia and P. P. Feofilov, this resonance emission is found not only in HgI_2 and CdS but also in PbI_2 and AgI crystals.

[7] E. F. Gross and M. L. Belle, J. Tech. Phys. (USSR) 25, 948 (1955).

[8] E. F. Gross and A. A. Kaplianskii, J. Tech. Phys. (USSR) 25, 1661 (1955).

[9] S. Nikitine and M. Sieskind et al., Comptes rend. 238, 1786 (1954).

[10] S. Nikitine and M. Sieskind, Comptes rend. 240, 1324 (1955).

[11] E. F. Gross and A. A. Kaplianskii, J. Tech. Phys. (USSR) 25, 2061 (1955).

[12] E. F. Gross and N. A. Karryev, Doklady Akad. Nauk SSSR 84, 471 (1952).

[13] E. F. Gross and M. A. Iakobson, J. Tech. Phys. (USSR) 25, 364 (1955); Doklady Akad. Nauk SSSR 102, 485 (1955); J. Tech. Phys. (USSR) 26, No. 6 (1956).

[14] E. K. Putseiko, Doklady Akad. Nauk SSSR 67, 1009 (1949); Bull. Acad. Sci. USSR, Phys. Ser. 16, 34 (1952).

[15] D. V. Chepur, J. Tech. Phys. (USSR) 25, 2411 (1955).

[16] G. Bergmann and J. Hänsler, Z. Physik 100, 50 (1936).

[17] E. K. Putseiko, Bull. Acad. Sci. SSSR, Phys. Ser. 15, 707 (1951).

[18] R. Frerichs, Phys. Rev. 72, 594 (1947).

[19] C. Klick, Phys. Rev. 89, 274 (1953).

[20] H. Gobrecht and A. Bartschat, Z. Physik 136, 224 (1953).

[21] E. F. Gross, A. A. Kaplianskii and B. V. Novikov, J. Tech. Phys. (USSR) 26, 697 (1956).*

[22] E. F. Gross, A. A. Kaplianskii and B. V. Novikov, J. Tech. Phys. (USSR) 26, No. 4 (1956).**

[23] F. Kröger, Physica 7, 1 (1940).

[24] R. Hebb, Phys. Rev. 81, 702 (1951).

[25] F. Kämpf, Ann. Physik 66, 463 (1921); Z. Physik 38, 104 (1926).

Received May 22, 1956

Leningrad Physico-Technological Institute,
Academy of Sciences USSR

---

* [Soviet Physics – Technical Physics, p. 674].

** [Soviet Physics – Technical Physics, p. 900].

STATIC DISTORTIONS OF CRYSTALS DETERMINED BY DIFFERENT X-RAY WAVE LENGTHS

V. A. Il'ina and V. K. Kritskaia

(Presented by Academician G. V. Kurdiumov May 4, 1956)

Our investigations of the lattice distortions of cold-deformed iron and the static deformations of a solid solution in martensite crystals showed that the magnitude of these deformations ($\sqrt{\overline{u^2_{st}}}$) which was obtained from measurement of cobalt x-ray reflections is greater than when molybdenum x-rays are used on the same materials [1-3]. The difference in the magnitudes of the deformations cannot be attributed to experimental errors as it is too large. For example, for martensite containing 0.41% C $\sqrt{\overline{u^2_{st}}}$ as measured with cobalt x-rays was 0.09 A; with molybdenum x-rays it was 0.06 A, the difference thus being 40%. A similar ratio was obtained for deformed iron. Discrepancies for $\overline{u^2_{st}}$ as determined by radiation with two different wave lengths in the case of deformed tungsten were also reported in [4]. Since the size of the deformations of the lattice is a characteristic of the state of the material it should not depend on the mode of measurement if the material is not subjected to any additional treatment. Consequently the difference in $\overline{u^2_{st}}$ when two different radiations are used could be a result of neglecting some factors which come into play differently under different radiation.

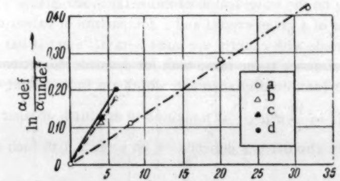

Fig. 1. ln ($\alpha_{def}/\alpha_{undef}$) as a function of $\Sigma h_2^2 - \Sigma h_1^2$ for α-iron as measured with x-rays from: a) Mo; b) Co, c)Cr, d)Fr

For the purpose of studying the effect of hardness of the x-rays on the results for $\sqrt{\overline{u^2_{st}}}$ we used four different sources of x-rays: molybdenum, cobalt, iron and chromium. The objects investigated were samples of deformed α-iron and α-solid solution of iron with 0.8% Nb. We determined distortions of the third kind in iron after plastic deformation (filing) and static distortions of the solid solution in the Fe-Nb alloy. The samples were prepared out of filed powders. Before x-raying the Fe-Nb powder was heated at 800° for 2 hours.

The static distortions were determined from intensity measurements of a large number of reflections (from $\Sigma h_i^2 = 2$ to $\Sigma h_i^2 = 62$), which eliminated the possibility of random errors. $\overline{u^2_{st}}$ was calculated from [1]

$$\ln \frac{\alpha_1}{\alpha_2} = \frac{4\pi^2}{3a^2}\overline{u^2}\,[(h_2^2 + k_2^2 + \ell_2^2) - (h_1^2 + k_1^2 + \ell_1^2)],$$

where for the determination of the 3rd kind of distortions in deformed iron

$$\frac{\alpha_1}{\alpha_2} = \frac{\alpha_{\text{def iron}}}{\alpha_{\text{undef iron}}};\ \alpha = \frac{J_{h_1k_1\ell_1}}{J_{h_2k_2\ell_2}},$$

and for static distortions of the solid solution in Fe-Nb

$$\frac{\alpha_1}{\alpha_2} = \frac{\alpha_{\text{solid sol}}}{\alpha_{\text{undef iron}}},.$$

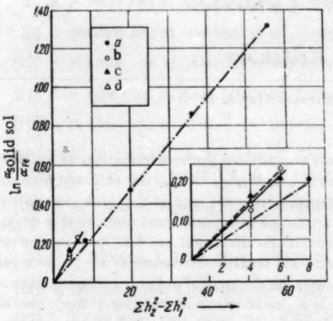

Fig. 2. $\ln(\alpha_{\text{solid sol}}/\alpha_{\text{iron}})$ as a function of $\Sigma h_2^2 - \Sigma h_1^2$ for a Fe-Nb solid solution as measured with x-rays from: a) Mo, b) Fe, c) Co, d) Cr.

Figures 1 and 2 show the dependence of the logarithm of α_1/α_2 on the order of reflection for these materials (iron and the Fe-Nb alloy).

As can be seen from Figs. 1 and 2, the straight lines passing through the points obtained with molybdenum x-rays in both cases have a considerably smaller slope than the straight lines through points obtained with greater wave lengths (K_α-Co, K_α-Fe and K_α-Cr). The slope of the last three lines is almost identical. The calculated static lattice distortions $\sqrt{\overline{u^2_{st}}}$ for deformed iron and the Fe-Nb solid solution are given in Table 1. We there also give our earlier results for tempered carbon steel [2, 3]. The experimental data showed very clearly that the values of the static distortions obtained with soft x-rays such as those from chromium, iron and cobalt give identical values of $\sqrt{\overline{u^2_{st}}}$ within the limits of experimental error and that these values are considerably greater than those obtained with molybdenum x-rays.

The literature as a rule gives such measurements made with relatively soft x-rays. Therefore the data of different authors were in satisfactory agreement. Because of the discovered divergence in the values of $\sqrt{\overline{u^2}}$ depending on the wave length of the x-rays, this quantity can be only regarded as an arbitrary value of the static distortions of a given crystal and a comparison of values of $\sqrt{\overline{u^2_{st}}}$ has meaning only if the intensity measurements were made with exactly the same x-rays. Sinct it has been shown experimentally that the attenuation law for x-ray interference is the same both for dynamic distortions (thermal vibrations of the atoms) and static lattice distortions (atomic displacements which are independent of time) and is described by the factor $e^{-G\frac{\sin^2\vartheta}{\lambda^2}}$, where $G = \frac{16}{3}\pi^2\overline{u^2}$, it remained to establish whether for the determined magnitude of the thermal displacements there also exists a dependence on wave length such as was found in the case of static distortions.

TABLE 1

Static Distortion as Determined with Different X-Rays for Deformed Iron and Fe-Nb and Fe-C Solid Solutions

	K_α-Cr	K_α-Fe	K_α-Co	K_α-Mo
Deformed Armco iron	0.142	0.144	0.135	0.093
Annealed Fe$^+$ 0.8% Nb alloy	0.148	0.148	0.151	0.121
Martensite with 0.41% C	—	—	0.090	0.060

The effect of different hardness of the x-rays on the magnitude of the dynamic lattice distortions (or on the characteristic temperature) was studied by us for silver and aluminum. These materials were selected because of their relatively weak interatomic bonds which are characterized by relatively large amplitudes of thermal vibrations of the atoms and small values of $m\theta^2$ (m is the atomic mass and θ is the characteristic temperature); this made it possible to determine the change of the thermal factor for intensity under soft x-rays with considerable accuracy. The Ag and Al were photographed with molybdenum and cobalt x-rays at room temperature and the temperature of liquid nitrogen. Molybdenum x-rays were used to determine the following reflections: (220), (311),(511), (531); cobalt x-rays were used for (111), (200), (220), (311), (331), (420).

The mean square atomic displacements for thermal vibrations and the characteristic temperature were determined from the relation

$$\ln\frac{\alpha_{+23^\circ}}{\alpha_{-185^\circ}} = \frac{4\pi^2}{3a^2}\left(\overline{u^2}_{+23^\circ} - \overline{u^2}_{-185^\circ}\right)\left[(h_2^2+k_2^2+l_2^2)-(h_1^2+k_1^2+l_1^2)\right] = \\ = \frac{3\hbar^2}{a^2mk}\varphi(\theta)\left[(h_2^2+k_2^2+l_2^2)-(h_1^2+k_1^2+l_1^2)\right],$$

where

$$\alpha_{+23^\circ} = \left(\frac{J_{h_1k_1l_1}}{J_{h_2k_2l_2}}\right)_{+23^\circ}; \quad \alpha_{-185^\circ} = \left(\frac{J_{h_1k_1l_1}}{J_{h_2k_2l_2}}\right)_{-185^\circ}; \quad \varphi(\theta) = \frac{1}{\theta}\left[\frac{\Phi(\theta/T_2)}{\theta/T_2} - \frac{\Phi(\theta/T_1)}{\theta/T_1}\right].$$

Figures 3 and 4 give the dependence of $\ln\frac{\alpha_{+23^\circ}}{\alpha_{-185^\circ}}$ on the difference of the sums of the squares of indices for the reflecting planes in the case of both silver and aluminum. The experimental points (which correspond to values of $\ln\frac{\alpha_1}{\alpha_2}$) which were obtained with K_α-Co and K_α-Mo lie practically on a single straight line from whose slope we also determined $\Delta\overline{u_d^2}$, the characteristic temperature and $\sqrt{\overline{u_d^2}}$ (the root mean square atomic displacement for thermal vibrations).

These results show that independently of the x-ray wave length the root mean square amplitudes of thermal vibrations ($\sqrt{\overline{u^2}}$) and the characteristic temperatures (θ) obtained from measurements at two temperatures are identical (Table 2). These results are in good agreement with the data for the characteristic temperature obtained from specific heat measurements [5, 6].

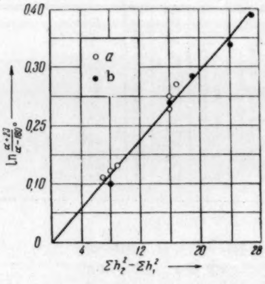

Fig. 3. ln ($\alpha_{+23^\circ}/\alpha_{-185^\circ}$) as a function of ($\Sigma h_2^2 - \Sigma h_1^2$) for silver, obtained with cobalt (a) and molybdenum(b) x-rays.

TABLE 2

	θ	$\sqrt{\overline{u^2}_{+23^\circ}}$, A
Aluminum	400	0.178
Silver	210	0.166

Thus despite the fact that the attenuation of x-ray interference intensities as a function of the reflecting plane indices both in the presence of static crystal distortions and with augmented thermal vibrations (dynamic distortions) follows the same law, the absolute values of the static distortions obtained through the intensity measurements depends on the x-ray wave length, while there is no such dependence on the wave length for the mean square amplitude of the thermal vibrations. It follows herefrom that the expression for the exponential factor e^{-2M}, which was deduced by Debye and Waller to allow for attenuation due to displacement of atoms from the sites of an ideal lattice during thermal vibrations requires corrections when applied to the calculation of the static displacements of atoms in solid solutions or plastic deformation of metals.

The cause of the divergence of results for $\sqrt{\overline{u_{st}^2}}$ obtained with different x-rays is still not known. It is possible that some part is played here by the distribution of these distortions both with regard to their magnitude and position in the volume of the crystal, which differs from the distribution of the atomic thermal vibrations.

For a correct fundamental explanation of these results further investigations are required, principally in the direction of developing a theory for the scattering of x-rays by a distorted lattice.

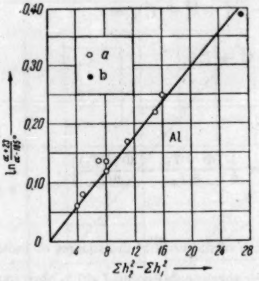

Fig. 4. $\ln(\alpha_{+23°}/\alpha_{-185°})$ as a function of $(\Sigma h_2^2 - \Sigma h_1^2)$ for aluminum, obtained with cobalt (a) and molybdenum (b) x-rays.

Received April 29, 1956

LITERATURE CITED

[1] V. A. Il'ina, V. K. Kritskaia and G. V. Kurdiumov, Problems of Metallography and the Physics of Metals, Collection No. 2 (1951).

[2] V. A. Il'ina, V. K. Kritskaia and G. V. Kurdiumov, Doklady Akad. Nauk SSSR 85, 4, 773 (1952); 85, 5, 997 (1952).

[3] V. K. Kritskaia, G. V. Kurdiumov and N. M. Nodia, J. Tech Phys. (U.S.S.R.) 25, 2, 177 (1955).

[4] A. Kokhanovska, Czechoslov. Phys. Jour. 4, November, 463 (1954).

[5] R. W. James, The Optical Principles of the Diffraction of X-Rays (1950).

[6] Ia. S. Umanskii and B. N. Finkel'shtein, et al, Physical Metallography (1955).

Institute of Metallography and Physics of Metals
Central Research Institute for Ferrous Metallurgy

ON THE RELATION OF THE PHYSICAL PROPERTIES OF CRYSTALS TO MOLECULAR CONCENTRATION

P. A. Savintsev

(Presented by Academician A. F. Ioffe May 9, 1956)

Crystals are often subjected simultaneously to considerable mechanical, thermal and electrical influences. In such instances it is necessary to evaluate a large group of crystal properties.

It has been shown [1, 2] that there is a relation between the properties of ionic crystals and the energy of the lattice. However, experiments which aim to determine the lattice energy are complicated and there is no data on the energy of crystals containing impurities. Therefore it is useful to find a physical quantity which is easily determined by experiment and is related to the mechanical, thermal, electrical and other properties of a crystal.

TABLE 1

Salts	α	U	E_s	σ	B	ε	nD	$\beta \cdot 10^6$	Heat of Fusion	Heat of Sublimation	Heat of Formation of solid compound
LiF	77	240	3.1	$0.6 \cdot 10^{-2}$	25500	1.9	1.38	30.7	6	63	145
LiCl	49	193	—	$1.5 \cdot 10^{-2}$	19000	—	1.66	40.7	5	47	—
LiBr	40	183	—	—	—	—	1.78	46.7	4.5	45	—
LiI	30	171	—	—	—	—	1.95	55.7	—	44	—
NaF	65	215	2.4	$1.7 \cdot 10^{-3}$	26000	1.75	1.33	32.7	7.6	72	135
NaCl	37	180	1.5	$1.3 \cdot 10^{-3}$	22000	2.25	1.53	36.7	7.0	57	99
NaBr	31	172	1.0	$1.3 \cdot 10^{-3}$	20600	2.65	1.64	39.7	6.1	54	86
NaJ	24	161	0.8	$4.0 \cdot 10^{-3}$	—	2.93	1.79	46.5	5.2	50	65
KF	41	190	1.8	$2.0 \cdot 10^{-4}$	27200	1.83	1.35	33.3	6.5	50	134
KCl	26	164	1.0	$2.0 \cdot 10^{-4}$	23900	—	1.50	33.7	6.4	52	107
KBr	22	158	0.7	$2.0 \cdot 10^{-4}$	22800	—	1.55	36.7	6.2	50	95
KI	19	149	0.6	$1.5 \cdot 10^{-4}$	20500	—	1.68	41.7	4.1	49	79
RbF	28	181	—	—	—	—	1.38	—	6	53	—
RbCl	23	159	0.8	$5.0 \cdot 10^{-6}$	24600	—	1.49	32.8	5	52	106
RbBr	20	152	0.6	$3.5 \cdot 10^{-5}$	23500	—	1.55	34.7	5	51	95
RbJ	15	144	0.5	—	—	—	1.64	39.7	5	50	83

Remarks. U is the lattice energy in kcal/mole; E_s is the electric strength in mv/cm; ϵ is the electronic component of the dielectric constant; σ is the ionic conductivity at the melting point; B is a constant in the conductivity equation $\sigma = Ae^{-B/T}$; β is the coefficient of linear expansion; n_D is the refractive index of light.

We have concluded that a large number of constants which characterize crystal properties depend on the molecular concentration. We denote this quantity by α and obtain it from the formula:

$$\alpha = \frac{D}{M} \cdot 10^3,$$

where D is the crystal density and M is the molecular weight. The relation of α to the properties of alkali halide crystals can be seen from Table 1.

It must be noted that the coefficients k which relate the physical constants to α change in going from the compounds of one metal to the compounds of another metal. Sometimes the coefficients k differ so little that they can be assumed to coincide (see Figs. 1, 2, 3).

In Table 2 we continue the comparison of mechanical and electrical characteristics with α. Here γ/γ_0 gives the relative values of the surface energy which we determined by mutual polishing [3]. It is seen from Table 2 that with increasing α the hardness of the crystals increases but that the dielectric loss (tan δ at 10^6 cycles) and the elastic limit decrease. With increasing α a tendency is noted toward smaller shear modulus and Young's modulus. We consider it necessary to verify the numerical values of Young's modulus and the shear modulus for several salts.

Table 3 gives a comparison of the properties of oxides of the second periodic group with α. The data in this table show that as α increases there is also an increase in the heat of sublimation, melting point, lattice energy and hardness, while there is a lowering of the specific heat, entropy and heat of hydration. For the purpose of constructing Tables 1, 2 and 3 we used data from [1-12].

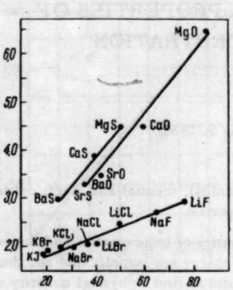

Fig. 1.

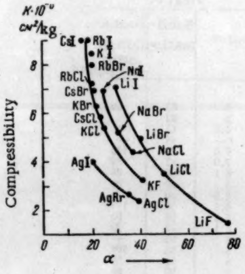

Fig. 2.

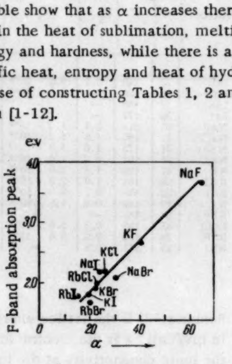

Fig. 3.

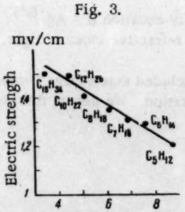

Fig. 4.

TABLE 2

Salts	α	Hardness			Shear modulus kg/mm²	Young's modulus kg/mm²	Elastic limit kg/mm²	tan $\delta \cdot 10^{-4}$	γ/γ_0
		scratching	boring	vibration dampness					
LiF	77	—	—	—	3204	14000	—	0.4	—
LiCl	49	—	—	25	1696	6000	—	—	—
LiBr	40	2.6	—	—	1718	1900	—	—	—
LiI	30	—	—	—	—	—	—	—	—
NaF	6.	—	—	—	—	—	—	—	—
NaCl	37	2.5	1.1	20	1234	4400	72	0.6	1.45
NaBr	31	2.4	—	—	923	4780	—	—	1.20
NaJ	24	—	—	—	—	—	—	—	—
KF	41	—	1.3	—	857	7340	—	—	—
KCl	26	—	0.8	7	—	—	50	0.7	1
KBr	22	2.3	0.6	—	369	4470	40	1.0	0.91
KJ	19	2.2	—	—	387	2470	31	1.3	—

TABLE 3

Oxides	α	U	Mohs hardness	Specific heat	Entropy	Heat of			m.p. °K
						Hydration	Formation	Sublimation	
MgO	85	940	6.5	8.93	6.40	9.7	143.5	130	3073
CaO	59	853	4.5	10.23	9.50	15.9	151.9	128	2858
SrO	43	791	3.5	10.76	13.0	19.5	141.1	117	2703
BaO	35	747	3,3	11,34	16.8	24,5	134.0	90	2196

We note that dependence of several properties on α is also observed in organic liquid dielectrics.

It is seen from Fig. 4 that the electric strength of a homologous series of liquiddielectrics diminishes as α increases. In solid dielectrics the electric strength increases with α (Table 1). This confirms [13] concerning the difference in the breakdown mechanisms of solid and liquid dielectrics.

It is observed that other properties of metals such as durability are dependent on α [4, 14].

Thus the molecular concentration α can be regarded as a collective characteristic of many properties of matter.

I wish to thank Professor A. A. Vorob'ev for discussions and valuable suggestions.

LITERATURE CITED

[1] A. A. Vorob'ev and E. K. Zavadovskaia, Doklady Akad. Nauk SSSR 81, 3 (1951); Bull. Tomsk Poly. Inst. (U.S.S.R.) 83 (1956).

[2] A. A. Vorob'ev, Works of the Siberian Physico-Technical Institute (U.S.S.R.) 5, 3 (1939); Bull. Tomsk Poly. Inst. (U.S.S.R.) 83 (1956).

[3] P. A. Savintsev and V. V. Kutsepalenko, Bull. Tomsk Poly. Inst. (U.S.S.R.) 83 (1956); Works of the Siberian Physico-Technical Inst. (U.S.S.R.) 34, (1955).

[4] V. D. Kuznetsov, Physics of Solids 1, 1937; 2, 1941; 4, 1947.

[5] V. M. Goldschmidt, Ber. 60, 1263 (1927); Z. tech. Phys. 8, 251 (1927).

[6] A. Hippel, J. Appl. Phys. 8, 12 (1937).

[7] N. S. Kurnakov, Selected Works 1 (1936); 2 (1939).

[8] Physical Constants, Ia. G. Dorfman and S. E. Frish, editors (1937).

[9] Technical Encyclopedia: Physical, Chemical and Technological Quantities (1927).

[10] A. A. Vorob'ev and K. A. Vodop'anov, Doklady Akad. Nauk SSSR 94, 3 (1954).

[11] V. Zeit, Progr. Phys. Sci. (U.S.S.R.) 18, 4 (1937).

[12] E. K. Zavadovskaia, Bull. Tomsk Poly. Inst. (U.S.S.R.) 83 (1956).

[13] A. A. Vorob'ev and A. F. Kalganov, Bull. Tomsk Poly. Inst. (U.S.S.R.) 83 (1956).

[14] M. M. Khrushchor and M. A. Babichev, Doklady Akad. Nauk SSSR 88, 3 (1953).

Received April 27, 1956

S. M. Kirov Tomsk Polytechnic Institute

K-MESON DECAY OF A SLOW SECONDARY PARTICLE

A. A. Varfolomeev, R. I. Gerasimova and L. A. Karpova

(Presented by Academician L. A. Artsimovich June 9, 1956)

The scanning of a stack of emulsions irradiated in the stratosphere [1] revealed the K-meson decay of a secondary particle.

From a 12+0n star, which is evidently primary, a slow particle emerges leaving track a (Fig. 1) of length 26μ. From its end begin the tracks of two charged particles (b and c in Fig. 1) forming an angle of 165 ± 10° with each other and almost at right angles to track a (in the undeveloped emulsion). Track b is dense without gaps and without tracks of fast δ-electrons; its length is 4.5± 0.5μ. Track c has small grain density and terminates in the emulsion at 16.25 ± 0.25 mm from the vertex of the secondary star without giving rise to any other tracks of charged particles.

In the emulsion track c is almost parallel to the plane of the plate so that one layer contains a section of the track in 12 mm. At the point where the track disappears particle c is not stopped but interacts in flight with the resultant formation of neutral particles. In order to determine the mass of particle c we measured the grain density and the gap density: 1) in track c as a function of the distance ΔR from the point of disappearance of the track, and 2) in 7 pion tracks, one τ-meson track and three proton tracks as a function of the residual range R. The mass of particle c was calculated from the formula $M_c = m\Delta R/\Delta r$, where m is the pion or proton mass, ΔR is the distance between sections with grain densities g_1 and g_2 (or gap densities G_1 and G_2) in track c and Δr is the distance between sections with the same grain densities g_1 and g_2 (or G_1 and G_2, respectively) in the tracks of the pions or protons. For M_c as compared with pion tracks we obtain $(1160 \pm 180)\ m_e$ by the (gΔR) method and $(80 \pm^{400}_{180})\ m_e$ by the (G,ΔR) method, and from a comparison with proton tracks $(950 \pm^{330}_{210})\ m_e$ by the (g,ΔR) method.

Figure 2 gives for comparison the grain density curves in the tracks of pions, particle c and protons as a function of distance from the point in the tracks where the density of all tracks is identical. The indicated errors are statistical. The probability that track c belongs to a proton is estimated as $\sim 10^{-7}$.

The measurements of multiple scattering in a constant cell gave values of pβ equal to (135 ± 22) Mev/c for the initial section in 4 mm and (131 ± 24) Mev/c for the final section in 2.3 mm.

On the basis of the above track c was ascribed to a K^--meson. On the assumption that the mass of particle c is $\sim 965\ m_e$ its initial energy was determined to be 65 ± 5 Mev. The indicated errors are due to the inaccuracy in determining the total residual track of the particle ($R_k = 23.5 \pm 2.0$ mm), track straggling and inaccuracy of the range-energy relation that was used (1%).

It is difficult to judge the nature of particle a from its track, which is short and forms a steep angle in the emulsion. However, the grain density indicates that particle a is slow and that in any event its kinetic energy is insufficient to produce a K-meson.

None of the known instable particles decays with emission of a K particle. Thus it must be concluded that in this case the K^--meson is a secondary particle from some "heavy" hyperon with mass $m_H \geqslant m_N + m_K + 60$ Mev or "heavy" meson with mass $m_X \geqslant m_K + 60$ Mev, where m_N and m_K are the masses of the nucleon and K-meson, respectively. The bc star could in principle be produced either by nuclear disintegration induced by a "heavy"-hyperon (meson) or from its decay, or from the decay of an unstable fragment associated with the "heavy" hyperon (meson).

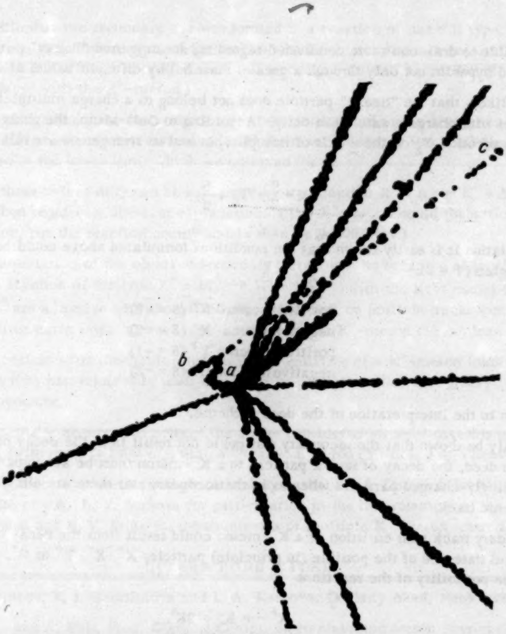

Fig. 1.

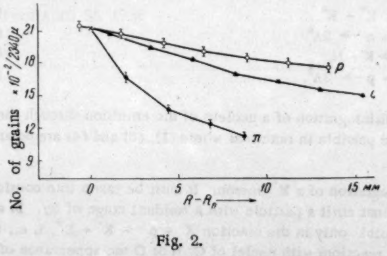

Fig. 2.

The assumed "heavy" hyperon (meson) can decay with emission of a K^--meson. Yet such decay is forbidden energetically. But it can be seen that the "heavy" hyperon (meson) has a relatively long decay period ($\sim 10^{-12}$ sec) so that either it itself or the fragment which contains it can be stopped in the emulsion through ionization slow-down. Consequently some kind of forbiddenness exists as a result of which the decay of the "heavy" hyperon (meson) takes place "slowly".

We now turn to Gell-Mann's [2] scheme of shifted charge multiplets and consider what strangeness S the "heavy" meson or hyperon could have.

It is clear that the "heavy" meson cannot have strangeness S equal to 0, +1 or −1 since then nothing would forbid "fast" decay of the meson into pions or into a K-meson and a light neutral particle (photon or neutrino). In exactly the same way the "heavy" hyperon cannot have strangeness S equal to 0, −1 or −2, as otherwise it would be impossible to forbid "fast" (with conservation of strangeness) decay of the "heavy" hyperon into a nucleon and pions, a hyperon and pions, or a Ξ hyperon and a light neutral particle.

It is thus possible to draw one more conclusion regarding the suggested "heavy" particle: it must differ from known K-mesons and hyperons not only through a greater mass but by different values of strangeness S.

It also seems likely that the "heavy" particle does not belong to a charge multiplet containing among its components particles with charge greater than unity. According to Gell-Mann, the charge $\underline{q}$ of a particle, its nuclear charge $\underline{n}$, its projection T_z on the $\underline{z}$ axis of isotopic spin and its strangeness are related by the equation

$$q = \frac{n}{2} + T_z + \frac{S}{2}. \tag{1}$$

By the use of this relation it is easily shown that the conditions formulated above could be satisfied only by the following chargesinglets ($T = 0$):

positive meson X^+ ($S = +2$)
negative meson X^- ($S = -2$)
positive hyperon Y^+ ($S = +1$)
negative hyperon Ω^- ($S = -3$)

We now return to the interpretation of the decay scheme.

1) It can easily be shown that the secondary star could not result from the decay of a singly-charged elementary particle. Indeed, the decay of such a particle to a K^--meson must be accompanied by the emission of an even number of singly-charged particles whereas in the secondary star there are altogether two tracks in addition to the K^--meson track.

2) The secondary track with emission of a K^--meson could result from the decay of an unstable fragment containing in a bound state one of the possible (in principle) particles X^+, X^-, Y^+ or Ω^-. For this it would be necessary to assume the possibility of the reactions

$$X^+ \rightarrow K^- + 2K^0, \tag{1}$$
$$X^- + N \rightarrow K^- + N, \tag{2}$$
$$Y^+ \rightarrow K^- + K^+ + p, \tag{3}$$
$$\Omega^- \rightarrow K^- + \Lambda^0. \tag{4}$$

However, if the masses of the particles make the enumerated reactions possible it also becomes possible to have fast decays (conserving strangeness):

$$X^+ \rightarrow K^+ + K^0, \tag{5}$$
$$X^- + p + n \rightarrow 2\Lambda^0, \tag{6}$$
$$Y^+ \rightarrow K + N, \tag{7}$$
$$\Omega^- + n + p \rightarrow 3\Lambda^0. \tag{8}$$

3) The secondary star could not result from the disintegration of a nucleus of the emulsion through the capture of an X^+, Y^+ or Ω^-. The emission of a K^- meson is possible in reactions where (1), (3) and (4) are possible and, consequently, also (5), (7) and (8).

Let us consider separately the possibility of disintegration of a X^--meson. It must be taken into consideration that a heavy nucleus of the emulsion (Ag or Br) cannot emit a particle with a residual range of 5μ. In a reaction with hydrogen the emission of a K^--meson is possible only in the reaction $X^- + p \rightarrow K^- + \Sigma^+$, i. e., together with the emission of an unstable Σ^+ hyperon. In reactions with nuclei of C, N or O the appearance of a K^--meson and one charged particle is possible in the reaction

$$X^- + M_Z^A \rightarrow K^- + \Lambda^0 + M_Z^{A-1}.$$

It is entirely possible that the secondary star was formed in a reaction of just this type. If this hypothesis is correct (for which there is little substantiation) the mass of the X^--meson has a lower limit of $m_K + (176 + 60)$ Mev = 1430 m_e. (If track c is attributed to a K^+ meson the secondary star can be attributed to the decay of an unstable fragment associated with the X^+-meson.)

Thus far we know altogether three cases which have been interpreted as the decay of a slow secondary particle with emission of a K^--meson. In two instances [3, 4] the reaction energy was > 43 Mev and > 54 Mev, respectively, which is close to the lower limit which we observed for Q.

It is possible that these values of Q can be explained by the reaction $X^- + n \to K^- + \Lambda^0$. However, the case in [5] with $Q \approx 5$ Mev then requires a different explanation. (The X^--meson could theoretically decay in flight into a K^--meson and pion, but the reaction energy should then be $\gtrsim 100$ Mev.)

The suggested interpretation of the observed secondary star cannot be regarded as satisfactory for the additional reason that in a reaction of the type $X^- + M_Z^A \to K^- + M_Z^{A-1}$ with the light nuclei C^{12}, N^{14} and O^{16} the products C^{11}, N^{13} and O^{15} are β^+ active with short lifetimes. However, no positron tracks were observed. It is also remarkable that in all three cases where Q was large the track of the K^--meson did not lead to a star.

It thus remains uncertain what mechanism results in the emission of a K^--meson from a slow secondary particle. It is clear that they can result only from the decay of particles which are "heavy" compared with well-verified K-mesons and hyperons.

If Gell-Mann's scheme is accepted as correct the above considerations show that this particle could rather be a "heavy" X^--meson (with mass $\gtrsim 1400\ m_e$) than a "heavy" hyperon (Y^+ or Ω^-) or a heavy positive X^+-meson.

In conclusion the authors consider it their pleasant duty to thank L. I. Gurevich for his assistance with the work and discussion of the results, L. V. Surkova for participation in the measurement of the K-meson mass, and B. P. Bannik, Z. P. Gol'vina and E. V. Esina for measurements of multiple K^--meson scattering.

LITERATURE CITED

[1] A. A. Varfolomeev, R. I. Gerasimova and L. A. Karpova, Doklady Akad. Nauk SSSR 110, 5, 758 (1956).

[2] M. Gell-Mann and A. Pais, Proc. Glasgow Confer. on Nuclear and Meson Physics (1954), p. 342.

[3] W. F. Fry, J. Schneps and M. S. Swami, Phys. Rev. 97, 1189 (1955); 99, 1561 (1955).

[4] W. F. Fry, J. Schneps and M. S. Swami, Nuovo Cim. 2, 346 (1955).

[5] Y. Eisenberg, Phys. Rev. 96, 541 (1954).

Received April 25, 1956

THE TOTAL CROSS SECTIONS FOR THE INTERACTION OF NEUTRONS WITH Li^6 AND Li^7 FROM 10 TO 450 KEV

G. V. Gorlov, B. M. Gokhberg, V. M. Morozov and G. A. Otroshchenko

(Presented by Academician A. P. Aleksandrov June 9, 1956)

This work was done at the end of 1952 with an electrostatic accelerator which developed up to 1.9 Mev [1]. The source of monoenergetic neutrons was the reaction $T(p, n)He^3$ [2]. Neutrons with energies from 10 to 350 kev, depending on the angle of emission from the target, were obtained from 1205 kev protons; neutrons with energies of 400 and 450 kev were obtained from 1255 kev and 1305 kev protons. The tritium target was made in the form of a thin layer of titanium on a molybdenum backing (thickness 0.2 mm); the titanium was impregnated with tritium. When the incident beam consisted of 1205 kev protons the target thickness was equivalent to ~ 10 kev. Measurements were made in a 3 x 3 x 2.5 m cage whose walls were made of a mixture of paraffin and borax.

The total cross section for the interaction of neutrons with Li^6 and Li^7 was determined from measurements of the transparency of two samples. Sample No. 1 was made of metallic lithium enriched with the Li^6 isotope (atomic ratio 91.4% of Li^6; impurities with respect to lithium 1.5% by weight). Sample No. 2 was made of metallic lithium enriched with Li^7 (atomic ratio 99.5% of Li^7; impurities with respect to lithium 1.46% by weight). Both samples, which were cylinders of 25 mm diameter and 30 mm length, were put into aluminum containers of 0.2 mm wall thickness.

The neutron flux was measured by a "long" neutron counter which was described in [3]. In this experiment two such counters were used. One counter served as the monitor and was in a fixed position with respect to the target; the other counter measured the neutron flux at various angles in the presence and absence of a sample. Both counters were placed at a distance of about 1 m from the target.

Measurements of the transparency of samples 1 and 2 were performed as follows: 1) we measured the neutron flux in the absence of a sample; 2) we measured the neutron flux using sample 1; 3) we measured the neutron flux using sample 2; 4) we measured the background of scattered neutrons (from the apparatus, walls, etc.) which reached the detector. All measurements were referred to a single position of the detector. In measurements of the neutron flux passing through a sample the latter was placed in such a position that it would cover the solid angle of the detector as seen from the target.

TABLE 1

$E \pm \Delta E$, Kev	$\sigma \pm \Delta\sigma$, barns		$E \pm \Delta E$, Kev	$\sigma \pm \Delta\sigma$, barns	
	Li^6	Li^7		Li^6	Li^7
10±2	2.2±0.3	1.0±0.3	261±13	9.3±0.3	6.0±0.2
20±4.	2.4±0.3	1.2±0.2	272±13	9.3±0.2	6.9±0.2
50±7	1.4±0.3	0.9±0.2	284±13	8.3±0.4	6.7±0.2
100±11	1.4±0.3	1.1±0.2	297±12	8.2±0.2	5.5±0.2
150±13	1.9±0.2	0.8±0.2	319±9	6.2±0.2	3.0±0.2
175±13	3.1±0.3	1.0±0.3	343±9	5.1±0.2	2.1±0.2
200±13	4.0±0.2	1.4±0.2	400±9	3.0±0.3	1.3±0.2
225±13	6.1±0.2	1.9±0.2	450±9	2.6±0.3	0.9±0.2
250±13	8.5±0.2	3.6±0.2			

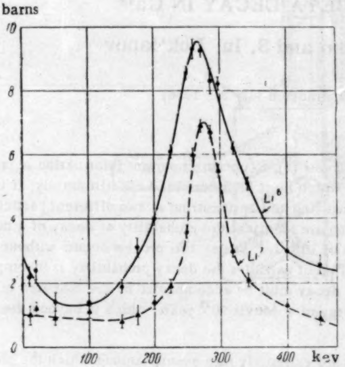

Fig. 1.

In determining the background a paraffin cone of 25 cm height was placed between the target and the detector; this practically entirely screened the detector from the direct neutron current issuing from the target. It should be noted that for measurements with neutrons above 100 kev the background consisted of from 3 to 5% of the measured current; at 50 kev the background was ~ 9%; at 20 kev it was ~ 25%; and, finally, at 10 kev it was ~ 42%. The background was measured with ± 3% accuracy.

In calculating the total cross section we introduced a correction for the background of scattered neutrons and for neutron scattering by the aluminum container walls (we note that the latter correction was smaller than the statistical error). The total cross sections obtained from samples 1 and 2 were converted into cross sections for Li^6 and Li^7 from the known isotopic composition of the samples. The results are given in Table 1.

The first column gives the values of the neutron energy with an indication of the energy dispersion associated both with the thickness of the tritium target and with the angular energy distribution of neutrons leaving the target and entering the recording counter. The last two columns give values of the total cross sections for Li^6 and Li^7. The indicated errors are statistical in accordance with the number of pulses recorded by the counter.

Figure 1 shows the total cross sections for Li^6 and Li^7 as a function of neutron energy.

As seen from Fig. 1 the total cross section for Li^7 reaches its peak $\sigma_t^{max} = 7.0 \pm 0.2$ barns at $E_{res} = 275$ kev. This is in good agreement with Adair [4]. The difference between our value of σ_t^{max} for Li^7 and the result given by Stelson and Preston [5] is explained by the fact that in our work the measurements were made with smaller energy resolution.

The total cross section for Li^6 which we obtained has a peak at $\sigma_t^{max} = 9.5 \pm 0.2$ barns for $E_{res} = 265$ kev. An increase of the cross section is also observed at small neutron energies; this is due to the reaction Li^6 (n, t)He^4. A comparision of our value for Li^6 with that published in 1954 by Johnson, Willard and Bair [6] shows good agreement within the limits of error for σ_t^{max}, E_{res} and the shape of the curve.

LITERATURE CITED

[1] G. V. Gorlov, B. M. Gokhberg, V. M. Morozov and G. A. Otroshchenko, Doklady Akad. Nauk SSSR 102, 2, 237 (1955).

[2] B. M. Gokhberg, G. V. Gorlov, V. M. Morozov and V. A. Shigin, J. Tech. Phys. (U.S.S.R.) 26, 985 (1956).

[3] B. Rossi and H. Staub, Ionization Chambers and Counters (1951).

[4] R. K. Adair, Phys. Rev. 79, 1018 (1950).

[5] P. H. Stelson and W. M. Preston, Phys. Rev. 84, 162 (1951).

[6] C. H. Johnson, H. B. Willard and J. K. Bair, Phys. Rev. 96, 985 (1954).

THE SEARCH FOR DOUBLE BETA DECAY IN Ca^{48}

E. I. Dobrokhotov, V. R. Lazarenko and S. Iu. Luk'ianov

(Presented by Academician L. A. Artsimovich July 31, 1956)

The investigation of double beta decay enables us, as we know [1], to obtain important information regarding the properties of the neutrino. Depending on the lifetime, which must be determined experimentally, it is possible to advance strong arguments for the existence of the neutrino and antineutrino as two different particles, or against this possibility. Thus, if the neutrino and antineutrino are identical the probability of decay of a nucleus with decay energy about 4 Mev corresponds to a lifetime of 10^{15}-10^{16} years; this process occurs without emission of a neutrino. If the neutrino and antineutrino are different particles the decay probability is incomparably smaller and in addition to the emission of 2 electrons the decay must be accompanied by the emission of 2 neutrinos. The lifetime of the nucleus for the same decay energy of 4 Mevis 10^{22} years, which is beyond the limits of contemporary experimental possibilities.

The serious difficulties which accompany attempts to record extremely rare events, among which the phenomenon under consideration is included, have resulted in contradictions in articles published over a long period [2-13] and have not enabled us to reach any definite conclusion regarding its existence. Only in 1955 did McCarthy [14] obtain sufficiently reliable data to apparently prove the eixstence of double beta decay for Ca^{48} with a half life of $1.1 \cdot 10^{17}$ years.* But a repetition with the same substance by Awshalom [15] which satisfied the conditions for reducing the background (measurements were made far below the earth's surface) gave a negative result: the half life had a lower limit of $2 \cdot 10^{18}$ years. Similarly, no double decay was observed for Nd^{150} in a recent article by Cowan, et al. [16]. The present article gives the results of experiments performed to detect double beta decay in Ca^{48}.

The isotopes of natural calcium were separated electromagnetically** and two pairs of samples were prepared, of which two were working samples and two were control samples. In an endeavor to reduce the content of inert atoms in the samples we used calcium fluoride as the chemical compound. Working samples Nos. 1 and 2, enriched with Ca^{48} to 76.2%, contained 423 and 259 mg of Ca^{48}, respectively. Control sample No. 2 was enriched with Ca^{44} (94.7%) and control sample No. 2 was enriched with Ca^{40} (99.9%). The weights of each pair of samples were chosen to make them equivalent according to the number of molecules of CaF. The impurities in the investigated material did not exceed 0.02% according to a chemical analysis. The samples were made by pressing CaF_2 powder into thin disks of 38 mm diameter. The binding material was a 1% solution of agar in water. The disks were placed in annular aluminum mountings faced at their ends with 30μ aluminum foil.

Measurements were made with two sets of apparatus, one of which (I) was on the earth's surface surrounded by 15 cm of lead and 3 cm of steel, while the other (II) was at a depth of 33 m below the surface (in the cosmic ray laboratory of the Moscow State University). In both installations both the measured and the control sample were placed alternately between two scintillation counters which were surrounded by a monitor counter with a liquid scintillator. The samples were alternated mechanically without opening the apparatus. As working counters we used FEU-12 photomultipliers, with FEU-19M photomultipliers as monitors. In the apparatus on the surface the working counters had tolane crystals while the monitoring counters contain three liters of the scintillator and

---

* Reference [1] contains the considerations which make Ca^{48} (and Nd^{150}) the most interesting objects of investigation in connection with the phenomenon under consideration.

** The authors are deeply grateful to V. S. Zolotarev for providing the separated calcium isotopes which were used in this work.

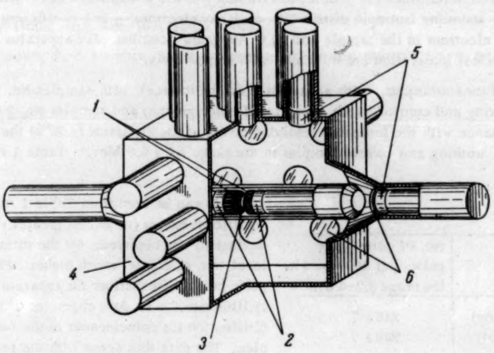

Fig. 1. Sketch of installation II. 1) Plastic scintillator; 2) working photomultipliers; 3) sample; 4) tank containing liquid scintillator; 5) monitor photomultipliers; 6) quartz windows.

two photomultipliers. The working counters used in the subterranean apparatus contained a plastic scintillator; the volume of the liquid in the monitor counter was 65 liters; this volume was scanned by 21 multipliers. Figure 1 shows schematically the arrangement of the principal elements of installation II.

Pulses from the two working counters which coincided within 0.5 μsec and were not accompanied by a pulse from the monitor were registered on film through the use of a double oscilloscope and then subjected to height analysis. The spread in the combined energy of two electrons recorded simultaneously in the vicinity of 4 Mev (the energy of double beta decay of Ca^{48} is 4.3 ± 0.1 Mev), which was caused by inhomogeneity of the scintillation crystals, apparatus drift, inaccurate measurement of pulse heights on the film, pulse height spread introduced by the multiplier and, finally, absorption within the samples, was estimated to be not more than ± 20%. The working counters were calibrated by a beta spectrometer up to 2.6 Mev with a reference point at 0.625 Mev (Cs^{137} conversion electrons). The calibration gave dependence of the pulse height at the multiplier output on electron energy, which was extrapolated to 7 Mev. An additional control of the energy calibration was obtained from the position of the peak corresponding to cosmic radiation with minimum ionization. The stability of the instrumental parameters was checked periodically, not less than once a day.

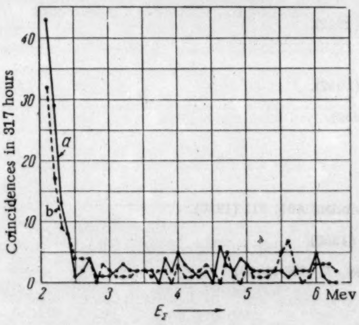

Fig. 2. Differential spectra of the combined energy of coincident pulses for Ca^{48}(a) and Ca^{40}(b). Channel width 0.1 Mev.

Let m be the mass of a given isotope in the working sample, A its mass number and Δn the difference between the number of pulses recorded per unit from the working and control samples. Then the half life with respect to the process of double decay is calculated from the formula

$$\tau = \ln 2 \frac{N_0}{A} \cdot \frac{k\eta m}{\Delta n}. \quad (1)$$

Here k is a factor which determines the geometric efficiency of the coincidence count without considering angular correlation, that is, assuming isotropic distribution of decay electrons, η is a coefficient which characterizes absorption of decay electrons in the sample and N_0 is Avogadro's number. For apparatus I and II the values of k obtained through numerical integration are 0.39 and 0.43, respectively.

We took two series of measurements: with apparatus I (on the surface), with samples No. 1 during 484 hours for each sample, working and control; with apparatus II (underground) and samples No. 2 during 317 hours for each sample. In accordance with the indicated resolving power of the apparatus (± 20%) the coincidence count was compared for the working and control samples in the range 4.0 ± 0.8 Mev.* Table 1 contains the results calculated for 100 hours.

TABLE 1

Apparatus	Sample	No. of coincident pulses per 100 hours in the range 3.2-4.8 mev
I	Ca^{48}(No. 1 working)	216 ± 7
	Ca^{44}(No. 1 control)	208 ± 7
II	Ca^{48}(No. 2 working)	10.6 ± 1.9
	Ca^{40}(No. 2 control)	8.2 ± 1.6

As can be seen from Table 1 in both series no significant excess (no excess greater than one standard deviation) was observed. On the surface the background level was, of course, much higher. Figure 2 shows the pulse height distributions for apparatus II, which clearly illustrate the random character of the pulse-height distribution for coincidences in the case of both samples. The data thus agree with the results of Awshalom and disagree with McCarthy.

The relatively small number of observed coincidences in the energy range of interest (in the underground measurements) requires extreme caution in evaluating the results. In each instance it can be stated that an excess of coincidences greater than twice the standard error is very improbable. Then Formula (1) with η = =0.67 and m = 0.259 gives $\tau > 1 \cdot 10^{18}$ years. This half life disagrees with theoretical estimates of the nuclear life time for "neutrinoless" decay and is thus an argument for the existence of the antineutrino as a real physical particle.

The authors consider it their pleasant duty to thank L. A. Artsimovich, Ia. B. Zel'dovich, Ia. A. Smorodinskii and P. E. Spivak for discussions and I. V. Galkin and V. F. Ivanov for assistance with the experiments.

LITERATURE CITED

[1] Ia. B. Zel'dovich, S. Iu. Luk'ianov and Ia. A. Smorodinskii, Progr. Phys. Sci. (U.S.S.R.) 54, 361 (1954).

[2] E. L. Fireman, Phys. Rev. 75, 323 (1949).

[3] E. L. Fireman and D. Schwarzer, Phys. Rev. 86, 451 (1952).

[4] J. S. Lowson, Phys. Rev. 81, 299 (1951).

[5] M. L. Kalkstein and W. F. Libby, Phys. Rev. 85, 368 (1952).

[6] R. M. Pearce and E. R. Darby, Phys. Rev. 86 1049 (1952).

[7] J. A. McCarthy, Phys. Rev. 90, 853 (1953).

[8] R. G. Winter, Phys. Rev. 85, 687 (1952).

[9] J. H. Fremlin and M. C. Walters, Proc. Phys. Soc. (London) A65, 911 (1950).

[10] M. G. Ingram and J. H. Reynolds, Phys. Rev. 78, 822 (1950).

[11] C. B. Levine, A. Ghiorso and G. T. Seaborg, Phys. Rev. 77, 296 (1950).

[12] R. G. Winter, Phys. Rev. 99, 88 (1955).

[13] J. F. Detoeuf and R. Moch, J. Phys. Rådium 16, 897 (1955).

---

* We estimated mean energy losses within the sample at 0.3 Mev.

[14] J. A. McCarthy, Phys. Rev. 97, 1234 (1955).

[15] M. Awshalom, Phys. Rev. 101, 1041 (1956).

[16] C. L. Cowan, F. B. Harrison, L. M. Longer and F. Reines, Nuovo Cim. 3, 649 (1956).

Received July 20, 1956

AN INVESTIGATION OF VACUUM-EVAPORATED SINGLE-CRYSTAL GERMANIUM FILMS

G. A. Kurov, S. A. Semiletov and Z. G. Pinsker

(Presented by A. V. Shubnikov June 16, 1956)

Semiletov [1] has shown the possibility of obtaining highly oriented (single crystal) germanium films by vacuum evaporation on hot single crystals of germanium. We have performed electrical measurements and investigated the strucutre of such films. Samples were prepared by evaporating in a vacuum (at $\sim 10^{-5}$ mm Hg) some pieces of n-type and p-type germanium with resistivity from 2 to 30 ohm · cm. Condensation took place either on polished surfaces of germanium single crystals which had previously been etched in hydrogen peroxide or on the cleavage surfaces of single crystals. During evaporation the temperature of the backing was maintained between 450 and 900°. The thickness of the films was from 20 to 30 μ.

An electronographic study showed that in order to obtain single-crystal films with perfect structure the evaporation must be performed on single crystals heated above 750-800°. At the lower temperature of the backing (500-700°) the film is formed with the structure of a mosaic single crystal. Electronograms of such films revealed many spots forming a regular network, thus showing the presence of separate blocks rotated relatively to each other by ~ 2-3°.

A different picture results from condensation on single crystals heated above 750-800°. Electronograms of such films show sharp Kikuchi lines and bands, which indicate the absence of mosaic structure in the samples [2]. It could have been assumed that the electrical properties of such films of ~ 10-20 μ thickness will not differ essentially from the properties of a massive sample. But measurements produced a quite unexpected result. It was found that a film of a few microns thickness shunts a crystal of ~ 1 mm thickness.

For example, in one of the experiments on a crystal of 0.7 mm thickness and resistivity $\rho = 10.5$ ohm · cm we evaporated (at 550°) a film of 18.5 μ thickness. As a result the effective resistivity of the entire sample (film + crystal) was reduced to 0.83 ohm · cm. The value for the film was $2.2 \cdot 10^{-2}$ ohm · cm. Because of the indicated difference in the electrical conductivity of the crystal and film we were also able to measure in the latter the Hall emf at room temperature and the thermal emf. The Hall constant for the film was ~ 3 cm^3/coulomb and the mobility of the current carriers (holes) was ~ 150 cm^2/v · sec. Thus for the film the Hall constant was 2 to 3 orders lower and the mobility one order lower than in the massive monocrystal. Similar results were obtained for films produced by evaporation on an etched surface or cleavage surface of a single crystal heated to 900°. It should be noted that all of the investigated films possessed hole conductivity independently of the type of evaporated material. Prolonged annealing of such samples at 500° did not change their properties essentially, in particular the type of conduction.

In order to check the possibility of film contamination during evaporation we performed the following experiment. N-type germanium was evaporated on a corundum plate. The resulting finely crystalline film (p-type) was then melted. During melting there were formed on the backing a few drops of germanium, each of ~ 0.5 mm diameter. After prolonged annealing at 500° the hole-type germanium was converted into the electronic type and its electrical conductivity was sharply reduced. In other words, the germanium acquired the properties of the evaporated material. This is evidence of the fact that the electrical properties of the films which we investigated result from defects in their structure and not from impurities introduced during evaporation.

A microscopic examination showed that condensation on an etched surface of a single crystal gives a picture which depends essentially on the orientation of the surface. The surface of the film reveals a great many protuberances and depressions. All of the protuberances (and depressions) are parallel and bounded by a few im-

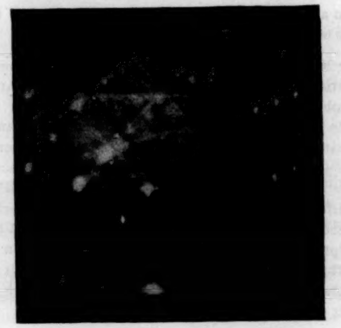

Fig. 1. Electronogram of a single crystal germanium film produced by evaporation at 900°.

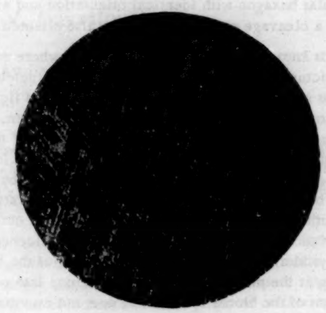

Fig. 2. A germanium film evaporated on a cleavage surface of a single crystal at 900° (450 x on a dark field).

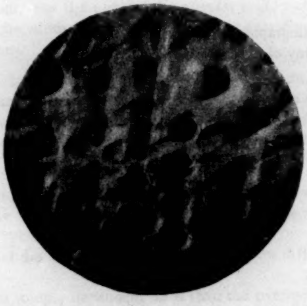

Fig. 3. A germanium film evaporated on a cleavage surface of a single crystal at 900°. (11,000 x).

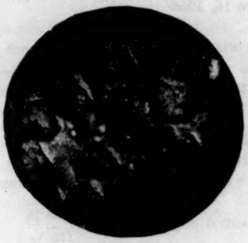

Fig. 4. Cleavage surface of a germanium single crystal (11,000 x).

portant crystallographic planes. The size of the proturbances reaches 30-40 μ. This picture is additional evidence of the single-crystal character of the film.

As was noted above, evaporation also took place on cleavage surfaces of single crystals. In one of such experiments a film was deposited only on the middle of the surface while the edge was screened. This sample enabled us to observe simultaneously both the film and the surface of the backing. For the purpose of revealing the fine structure the sample was lightly etched in hydrogen peroxide. Figure 2 is a photograph of the etched film. Etched figures are placed along segments of straight lines and form almost a continuous regular network with cells in the form of a rhombus with vertex angles of 60 and 120°. Figure 3 is an electron-microscopic photograph* of an impression of this same surface. We can see here that the etched figures on the film have the shape of a regular hexagon with identical orientation and are located along theedges of the rhombus. The etched figures on a cleavage surface (Fig. 4) are also oriented regularly but are arranged irregularly on the surface.

It is known that etching usually begins where defects are located. It can therefore be assumed that the etched picture (Fig. 2) reflects the symmetry of defect distribution in the given film. It should be noted that analogous symmetry in the arrangement of etched figures was observed on the (111) plane of a curved [3] or nonuniformly cooled [4] single crystal of germanium. Here slip occurred along the faces of an octahedron and the etched figures were arranged along the tracks of the slip planes. The analogy noted between the arrangement of etched figures on our film and the surface of a deformed single crystal evidently indicates that their defects are of the same character. The films investigated by us consist possibly of separate very small and identically oriented blocks that are separated by regions with lattice imperfections and are somewhat shifted with respect to each other. Such defeats apparently cannot be observed electronographically. The anomalous electrical properites of such films can be attributed to the influence of acceptor energy levels originating in the forbidden zone of the crystal and localized on the boundaries of the blocks. The low hole mobility in the films is the result of scattering at the places where the blocks come into contact. Our results also indicate that the observed lack of orientation of the blocks in the films does not essentially affect their electrical properties.

LITERATURE CITED

[1] S. A. Semiletov, Crystallography (U.S.S.R.) 1, 5, 542 (1956).

[2] S. A. Semiletov and Z. G. Pinsker, Crystallography (U.S.S.R.) 1, 2. 209 (1956).

[3] G. L. Pearson, W. T. Read and F. J. Morin, Phys. Rev. 93, 4, 666 (1954).

[4] E. Billig, Proc. Phys. Soc. (London) A, 235, 1200, 37 (1956).

Received June 16, 1956

Crystallographic Institute,
Academy of Sciences USSR

---

* Electron-microscopic photographs were taken at our request by A. L. Aleksandrov, whom we hereby thank.

TOTAL CROSS SECTIONS FOR THE INTERACTIONS OF 650 MEV PROTONS AND NUCLEI

V. I. Moskalev and B. V. Gavrilovskii

(Presented by Academician L. A. Artsimovich June 16, 1956)

This communication reports measurements of total cross sections for the interactions of 650 Mev protons with Be, C, O, Al, Cu, Sn, Pb and U. The experiments were performed on the synchrocyclotron of the Institute for Nuclear Problems of the Academy of Sciences USSR and employed the method and apparatus used in the determination of cross sections for p-p and p-d interactions [1, 2].

In the measurements of total nuclear cross sections for nucleons with energies of a few hundred million electron volts it is necessary to pay special attention to the geometrical conditions of the experiment because of the fact that elastic scattering at such energies is very strongly directed in the forward direction. Our apparatus included a telescope of three proportional counters connected for coincidence and a system of collimators which isolated a proton beam directed at the scatterer with a diameter of 10 mm and angular spread of about 0.1°; the liquid scintillation counter connected for coincidence with the telescope for recording of the attenuated beam had a diameter of 100 mm and uniform sensitivity over its entire surface within a few percent.

The Coulomb interaction between protons and nuclei hinders the measurements of cross sections for nuclear interactions of these particles with very "good" geometry such as is easily attained in similar experiments with neutrons. At 650 Mev a considerable fraction of proton diffraction scattering on heavy nuclei takes place in the angular region where the Coulomb scattering cross section is very large. Consequently, for these nuclei only measurements with "poor" geometry are feasible, from the results of which one can determine the inelastic cross sections. For light nuclei the angular region where the Coulomb interaction is important is considerably narrower than the width of the first diffraction peak, thus permitting quite reliable measurements of the total nuclear cross sections.

In our experiments with Be, C and Al the distances between the scintillation counter and the scatterers were such that the recording angle varied from 2 to 8°. Into the cross sections measured at various angles θ a correction was introduced for single Coulomb scattering which for Al does not exceed 2.5% at the smallest angles. Under the conditions of our experiment multiple Coulomb scattering could be neglected.

The correction for diffraction scattering at angles under 2° was calculated in two ways. By the first method the experimentally determined function $\sigma(\theta)$ was extrapolated to $\theta = 0$ with the aid of a straight line obtained by the method of least squares. However, the values of the total cross section obtained in this way are too high so that the integral angular distribution for diffraction scattering $\left(\int_{\theta}^{\pi} \frac{d\sigma_d}{d\Omega}\, d\Omega\right)$ at angles θ smaller than 1° is less steeply dependent on θ than the extrapolated straight line. Therefore in addition to this method the diffraction correction was calculated with the usual optical model [3]. This gave around 2% for Be and 4.5% for Al. These values were taken into consideration in the final result. The effect of secondary charged particles registered by the scintillator was very small.

The total cross sections for inelastic interaction of protons with nuclei from Be to U was determined from the measurements with 8° geometry. For Be, C and Al diffraction scattering was considered at angles greater then 8°. The corresponding correction as calculated for these nuclei from the optical model did not exceed 10%. For heavy nuclei, whose first diffraction minimum is found at angles θ smaller than 8° this correction was very small. The effect of secondary charged particles leaving the scatterer at angles smaller than 8° was estimated approximately from data obtained in our Institute by E. L. Grigor'ev and L. P. Solov'eva in connection with the study of nuclear disintegrations produced by 660 Mev protons in photographic emulsions [4]. The corresponding correction comprised about 1% for heavy nuclei. Corrections were also made to the inelastic cross section because of the effect of the Coulomb barrier of the nucleus (less than 3% for the heaviest nuclei).

TABLE 1

Element	σ_t	σ_a	σ_d	$\frac{\sigma_a}{\pi R^2}$ ($R=1.37\times$ $\times A^{1/3}\cdot 10^{-13}$ cm)
	10^{-27} cm²			
Be	272 ± 7	191 ± 8	81 ± 11	0.75
C	340 ± 10	227 ± 12	113 ± 16	0.73
O*	416 ± 30	—	—	—
Al	710 ± 32	418 ± 22	292 ± 39	0.79
Cu	—	850 ± 50	—	0.90
Sn	—	1285 ∓ 70	—	0.91
Pb	—	1930 ± 110	—	0.94
U	—	2215 ± 104	—	0.98

---

* The total cross section for oxygen was determined from the difference $\sigma(H_2O)-2\sigma(H)$ obtained from references [1, 2].

The energy of the protons in the beam impinging on the scatterers was 657 ± 5 Mev. Ionization losses of the protons in the scatterers did not exceed 15 Mev; therefore, the energy of protons in the center of the scatterers was about 650 Mev. Attenuation of the proton beam by scatterers was from 5 to 10%. The ratio of the number of quadruple coincidences to the number of triple coincidences, as measured without a scatterer, was not less than 98%. The intensity of the proton beam was maintained constant at about 150 particles per second.

Our values for the total cross sections σ_t and the inelastic cross section σ_a are given in Table 1.

The errors indicated in the table include both statistical errors of measurement, which comprise not more then 2-3%, and all indetermination associated with corrections. The values for the total diffraction scattering cross section σ_d are given by the difference $\sigma_t - \sigma_a$.

A comparison of our data on σ_t with the results obtained with 315 and 408 Mev protons [5, 6] shows that the total cross sections for light nuclei increase by about 10-20% as the proton energy is raised to 650 Mev. The inelastic cross sections which were measured for 134 Mev protons [7] agree within the limits of error with the cross sections at 650 Mev. With 860 Mev protons [8] the inelastic cross sections for Be, C and Al also agree within the limits of error with our data; for heavy nuclei the cross sections at 860 Mev are approximately 10% smaller. The total cross sections for light nuclei in [8] were determined by extrapolating $\sigma(\theta)$ to 0°; therefore the values obtained are the upper limits for the total cross sections.

It should be noted that the total cross sections of light nuclei for 650 Mev protons agree within the limits of error with cross sections measured for neutrons with 630 Mev effective energy [9], which is in agreement with the hypothesis of charge symmetry.

The data on σ_a for 650 Mev protons was used to determine the nuclear radii R. The calculations were performed according to the optical model [3] using the total cross sections for p-p and n-p interactions given in [1, 9]. The absorption coefficient K for these values of the elementary nucleon-nucleon cross sections is $0.36\cdot10^{13}$ cm^{-1}. The values of R for all nuclei from Be to U fit on the line $R = r_0 A^{1/3}$, where $r_0 = (1.37 \pm 0.03)\cdot 10^{-13}$ cm. Total cross sections and integral angular distributions of diffraction scattering for the light elements agree best with calculations based on the optical model when with the values of K and r_0 given above the real part of the complex potential V is set equal to 26 Mev.

From the ratios $\sigma_a/\pi R^2$ in Table 1 it follows that heavy nuclei are almost opaque to protons of the indicated energy while light nuclei still exhibit considerable transparency (~ 25%).

In conclusion we take this opportunity to thank V. P. Dzhelepov for discussions and S. V. Medved' for assistance with the measurements.

LITERATURE CITED

[1] V. P. Dzhelepov, V. I. Moskalev and S. V. Medved', Doklady Akad. Nauk SSSR 104, 380 (1955).

[2] V. P. Dzhelepov and V. I. Moskalev, Doklady Akad. Nauk SSSR 110, 4 (1956) [Soviet Physics – Doklady, p. 565].

[3] S. Fernbach, R. Serber and T. B. Taylor, Phys. Rev. 75, 1352 (1949).

[4] E. L. Grigor'ev and L. P. Solov'eva, Report of Institute for Nuclear Problems, Academy of Sciences USSR, 1956.

[5] H. G. de Carvalho, Phys. Rev. 96, 398 (1954).

[6] J. Marshall, L. Marshall and V. A. Nedzel, Phys. Rev. 91, 767 (1953).

[7] J. M. Cassels and J. D. Lawson, Proc. Phys. Soc. (London) A 67, 153 (1954).

[8] F. F. Chen, C. P. Leavitt and A. M. Shapiro, Phys. Rev. 99, 857 (1955).

[9] V. P. Dzhelepov, V. I. Satarov and B. M. Golovin, Doklady Akad. Nauk SSSR 104, 717 (1955).

Received June 16, 1956

Institute for Nuclear Problems
Academy of Sciences USSR

SOVIET PHYSICS – "DOKLADY" VOL. 1, NO. 5 MAY, 1957

(Translation of all papers in the "Physics" Sections of the Proceed
Academy of Sciences of the USSR, Vol. 110, Nos. 1-6, September-October, 1956)

CONTENTS

		Russian	
	Page	Issue No.	Page
Energy Distribution of Incoherent Radiation from Synchrotron Electrons. Iu. M. Ado and P. A. Cherenkov	517	1	35
Equations with Variational Derivatives and Distribution Functions for Systems with Complex Interaction. I. P. Bazarov	520	1	38
Pseudoscalar Interaction in Nonlinear Meson Theory. A. Borgardt	524	1	42
X-Ray Emission Spectra of Mn and Cu in a Heusler Alloy at Temperatures Around the Curie Point. E. E. Vainshtein and B. I. Kotliar	527	1	44
Sound Reflection by a Thin Rod in Water. L. M. Liamshev and S. N. Rudakov	530	1	48
Diamagnetic Resonance in Strongly Magnetic Bodies. Ia. G. Dorfman	534	2	201
Infrared Asymptotic Form of the Green's Function for Electrons to Order e^4. L. D. Solov'ev	536	2	203
On a Macroscopic Theory of Superconductivity for All Temperatures. V. L. Ginzburg	541	3	358
Exchange Interaction in Some Paramagnetics. S. -Kh. G. Kashaev	546	3	362
On the Isotope Shift in the Spectrum of Neodymium. F. A. Korolev and Iu. I. Osipov	549	3	365
Dispersion Relations for the Photoproduction of Pions. A. A. Logunov and B. M. Stepanov	552	3	368
On Thermal Agitation in Distributed Systems. S. M. Rytov	555	3	371
On the Departure from Weak Coupling in the Doubly-Charged Meson Field Theory. I. F. Ginzburg	560	4	535
Total p-d Cross Section from 390 to 650 Mev. V. P. Dzhelepov and V. I. Moskalev	565	4	539
An Experimental Investigation of the Angular Distribution and Polarization of Optical Radiation from Electrons in a Synchrotron. F. A. Korolev, V. S. Markov, E. M. Akimov and O. F. Kulinkov	568	4	542
The Potential in Pair Theories of Nuclear Forces. Iu. M. Lomsadze	571	4	545
A Method of Investigating the Electronic States of Diatomic Molecules. The Electronic States and Bond Distances of Alkali Metals and Their Hydrides. F. Sh. Shifrin	576	4	549
A Possible Example of Anomalous Decay of a Hyperfragment. A. A. Varfolomeev, R. I. Gerasimova and L. A. Karpova	579	5	758
Exciton Structure of the Spectral Curves of the Photoconductive Effect in Crystals. E. F. Gross, A. A. Kaplianskii and B. V. Novikov	582	5	761
Static Distortions of Crystals Determined by Different X-Ray Wave Lengths. V. A. Il'ina and V. K. Kritskaia	587	5	765

CONTENTS (continued)

	Page	Russian Issue No.	Russian Page
On the Relation of the Physical Properties of Crystals to Molecular Concentration. P. A. Savintsev	591	5	769
K-Meson Decay of a Slow Secondary Particle. A. A. Varfolomeev, R. I. Gerasimova and L. A. Karpova	594	6	959
The Total Cross Sections for the Interaction of Neutrons with Li^6 and Li^7 from 10 to 450 kev. G. V. Gorlov, B. M. Gokhberg, V. M. Morozov and G. A. Otroshchenko	598	6	963
The Search for Double Beta Decay in Ca^{48}. E. I. Dobrokhotov, V. R. Lazarenko and S. Iu. Luk'ianov	600	6	966
An Investigation of Vacuum-Evaporated Single-Crystal Germanium Films. G. A. Kurov, S. A. Semiletov and Z. G. Pinsker	604	6	970
Total Cross Sections for the Interactions of 650 Mev Protons and Nuclei. V. I. Moskalev and B. V. Gavrilovskii	607	6	972

The expanded program of the American Institute of Physics comprises translation of four leading Soviet physics journals, as listed below. These translations, by competent, qualified scientists, will provide all research laboratories and libraries with accurate and up-to-date information of the results of research in the U.S.S.R.

Soviet Physics — Technical Physics

A translation of the "Journal of Technical Physics" of the Academy of Sciences of the U.S.S.R. The 1956 volume, which was originally announced as containing eighteen issues, is instead being issued monthly, in expanded issues. All issues of the original Russian journal for 1956 will be translated. Approximately 4,000 Russian pages. Annually, $90.00 domestic, $95.00 foreign.

Soviet Physics — Acoustics

A translation of the "Journal of Acoustics" of the Academy of Sciences of the U.S.S.R. Four issues per year, approximately 500 Russian pages. Annually, $20.00 domestic, $22.00 foreign. The 1955 issues of "Journal of Acoustics" U.S.S.R. will also be published. Will consist of two volumes, approximately 500 pages, and the subscription price will be $20.00 for the set.

Soviet Physics "Doklady"

A translation of the "Physics Section" of the Proceedings of the Academy of Sciences of the U.S.S.R. Six issues per year, approximately 900 Russian pages. Annually $25.00 domestic, $27.50 foreign.

Soviet Physics — JETP

A translation of the "Journal of Experimental and Theoretical Physics" of the Academy of Sciences of the U.S.S.R. Twelve issues per year, approximately 2,600 Russian pages. Annually $60.00 domestic, $64.00 foreign. Back issues of Volume 1 and 2 are available at a special price of $30.00 for both to subscribers to Volume 3.

Subscriptions should be addressed to the American Institute of Physics, 57 East 55th Street, New York 22, N.Y.